UC Davis

UC Davis Electronic Theses and Dissertations

Title

Modeling Non-point Source Nitrate Groundwater Contamination at an Almond Orchard in the Central Valley, California

Permalink

https://escholarship.org/uc/item/2t9904gj

Author

Haynes, Hanni

Publication Date

2022

Peer reviewed|Thesis/dissertation

Modeling Non-point Source Nitrate Groundwater Contamination at an Almond Orchard in the Central Valley, California

By

HANNI HAYNES
THESIS

Submitted in partial satisfaction of the requirements for the degree of

MASTER OF SCIENCE

in

Hydrologic Sciences

in the

OFFICE OF GRADUATE STUDIES

of the

UNIVERSITY OF CALIFORNIA

DAVIS

Approved:

_____
Thomas Harter, Chair

_____
Helen Dahlke

_____
Laura Foglia

Committee in Charge

2022

- i -

TABLE OF CONTENTS

TABLE OF FIGURES

TABLE OF TABLES

ABSTRACT

Agriculture is responsible for 90% of nitrate leaching to groundwater in the Central Valley. This nitrate comes from excess fertilizer in the soil which is not taken up by crops. One method to reduce excess fertilizer, and therefore nitrate leaching, is by matching the crop's nitrogen demand through high frequency, low concentration (HFLC) fertilizer applications. This method has been implemented at the study site, a 56-ha commercial almond orchard in Modesto, CA, since 2017. Over five years of data have been collected from a vadose zone and groundwater monitoring well network at the orchard to study how this nutrient management practice impacts nitrate leaching rates as well as the nitrate concentrations in shallow groundwater. This project develops numerical models of water flow and nitrate transport used to 1) quantify the resulting reduction in nitrate loading rates from the orchard, and 2) predict when improvements in shallow groundwater quality may be measured. The models integrate flow and transport in the unsaturated zone and shallow groundwater at the field-scale. A key challenge investigated is the role that spatial variability observed in both the geologic media and in nitrate concentrations plays in the vadose zone and in groundwater. The models demonstrate that spatial variability observed in groundwater nitrate concentrations at the sub-field scale primarily results from sub-field scale spatial variability in nitrate leaching from the vadose zone. HFLC is predicted to reduce nitrate leaching from an already well-managed orchard by 40%. Low recharge rates (7 cm/year on average) caused by dry climate and efficient irrigation make for long response times (up to 50 years or more) in field-scale improvements in shallow groundwater quality. Additionally, nitrate concentrations in groundwater recharge under HFLC are predicted to remain above the public health criteria of 10 mg/L NO_3-N. These findings imply that under dry current climate conditions, reliance on nutrient efficiency goals alone may not resolve groundwater nitrate issues in the Central Valley.

ACKNOWLEDGEMENTS

First and foremost, I would like to thank my committee members for their mentorship. This thesis would not be possible without the support of my advisor, Thomas Harter. He gave a fledgling modeler a chance to spread her wings. Whenever I needed guidance, Thomas' ideas would propel me in the right direction. I am also thankful for the time Laura Foglia and Helen Dahlke spent helping me improve this project. Laura's advice helped me develop the groundwater model, and Helen's diligent review of my thesis led to improvements in the text.

Next, this project would not be possible without the hard work of the whole orchard project team. The team put years of work into this project before I arrived at UC Davis. Hanna Gurevich developed the HYDRUS model that the vadose zone model in this project is based on. Even though she was on the other side of the world, she taught me how to use her model and R scripts. Will Lennon collected much of the field data used in this project. Teena Stockert and Iael Raij-Hoffman also worked hard to support this project. The enthusiastic cooperation of the growers at the orchard study site was necessary to the success of this project.

On a personal note, I am grateful for the friendship of my peers in the Hydrologic Sciences Graduate Group. I often still reflect with gratitude for my former undergraduate mentors in the Earth and Oceanographic Science Department at Bowdoin College, Rachel Beane and Emily Peterman. Special thanks to my partner, Matt Blair, for moving across the country with me so I could pursue this degree. And thank you to my sister and mother for supporting my dreams. This work is dedicated to my father, who graduated with a PhD in immunology from UC Davis in 1985 and passed away in 2013. My father's example helped inspire me to be the scientist who I am today.

CHAPTER 1. Introductory Remarks

1.1 Background and Motivation

Increasing levels of nitrate emerging in groundwater wells in the Central Valley today are the result of decades of inefficient nutrient management practices by farmers. As California agriculture has grown over the past century into a $49 billion industry ("CDFA Agricultural Production Statistics"), fertilizer application has matched pace; the resulting nitrogen loading to groundwater in the 2000s is now 10 times greater than in the 1940s (Harter et al. 2017). Since the 1940s nutrient use efficiency of synthetic fertilizers on crops in the Central Valley has increased modestly from 33% to 53% (Harter et al. 2017); however, more improvements are needed to protect groundwater quality. The regulatory approach to reducing nitrogen loading in groundwater, and thus improving future groundwater quality in the Central Valley, is to encourage nutrient management practices for farmers that increase their nutrient use efficiency.

The challenge in developing efficient nutrient management strategies is quantifying the relationship between the amounts and timing of fertilizer and irrigation applications and observed nitrate concentrations in groundwater. Quantifying this relationship requires measurements that track the course of nitrogen and water inputs at the surface, through the soil, and into the underlying aquifer. It can also take decades for measurable impacts on groundwater quality to manifest in nearby wells due to the slow flow and mixing in groundwater. Predictions of groundwater age and source area of wells therefore provide valuable context needed to interpret nitrate measurements. Paired vadose zone and groundwater models can be used to estimate the transport timescales and source areas of nitrate in wells. Models also offer a timely solution to predict how agricultural management practices will impact groundwater quality over decadal time scales.

Nitrogen loading to groundwater by agriculture in the Central Valley is currently tracked by regulators using a simple mass balance model. For the mass balance model, farmers annually report nitrogen applications through fertilizer and removal through harvest. However, previous studies of nitrate transport in the vadose zone have recognized that in areas with highly heterogeneous geology, such as the alluvial systems that comprise much of the Central Valley, the presence of contrasting sediment textures with variable soil hydraulic properties may influence nitrate transport by offering preferential flow pathways for water (Onsoy et al. 2005; Baram et al. 2016A). Some previous studies still find mass balance to be a good proxy to estimate nitrate leaching (Botros et al. 2012; Baram et al. 2016B). Physics-based models, such as the ones in this study, can evaluate mass balance estimates while accounting for geologic heterogeneity.

Finite-element models such as the one used in this study, HYDRUS (Simunek et al. 2013), may realistically represent physical processes, but face computational limitations at the regional scale. Thus, the nitrogen mass balance has been used instead to approximate loading rates in regional groundwater nitrate models (Bastani and Harter 2019; Kourakos et al. 2012). Another model used to estimate nitrate loading at the regional scale is the Soil and Water Assessment Tool, which is a simplified physical model (Neitsch et al. 2011). The results of the field-scale model developed in this study contextualize nitrate loading rates used for regional models

Ultimately, nitrate transport models will be applied to understand nitrate leaching from agriculture at the regional scale. Regional groundwater nitrate models may be used as regulatory planning tools by predicting an exceedance probability for nitrate concentrations in wells within an area. Uncertainty in the mean concentration predicted in wells at the regional scale increases with the variability of loading rates across the different land uses in the area, as well as the loading rate variability within individual land use categories (Kourakos et al. 2012). Planning for groundwater quality at the

regional scale may therefore also require knowledge of spatial variability of nitrate loading within the same land use, which is a topic that is still poorly understood. The field scale model in this study considers the relationship between shallow groundwater nitrate concentrations and nitrate loading rates across different parts of an almond orchard.

1.2 Objectives

In order to demonstrate the impacts of nutrient management practices on nitrate leaching to groundwater, this project uses detailed data collected at an almond orchard to develop a field-scale vadose zone to shallow groundwater nitrate transport model. Data is collected for several growing seasons before and after a change to an experimental nutrient management practice meant to improve nutrient use efficiency at the orchard. The model is used to predict spatial and temporal patterns in nitrate concentrations in shallow monitoring wells spanning a 56-ha orchard over the past 30 years and for the next 30 years into the future. Nitrate loading to groundwater in this physics-based model is compared to mass-balance estimates to indicate the accuracy of the simple approach used by farmers and regulators today. This model demonstrates how nutrient management practices adopted by farmers influence the spatial and temporal distribution of nitrate in shallow groundwater. The model also investigates the role that spatial variability observed in both the geologic media and in nitrate concentrations plays in the vadose zone and in groundwater. The objective of this study is to address the following research questions:

1) Does switching to an experimental nutrient management practice reduce nitrate leaching from the orchard compared to the previous standard management practice? Do numerical and mass balance models predict the same outcome? (Chapter 2)

2) If nitrate leaching is being reduced, then how long will it take to observe improvements in shallow groundwater quality underlying the orchard? (Chapter 2 and 3)

3) What is the relationship between spatial variability in nitrate leaching and shallow groundwater concentrations at the field scale, and what role does soil heterogeneity play in nitrate transport? (Chapter 2 and 3)

1.3 References

Baram, S., V. Couvreur, T. Harter, M. Read, P. H. Brown, J. W. Hopmans, and D. R. Smart. 2016A. "Assessment of Orchard N Losses to Groundwater with a Vadose Zone Monitoring Network." *Agricultural Water Management* 172 (July): 83–95. https://doi.org/10.1016/j.agwat.2016.04.012.

Baram, S., V. Couvreur, T. Harter, M. Read, P.H. Brown, M. Kandelous, D.R. Smart, and J.W. Hopmans. 2016B. "Estimating Nitrate Leaching to Groundwater from Orchards: Comparing Crop Nitrogen Excess, Deep Vadose Zone Data-Driven Estimates, and HYDRUS Modeling." *Vadose Zone Journal* 15 (11): 1–13. https://doi.org/10.2136/vzj2016.07.0061.

Bastani, Mehrdad, and Thomas Harter. 2019. "Source Area Management Practices as Remediation Tool to Address Groundwater Nitrate Pollution in Drinking Supply Wells." *Journal of Contaminant Hydrology* 226 (October): 103521. https://doi.org/10.1016/j.jconhyd.2019.103521.

Botros, Farag E., Yuksel S. Onsoy, Timothy R. Ginn, and Thomas Harter. 2012. "Richards Equation–Based Modeling to Estimate Flow and Nitrate Transport in a Deep Alluvial Vadose Zone." *Vadose Zone Journal* 11 (4): vzj2011.0145. https://doi.org/10.2136/vzj2011.0145.

"CDFA Agricultural Production Statistics." n.d. Accessed September 4, 2022. https://www.cdfa.ca.gov/Statistics/.

Harter, Thomas, Kristin Dzurella, Giorgos Kourakos, Allan Hollander, Andy Bell, Nick Santos, Quinn Hart, Aaron King, Jim Quinn, and Gail Lampinen. 2017. "Nitrogen Fertilizer Loading to Groundwater in the Central Valley." *Final Report to the Fertilizer Research Education Program, Projects*, 11–0301.

Kourakos, George, Frank Klein, Andrea Cortis, and Thomas Harter. 2012. "A Groundwater Nonpoint Source Pollution Modeling Framework to Evaluate Long-Term Dynamics of Pollutant Exceedance Probabilities in Wells and Other Discharge Locations." *Water Resources Research* 48 (6). https://doi.org/10.1029/2011WR010813.

Neitsch, Susan L., Jeffrey G. Arnold, Jim R. Kiniry, and Jimmy R. Williams. 2011. "Soil and Water Assessment Tool Theoretical Documentation Version 2009." Texas Water Resources Institute.

Onsoy, Y. S., T. Harter, T. R. Ginn, and W. R. Horwath. 2005. "Spatial Variability and Transport of Nitrate in a Deep Alluvial Vadose Zone." *Vadose Zone Journal* 4 (1): 41–54. https://doi.org/10.2113/4.1.41.

Simunek, Jirka, M. Th Van Genuchten, and M. Sejna. 2013. "The HYDRUS-1D Software Package for Simulating the One-Dimensional Movement of Water, Heat, and Multiple Solutes in Variably-Saturated Media, Version 4.17." *HYDRUS Software Series 3*, 342.

CHAPTER 2. Quantifying nitrate leaching response to nutrient management at an almond orchard using mass balance and numerical models.

2.1 Abstract

Increasing levels of nitrate emerging in groundwater wells in the Central Valley today are the result of decades of inefficient nutrient management practices by farmers. This study quantifies the impact of high frequency, low concentration (HFLC) nutrient management on the reduction of nitrate leaching from an almond orchard located near Modesto, CA, using two approaches: a numerical vadose zone model and the nitrogen mass balance. Both approaches are based on data spanning nine growing seasons (2013-2021). Spatial variability in nitrate leaching at the field scale is evaluated by calculating water and nitrate fluxes for different portions of a 56-ha orchard. The vadose zone model is conceptualized as twenty 1D soil profiles spread throughout the almond orchard and simulated in HYDRUS. Water and nitrogen mass balance estimates based on historic data collected from 2013-2021 are generally consistent with the vadose zone model results. Average nitrate leaching rates were around 50 kg/ha/year but vary from <1 to 340 kg/ha/year based on the amount of precipitation, overlying tree age, and differences in profile sediment texture. Sediment heterogeneity combined with changing nitrate loading rates over time created high spatial variability in nitrate leaching to groundwater, even within orchard blocks under the same fertilizer and irrigation treatments. HFLC practices are predicted to increase the long-term nutrient use efficiency (NUE) of the orchard, which was already well-managed prior to the experiment. Both the numerical model and mass balance predict that the switch to HFLC produced a ~40% reduction in nitrate loading to groundwater. Dry climate and efficient irrigation at the orchard results in low recharge rates (7 cm/year). With such low recharge rates, it will take 10 years to see benefits of HFLC at the water table, and over 30 years for the 7 m deep vadose zone to reach a new steady state.

2.2 Introduction

Extensive usage of synthetic nitrogen (N) fertilizer allows world food production to keep pace with population growth, and is a key innovation of modern agriculture (Stewart et al. 2005). However, poorly optimized application of fertilizer leads to non-point source nitrate contamination of groundwater in agricultural areas. Nitrate contamination of groundwater is recognized as a public health issue of global importance by the United Nations (UNESCO 2022), as well as federally in the United States (Dubrovsky et al. 2010); and, it has been identified as an urgent concern in California (Harter and Lund 2012). The diffuse nature of non-point source nitrate contamination in groundwater makes remediation extremely challenging. The best way to address this problem is to prevent pollution in the first place by controlling N loading in agricultural discharges.

While recognized as a widespread water quality concern today, agricultural discharges are not federally regulated in the United States and were unregulated in California until the twenty-first century. In California, waste discharge requirements were created for irrigated agriculture discharges to surface water (in 2002) and groundwater (in 2012). These waste discharge requirements require farmers to follow nutrient management practices that limit pollutants entering surface water and groundwater and created requirements for tracking and reporting nitrogen use. Likewise, in 1991 the European Union initiated the Nitrates Directive, which requires member nations to establish practices that will limit fertilizer application rates in at-risk areas. Regulatory approaches to reducing N loading from agriculture focus on tracking and limiting excessive N application, thus improving the efficiency of its use.

Regulators are interested in supporting the development of nutrient management practices which reduce nitrate leaching. But, because there is no direct method to measure nitrate leaching from the vadose zone, it is difficult to quantify a reduction in nitrate leaching caused by more efficient nutrient management practices. A simple indicator for potential N losses to the environment is to compare the

mass balance between N applied in fertilizer to N harvested in the crop (Van Groenigen et al. 2010). The difference in the mass balance is the N surplus. The ratio of N outputs to inputs is the nitrogen use efficiency (NUE). A perfect balance of nitrogen applied to and taken up by crops results in a 100% NUE and no leaching. A practical upper limit to NUE is thought to be about 80-90% (EU Nitrogen Expert Panel 2015); but, the overall NUE for the Tulare Lake Basin and Salinas Valley is estimated at only 40-60% (Harter and Lund 2012). With statewide average synthetic fertilizer use averaging 514,000 tons N/year (Harter and Lund 2012), a conservative estimate of 60% NUE and fertilizer costs at $0.50/lb-N, this represents the loss of at least $200 million of fertilizer every year in California.

Constant crop management over several years is assumed to create a steady-state mass balance (Meisinger and Randall 1991), which means that deficiencies in the NUE imply excess N in soil. Under steady state conditions, most excess N in soil will presumably leach to groundwater. N mass balance is calculated annually and produces only one datapoint per land management unit (field) per year. Studies evaluating nutrient management practices typically span only two or three growing seasons. Thus, it is difficult for such studies to find a statistically significant difference between treatments, especially when improvements are relatively small compared to natural variability in NUE (Syvertsen and Jifon 2001).

Studies which evaluate the performance of nutrient management practices should continue for three growing seasons or more if possible; and the mass balance method should be validated by alternative methods to estimate nitrate leaching such as numerical models or field measurements. While the mass balance is a quick and easy, cost-effective tracking tool for regulators and farmers, it is an oversimplification of complex flow and transport processes in the vadose zone. Mass balance models rely on the assumption of steady state and uniform flow conditions (plug flow) (Selker et al. 1999). Meanwhile, field measurements of soil water potential and porewater nitrate concentrations in the vadose zone suggest that non-uniform flow paths are more likely to occur in soils characterized by heterogeneous

unconsolidated sediments, which accelerate some N fluxes to the water table through preferential flow paths. Field measurements collected at several orchard study sites in the Central Valley demonstrate high spatial and temporal variability in nitrate leaching from the vadose zone (Baram et al. 2016A; Onsoy et al. 2005; Gurevich et al. 2021). Onsoy et al. (2005), for example, concluded that heterogeneity in soil hydraulic properties was primarily responsible for the variability in nitrate concentration; and, as a result, N transport to the water table is characterized by preferential flow and highly localized fluxes through the most conductive sediment textures (i.e., sand). Numerical models use physics to simulate water and nitrate fluxes through the unsaturated zone and can even include representations of small-scale soil heterogeneity—a more faithful representation of the actual complexity of the system. Despite the added complexity, prior studies have found long-term N fluxes in numerical models to be consistent with fluxes predicted by the simple mass balance model (Botros et al. 2012; Baram et al. 2016B). This finding has significant implications for future regulations and standards adopted by farmers and would benefit from the support of a robust body of evidence.

This study quantifies the impact of a promising nutrient management practice on the reduction of N leaching from an almond orchard located in the Central Valley, California. N leaching before and after the implementation of the new nutrient management practice is estimated using both a numerical model of the vadose zone and the N mass balance. These models are based on a lengthy data collection period spanning nine growing seasons at the orchard (2013-2021). The results of the numerical model are compared to the N mass balance based on the farmer's fertilizer and harvest records as a validation. Because the numerical model is physics-based, it is used to estimate the amount of time it will take for improvements in nutrient management to reduce N leaching rates, which, depending on the rate that water and nutrients traverse the vadose zone to groundwater, is likely to take several years. Lastly, the models evaluate spatial variability in nitrate leaching at the field scale by calculating water and nitrate fluxes for

different portions of the 56-ha orchard. In particular, the numerical model includes a representation of the heterogeneous sediment deposits at the orchard in order to model the impacts of soil heterogeneity on spatial variability in N leaching noted in prior studies.

2.3 Study Area

The study site is a 56-ha (140-acre) commercial almond orchard located west of Modesto in Stanislaus County, California. The study site has been an almond orchard for more than 30 years. The geology at the orchard is characterized in prior work described in Gurevich et al. (2021). The orchard is located on alluvial fan deposits of the Tuolumne River, which is located approximately 3.4 km (2 miles) to the south. Sediments are heterogeneous, interbedded coarse channel sands and fine floodplain deposits. The average thickness of the vadose zone is approximately 7 m. Intra-annual variability in the water table has been less than one meter throughout 2017-2021. The water table has fluctuated by less than 2 m over the past 50 years. The ground surface elevation at the orchard is 18-19 m above sea level.

Since September 2017, an experimental nutrient management practice has been implemented at the orchard. This nutrient management practice aims to increase NUE by matching the timing and application rates of fertilizer to the crop uptake. This is accomplished by applying fertilizer in smaller, more frequent doses at a time and rate that coincides with the almond tree's nitrogen demand. The nutrient management practice is aptly referred to as high frequency, low concentration, or HFLC. In HFLC, fertilizer is applied in frequent, small doses that are dissolved and delivered through the irrigation system (a process called fertigation). Fertilizer is added to the irrigation system in the last 30 minutes of each irrigation event, which typically last around two days, in order to minimize leaching.

Almond nitrogen demand varies throughout the growing season depending on the stage of the annual growth cycle (Brown et al. 2020). Trees are dormant during the winter and bloom in the spring using stored nitrogen. Nitrogen uptake from the soil begins once most of the leaves are out and continues

through the growing season in order to develop and fill the kernels. Once the leaves fall, the tree is dormant again. The grower estimates the N demand for the orchard at the beginning of the season based on the past growing season yield, climate, and experience. Leaf tissue analyses are conducted in April and July to check the progress of the crop (Silva et al. 2013). Leaf tissue analyses are checked to make sure nutrient concentrations in leaves are meeting critical values necessary for a good yield. Fertilizer application rates are adjusted mid-growing season accordingly to match the progress of the crop indicated by the leaf tissue analysis. Small, frequent fertilizer applications in HFLC allow for more flexibility in adjusting fertilizer application rates to orchard productivity. In contrast, traditionally, nitrogen applications are split into only a few fertilization events per growing season (e.g. three to four applications in almonds; Brown et al. 2020). At the study site, traditional fertilizer applications before HFLC ranged from 13-90 kg N/ha (12-80 lbs N/ac), compared to 13-17 kg N/ha (12-15 lbs N/ac) with HFLC. This results in elevated soil nitrogen following applications, some of which may be leached from the soil before the crop can use it.

Compared to conventional fertilization practices, the HFLC nutrient management practice has been observed to raise NUE and/or lower leaching in field crops such as tomatoes (Farneselli et al. 2015), onions (Rajput and Patel 2006), potatoes (Badr et al. 2011), as well as citrus orchards (Thompson et al. 2000; Syvertsen and Sax 1999), pistachios and almonds (Baram et al. 2016B). Though, NUE improvements are not consistently observed when increasing application frequency in sandy soils (bell peppers, Storlie et al. 1995; broccoli, Thompson et al. 2003), which has a lesser ability to retain nutrients and moisture compared to loamy or clayey soils.

Previous work at the orchard considered in this study evaluated water and N mass balance data, field measurements in and just below the root zone, collected groundwater samples for nitrate, and developed a numerical model of water and nitrate transport in the vadose zone just for the 2013-2017

growing seasons, before HFLC was adopted (Gurevich et al. in preparation). The initial modeling found that variable water and nutrient management efficiency for the young trees compared to old trees created significant nitrate concentration variability in the root zone. The initial model also found that under current management and climate, it would take longer than 5 years for nitrate applied at the surface to reach groundwater. The current study extends the existing model to evaluate the long-term impact of HFLC nutrient management on nitrate leaching at the orchard scale. Additionally, the model in this study considers two causes of nitrate leaching variability which have been identified in previous research but have not been directly compared: 1) orchard water and nutrient management efficiency as it relates to tree age, and 2) sediment heterogeneity in the vadose zone.

2.4 Methods

This study evaluates the impact of HFLC nutrient management on groundwater quality at a commercial almond orchard by using a numerical model of the vadose zone to calculate water and N fluxes to groundwater. The model estimates are tested by comparing simulation outputs to the monthly and annual water and nitrogen mass balance record from 2013-2021. An existing HYDRUS model of the orchard covering the years 2013-2017 is extended to model a 90-year period from 1957-2047, which includes the orchard before and after the switch in nutrient management practices that occurred in 2017. This section describes how data was gathered and prepared for the mass balance and numerical model. Daily data were gathered for each of the six orchard blocks (NE1, NE2, NW, SW1, SW2, SE) for growing seasons 2013-2021 (Figure 2-1).
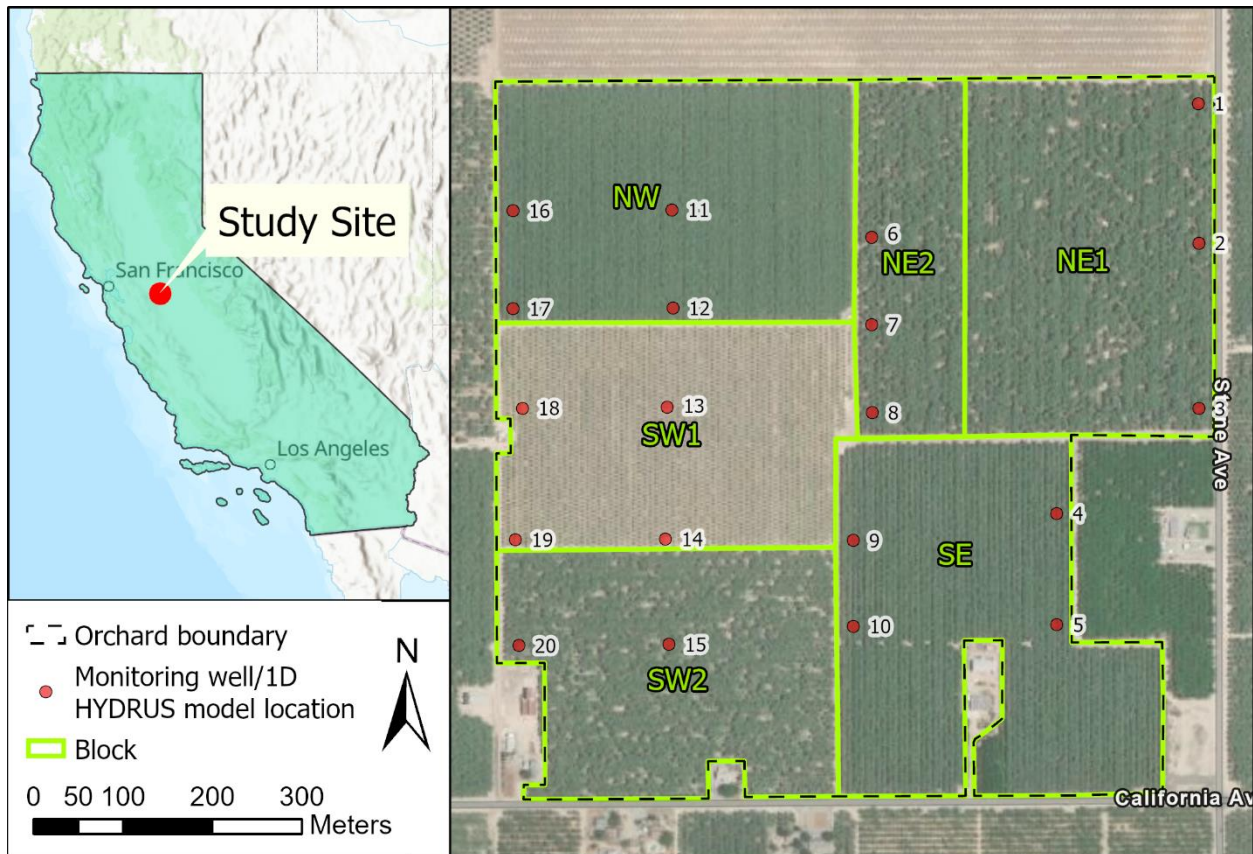
Figure 2-1. Site Location. *The 56-ha orchard is divided into six blocks: NE1, NE2, NW, SW1, SW2, and SE. Trees within a block are planted at the same time. As the blocks age, individual trees may be removed and replanted. The locations of the vadose zone model profiles are the same as the monitoring well locations.*

2.4.1 Water Fluxes

Nitrate is highly soluble and is transported to groundwater through soil moisture. Nitrate leaching predictions are therefore subject to movement of water through the vadose zone. Water inputs to the vadose zone water mass balance are precipitation and irrigation. Water outputs leaving the vadose zone are evaporation, transpiration, and deep percolation (i.e., recharge) to the water table. While evaporation and transpiration can be measured (see below data sources), deep percolation is a water output that cannot

be directly measured. One way to estimate recharge is to solve Richard's equation via a numerical model. Recharge is also estimated from the water mass balance according to Equation 2-1.

$$Recharge = Precipitation + Irrigation - Evaporation - Transpiration - \Delta Storage \qquad \text{(2-1)}$$

Because the simulated period spans several years with both wet and dry years, the net change in water stored in the vadose zone is assumed to be zero. Precipitation data is obtained from the nearest California Irrigation Management Information System (CIMIS) station (Modesto 71) located approximately 9 km west-northwest from the Site. Irrigation rates were based on the grower's records and ranged from 95-103 cm/year. For growing seasons 2020 and 2021 irrigation rates were logged with a computerized flow meter at the orchard. Evapotranspiration (ET) is estimated from the reference ET (ETo) measured at the same CIMIS station. ETo is evapotranspiration from a well-irrigated clipped grass and is converted into an estimate of ET for the almond orchard (ETc) by using a crop coefficient (Kc) (Equation 2-2). ETc is an estimate of potential crop ET under ideal growing conditions. Actual crop ET (ETa) may be equal to ETc but is typically lower if the crop water requirement is not met with precipitation and irrigation at the field. HYDRUS calculates ETa from the input ETc according to a water stress response function (see Section 2.4.3.2.1 **Water and Solute Uptake by Trees**).

$$ETc = ETo \times Kc \qquad \text{(2-2)}$$

The crop coefficient is specific to the day of the year, and the crop age and type. The crop coefficient for mature almonds by Doll and Shackel (2016) were used to calculate the ETc for mature almond trees. Almond trees are considered mature when they are at least 6 years old. The transpiration rates of young trees (less than 6 years since planting) are less than that of mature trees. Known replanting dates for the orchard blocks are presented in Table 2-1. For trees that were planted within the last 5 years, the crop

coefficients were proportionally reduced according to the age-corrected mid-season crop coefficient described in Drechsler et al. (2022).

For the numerical model, ET was split into its component evaporation and transpiration. Bellvert et al. (2018) found that the evaporation proportion of ET at a micro-sprinkler irrigated almond orchard decreases as the number of days since the last irrigation event increases. ET was scaled according to Bellvert et al. (2018): on the first day of an irrigation or precipitation event evaporation is 24% of the ETc after which it decreases linearly until reaching zero on the seventh day if no additional rainfall or irrigation has occurred.

Modeled ET predicted using the age-adjusted crop coefficients is compared to satellite-measured ETa data. The satellite-measured ETa data was obtained from the California Actual Evapotranspiration Mapping Program (CalETa; Paul et al. 2018). The CalETa dataset is a 30-m resolution dataset of daily ETa in California calculated from Landsat imagery combined with climate conditions measured at CIMIS stations and processed through a Surface Energy Balance System (SEBS; Su 2002). Daily ETa per orchard block is calculated as an average of the 30-m pixels in CalETa.

2.4.2 N Fluxes

Inorganic nitrogen compounds will readily convert to nitrate in the oxygenated soil of the root zone at the almond orchard. Nitrogen sources include fertilizer, atmospheric deposition, nitrate in irrigation water, and mineralization of nitrogen from decomposing organic matter. Nitrogen is removed from the soil as it is taken up through the roots of the almond tree, as well as through denitrification by microbes. Any remaining nitrogen in the soil may accumulate in the vadose zone, or it may potentially leach to groundwater with recharge. Like recharge, nitrate leaching rates also cannot be directly measured. Nitrate loss through leaching may be estimated from the nitrogen mass balance in Equation 2-3.

$$N\ Leached = Fertilizer + Atmospheric\ deposition + N\ in\ irrigation + Mineralization$$

$$- Root\ uptake\ for\ crop - Root\ uptake\ for\ tree\ growth \qquad (2\text{-}3)$$

$$- denitrification - \Delta Storage$$

Under constant management practices over several years, the net nitrogen accumulation in the soil profile is assumed to be zero.

The grower provided annual fertilizer records for the orchard blocks. Fertilizer is dissolved and delivered through the irrigation system. Fertigation records include the date, pounds of N applied per acre, and N source (UAN32 or CAN17). Total fertilizer application amounts per block are estimated by the grower based on expected yield early in the growing season (March) and updated following leaf analysis in April and May. Fertilizer application estimates account for residual N in the soil in spring. During growing seasons 2013-2017, six or seven fertigation events were performed per year, plus one fall application after harvest. During the HFLC treatment years, growing seasons 2018-2021, fertigation was performed approximately weekly throughout the growing season from March through July, plus a fall application, for a total of 15 to 19 fertigation events. The fertilizers used were primarily UAN32 and CAN17. Irrigation water provided by the Modesto Irrigation District is sourced from surface water and has a negligible nitrate content. Atmospheric deposition of nitrogen is assumed to be 20 kg N/ha/year due to the presence of confined animal facilities in the vicinity of the Site (Harter et al. 2017). Mineralization is an aerobic biological process in which microbes decompose organic matter and organic nitrogen into inorganic forms of nitrogen (ammonium, which readily converts to nitrate). Mineralization is estimated to add about 40 kg N/ha/year at the almond orchard (Brown 2010).

Nitrogen is taken up by the trees through roots and used to develop plant tissues that are harvested (kernels and hulls) and also for tree growth. The N uptake for tree growth varies with tree age and ranges from 30-65 lbs N/ac/year (Brown et al. 2020). The N content of the harvested kernels is

generally estimated as 68 lbs N/ 1,000 lbs. kernels yield (Brown et al. 2020). This ratio was used to estimate the N uptake for growing seasons 2013-2017 where the grower provided the annual harvest records in lbs kernels per block. For 2018-2021, the N content of the harvested kernels and hulls was found via laboratory analysis of harvest samples collected from the orchard. Denitrification is an anaerobic microbial process which converts nitrate into gaseous forms of nitrogen. Denitrification is estimated to account for a 5% loss of applied N within the root zone (Khalsa et al. 2020). Limited denitrification is expected below the root zone (1 m depth) (Harter et al. 2005; Onsoy et al. 2005).

2.4.3 Numerical Model Development

Unsaturated flow and nitrate transport in the vadose zone were modeled numerically in the software HYDRUS-1D (Simunek et al. 2013). The HYDRUS-1D model was adapted from a HYDRUS model previously developed for the site, as described in Gurevich et al. (manuscript in preparation). The model consists of 20 profiles described in Gurevich et al. (2021) which are modeled individually in HYDRUS-1D. Locations of the 20 profiles are spread throughout the orchard. The profiles are coincident with the locations of existing shallow groundwater monitoring wells. The profiles are discretized into 300 nodes spaced 2.3 cm apart for a total depth of 7 m below the ground surface.

The prior model was developed for a simulation period of 2013-2017, representing conditions before HFLC practices were implemented at the Site. Gurevich et al. (manuscript in preparation) found that it takes up to 15 years for forcing stresses at the surface to impact nitrate concentrations at the bottom of the profile. Because the goal is to model nitrate leaching reaching the water table (located at the bottom of the model at approximately 7 m depth), the model was extended backward into the past to include the 60-year period leading up to 2017. The first 60-year period is simulated assuming farming under fertigation practices used between 2013-2017. Note that farming practices prior to 2013 are not represented in this study. At some point prior to 2013, orchard irrigation methods switched from flood

irrigation to drip and micro-sprinklers, which would result in significantly higher recharge rates modeled in this study. Historic management practices at the orchard before 2013 were not considered in this study in order to model a clear water and nitrate flux signal through the vadose zone created over a hypothetical long-term by 2013-2017 management practices.

A second goal is to compare the nitrogen leaching impacts of 2013-2017 fertigation practices to those created by HFLC. So, the model period was extended forward to include conditions under HFLC during growing seasons 2018-2021 as well as 30 years into the future. The total simulation length is 90 years, including a 30-year warm-up, 30 years before HFLC, followed by 30 years with HFLC.

Almond tree productivity peaks at 15 years and declines thereafter; due to a decrease in productivity, orchard blocks are typically removed and replanted by 25 years of age. Once replanted, young trees take 3 to 4 years to mature enough to produce a commercially viable harvest. During the 90-year simulation period, trees would age, and almond orchard blocks would be replanted approximately every 15-25 years. Known replanting dates for the orchard blocks are presented in Table 2-1. Gurevich et al. (manuscript in preparation) found that because fertigation and irrigation is less efficient for young trees, tree age has a significant impact on water fluxes and nitrate concentrations leaving through the bottom of the profile. For this reason, the effects of tree aging on irrigation, transpiration, and fertilization rates are reflected in the model boundary conditions.

Initial conditions for soil moisture and nitrate concentration were determined by repeating growing season 2017 (a relatively wet year) until a steady state was reached (Gurevich et al. manuscript in preparation).

2.4.3.1 Boundary Conditions

Atmospheric boundary conditions were set at the top of the profile. Atmospheric boundary conditions include daily stresses from combined precipitation and irrigation, evaporation from the soil, and potential

transpiration from the trees, gathered for the growing seasons 2013-2021 (see Section 2.4.1 Water

Fluxes). To create a 90-year simulation, the 9 years of atmospheric data were cycled to fill in unknown

data before 2013 and after 2021. Historic climate data collected before 2013 were not used because the

irrigation rates should be matched to the climate. The nine years of climate data in the model included

both wet and dry years, with an overall climate drier than average during this period. During the 90-year

simulation period the trees age and are replanted every 25 years unless grower records or aerial imagery

indicated otherwise. Tree age is simulated by adjusting irrigation, transpiration, and fertilization rates.

Following communication with the grower at the Site, trees are removed in December of their 25th year

and replanted the following September (Table 2-1).

Table 2-1. Tree Replanting Dates by Orchard Block

	NE1	NE2	NW	SW1	SW2	SE
Starting age (years):	*(8)*	*(14)*	*(25)*	*(8)*	*(8)*	*(0)*
Profile no.	1,2,3	6,7,8	11,12,16,17	13,14,18,19	15,20	4,5,9,10
Block replanted	1976	1970	1959	1976	1976	1958
in September of	2002*	1996*	1985	2002*	2002*	1985
year:	2022*	2022*	2011*	2018*	2028	2010*
			2037	2044		2036

*Known replanting year based on grower records or aerial imagery

During the intermittent time, no additional irrigation or fertilizer is added to the block and

transpiration is zero. Transpiration was modified using an age-adjusted crop coefficient as described in

Section 2.4.1 Water Fluxes. Irrigation and fertilizer are adjusted to tree age by multiplying the mature

tree application rate by a factor listed in Table 2-2. The factor was determined based on irrigation and

fertilizer records provided by the grower for 2013-2021.

Table 2-2. Irrigation and Fertilizer Adjustment for Tree Age

Age of trees in block (years)	Irrigation adjustment factor	Fertilizer adjustment factor
1	0.5	0.36
2	0.5	0.36
3	0.75	0.45
4	1	0.75
5	1	0.75
6-25	1	1

During HFLC treatment in growing seasons 2018-2021, young trees in block SW1 received fewer fertigation events than mature trees. For this reason, the fertigation record for block SW1 from 2018-2021 was used for the fertigation of other young tree blocks in the model for HFLC years 2018-2047. The fertilizer mass applied per unit area is dissolved in a concurrent irrigation event. The upper boundary condition for nitrate solute transport is therefore a time-variable fixed concentration.

A constant head boundary of zero, representing the water table, was set at the bottom at 7 m depth. A zero-gradient condition was used as the lower boundary for nitrate solute transport.

2.4.3.2 Parameterization

2.4.3.2.1 Water and Solute Uptake by Trees

Root water uptake is modeled with the Vrugt et al. (2001) 1-D root distribution model coupled with Feddes et al. (1978) water stress response function. Baram et al. (2016B) found that 90% of the roots in an almond orchard are within a depth of 1m. The parameterization of the root distribution model was max rooting depth (z_m) of 1 m, max uptake depth (z^*) at 0.27 m, and a shape parameter, $p_z = 3$ (Vrugt et al. 2001). The root distribution was independent of tree age (root growth was not included). The water stress response function uses the deciduous fruit tree parameterization in the HYDRUS-1D desktop application ($h_1 = -10$ cm, $h_2 = -23$ cm, $h_{3max} = -500$ cm, $h_{3min} = -800$ cm, $h_4 = -8000$ cm). HYDRUS calculates actual transpiration based on the water stress and the potential transpiration. With compensated root water uptake, a root adaptability factor allows reduced water uptake in stressed parts of the root zone to be

compensated with increased uptake from other parts of the root distribution (Simunek et al. 2010).

Uncompensated root water uptake was found to result in modeled ETa less than the ETa measured

through CalETa remote sensing data for the Site; therefore, a root adaptability factor of 50%

compensation was used to bring the modeled and measured ETa closer together.

Nutrients used by the tree for growth and to produce a crop are taken up from the soil by the

roots. Nitrate uptake is modeled as passive uptake through the compensated root water uptake multiplied

by the dissolved nitrate concentrations, up to a certain maximum concentration ($cRoot_{max}$). Gurevich et al.

(manuscript in preparation) found $cRoot_{max}$ to range from 0.015 to 0.08 mg/cm^2 by fitting the 2013

cumulative nitrate uptake at profile 1 in the NE block to the almond tree nitrate demand curve. For this

study, the model $cRoot_{max}$ value was manually fit to 0.035mg/cm^2 to reduce residuals between field

measured and modeled total N uptake in all the blocks for growing seasons 2013-2021. Measured and

modeled N uptake was compared as a partial mass balance NUE_{growth} ratio between the total N uptake by

the roots and the applied fertilizer (Equation 2-4). Measured N uptake is estimated from the N content of

harvest yields. N uptake for tree growth ranges from 34-73 kg/ha (30-65 lb/ac) and depends on the tree

age (Brown et al. 2020). HYDRUS does not differentiate between N used towards the crop or tree growth.

$$NUE_{growth} = \frac{N_{crop} + N_{growth}}{N_{fertilizer}} \qquad (2\text{-}4)$$

2.4.3.2.2 Soil Hydraulic Parameters

Soil texture for twenty 7m-deep profiles located throughout the orchard was visually described using

standard soil textural field analysis at a spatial resolution of 1 cm. Laboratory textural analysis was

performed in 30 cm increments as described in Gurevich et al. (2021). A total of 19 soil textures were

identified, ranging from clay and loamy mixes to coarse sand. Ranges of likely values for the soil

hydraulic parameters (K_s, n, α) of the 19 soil textures were estimated by Gurevich et al. (2021), using the

Rosetta3 (Zhang and Schaap 2017) pedotransfer function. Parameter sets with unique parameter values were generated by Latin hypercube sampling within the ranges for each soil texture (Herman and Usher 2017). Monte Carlo simulations were performed using randomly selected parameter sets to incorporate parameter uncertainty in the model predictions. Gurevich et al. (manuscript in preparation) found that the distribution of model results plateaus quickly after 10 to 50 Monte Carlo simulations; there was little change in the coefficient of variation of water fluxes at the bottom of the profile using 100 or up to 200 simulations. For that reason, Monte Carlo simulations for 22 unique soil hydraulic property parameter sets were performed.

2.4.4 Analysis of Model Data

Model performance is evaluated by comparing model results to the water and N mass balance estimates for groundwater recharge, N leaching, and overall NUE during growing seasons 2013-2021. Monte Carlo simulations were averaged for individual profiles or for profiles within the same blocks. The standard deviation and the 5th and 95th percent quantiles (90% confidence interval) across the simulations were used to evaluate the impact of parameter uncertainty on model results. Model recharge and N leaching are summarized as monthly and annual water and N mass fluxes at the bottom of the model. N mass fluxes at the bottom boundary are equivalent to the water flux multiplied by the nitrate concentration at the boundary. Mass balance groundwater recharge and N leaching are calculated according to Equation 2-1 and Equation 2-2 in Sections 2.4.1 Water Fluxes and 2.4.2 N Fluxes. NUE is calculated by block every year using cumulative annual amounts according to Equation 2-5.

$$NUE = \frac{Output}{Input} = \frac{N_{crop} + N_{growth} + N_{denitrification}}{N_{fertilizer} + N_{atm.dep.} + N_{mineralization}} \qquad (2\text{-}5)$$

The impact of HFLC on N leaching was then evaluated by comparing modeled and mass balance estimates of NUE, modeled nitrate leaching concentrations and N leaching rates before and after switching management practices.

2.5 Results

First, the mass balance results are presented in Section 2.5.1 Mass Balance Results Section 2.5.2 Model Results presents the modeled water and N fluxes.

2.5.1 Mass Balance Results

2.5.1.1 Water Fluxes

Groundwater recharge was estimated for 2013-2021 using precipitation, irrigation, and ET mass balance (Figure 2-2). Average annual precipitation from 2013-2021 was 27 cm. The wettest year was water year 2017, with 45 cm of precipitation. Water year 2021 was the driest with 14.5 cm of precipitation. Irrigation was applied at a rate of 90-100 cm/year to mature orchard blocks. The average ET was 123 cm/year.

Annual Water Mass Balance
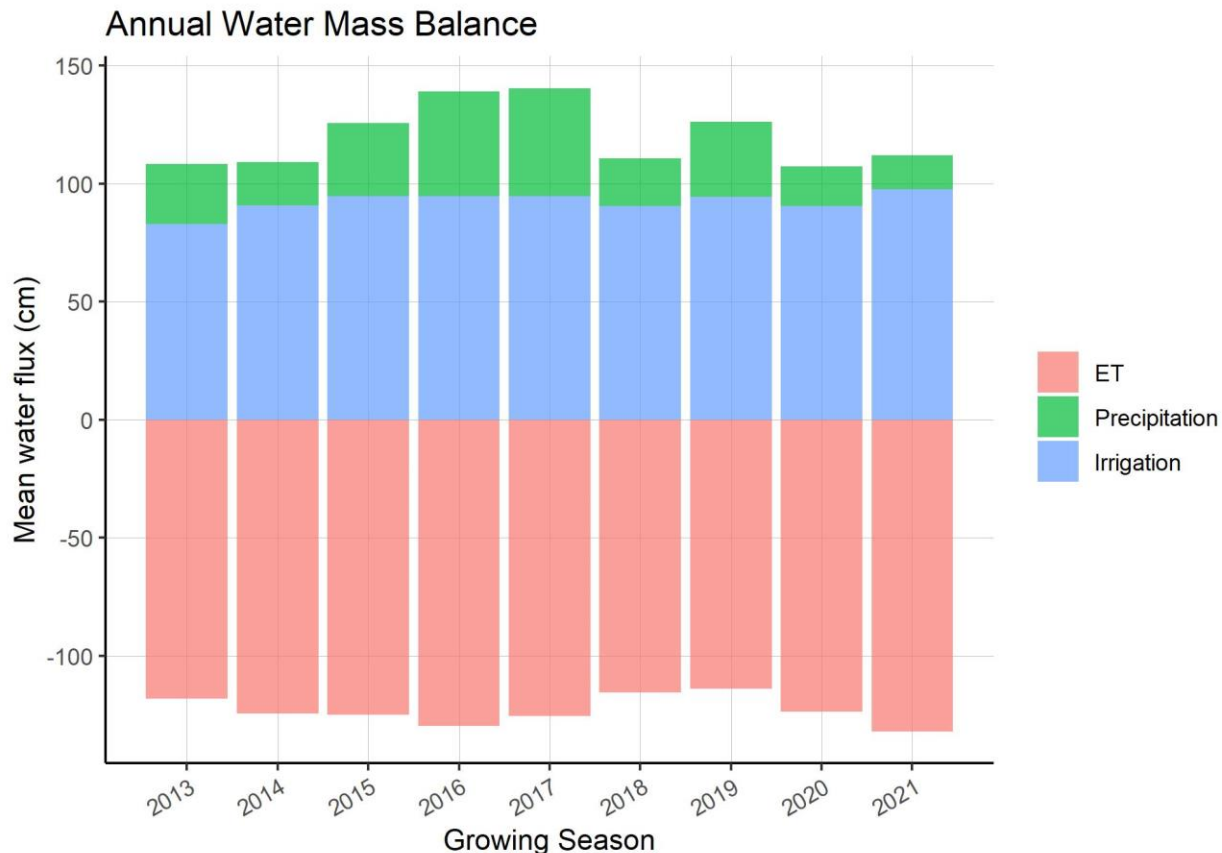
Figure 2-2. Annual Water Mass Balance. *The measured water mass balance for each growing season*

consists of precipitation and irrigation inputs, and ET output. Groundwater recharge is also an output from

the water mass balance (not shown) and is calculated from the difference between the inputs and outputs.

The net annual water mass balance was positive for wet years (2016, 2017, 2019) and negative

for dry years (2013-2015, 2018, 2020, 2021); see Figure 2-3. A net positive water mass balance may be

interpreted as the amount of water recharged to groundwater. During 2017 (the wettest year), the net

water mass balance was +15 cm. A net negative water balance indicates overall drying in the soil profile.

The overall annual average water mass balance was close to zero (-3 cm). This is an indication that the

climate is dry, and that the orchard is irrigated efficiently. Higher net positive water fluxes in blocks with

young trees (20 to 40 cm) indicate young trees are irrigated less efficiently. The net water mass balance during the dry years ranged from -10 cm to -20 cm.
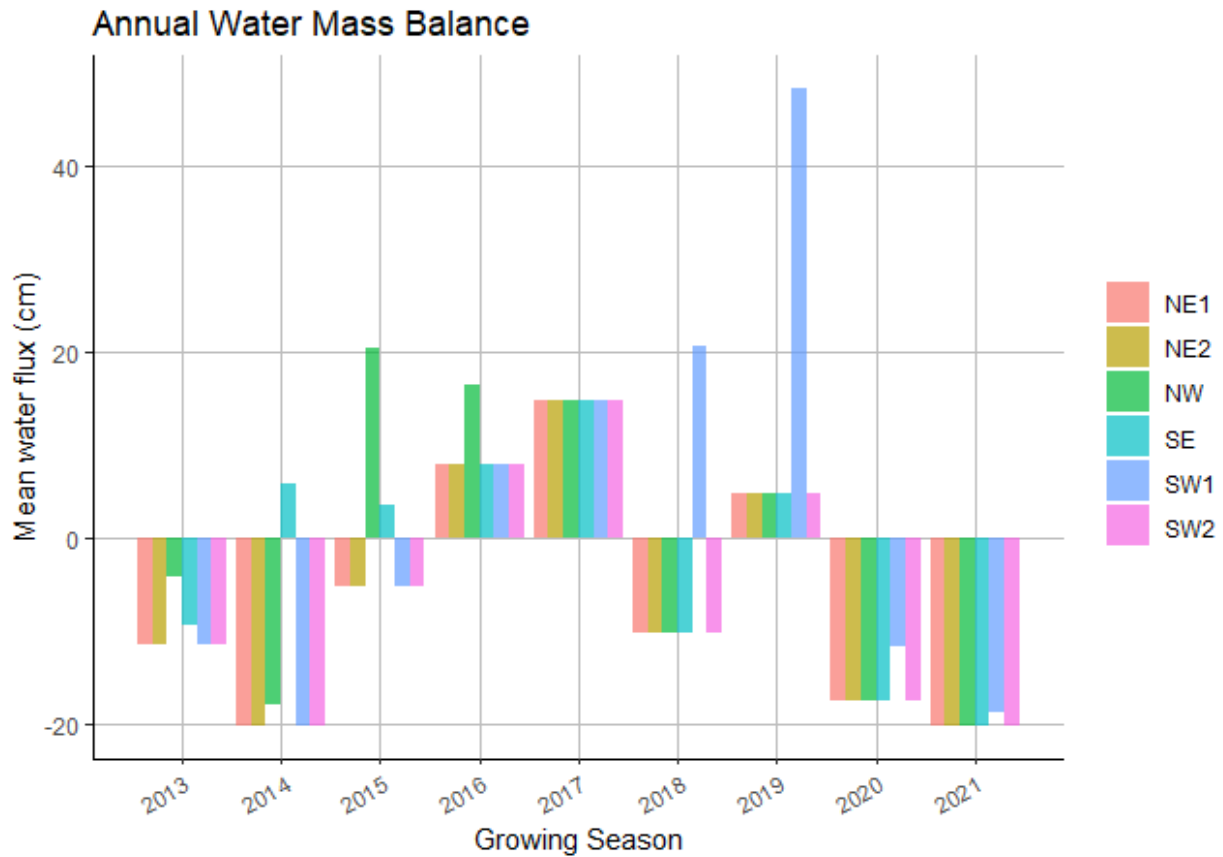
Figure 2-3. Annual Water Mass Balance: Net Water Flux. *The net water flux is the difference between the measured water inputs (precipitation and irrigation) and outputs (ET) and represents groundwater recharge. Positive net flux indicates net recharge, and negative flux represents net drying. The water mass balance is calculated annually individually for the six orchard blocks.*

Dry years with a net negative water balance still have periods of recharge during the rainy winter and at times when irrigation rates are higher (Figure 2-4). Monthly water mass balance computations suggest that recharge occurs during the months of October through April and sometimes in July. Monthly water mass balance shows recharge rates of approximately 5 cm/month during wet periods. Even during

the driest year, 2021, the average recharge rate during the winter was 3 cm/month. The cumulative winter

recharge each year averaged 24 cm during the period 2013-2021, with annual rates ranging from 8 cm in

2020 to 44 cm in 2017 (Figure 2-5). These mass balance estimates do not account for changes in water

storage in the soil and deep vadose zone that occur seasonally between summer and winter, and over

longer timescales between wet and dry years. The net annual water balance estimate represents a low-end

approximation of recharge from zero to 15 cm, whereas the cumulative monthly water balance represents

the high end of estimated recharge ranging from 8 cm to 44 cm.
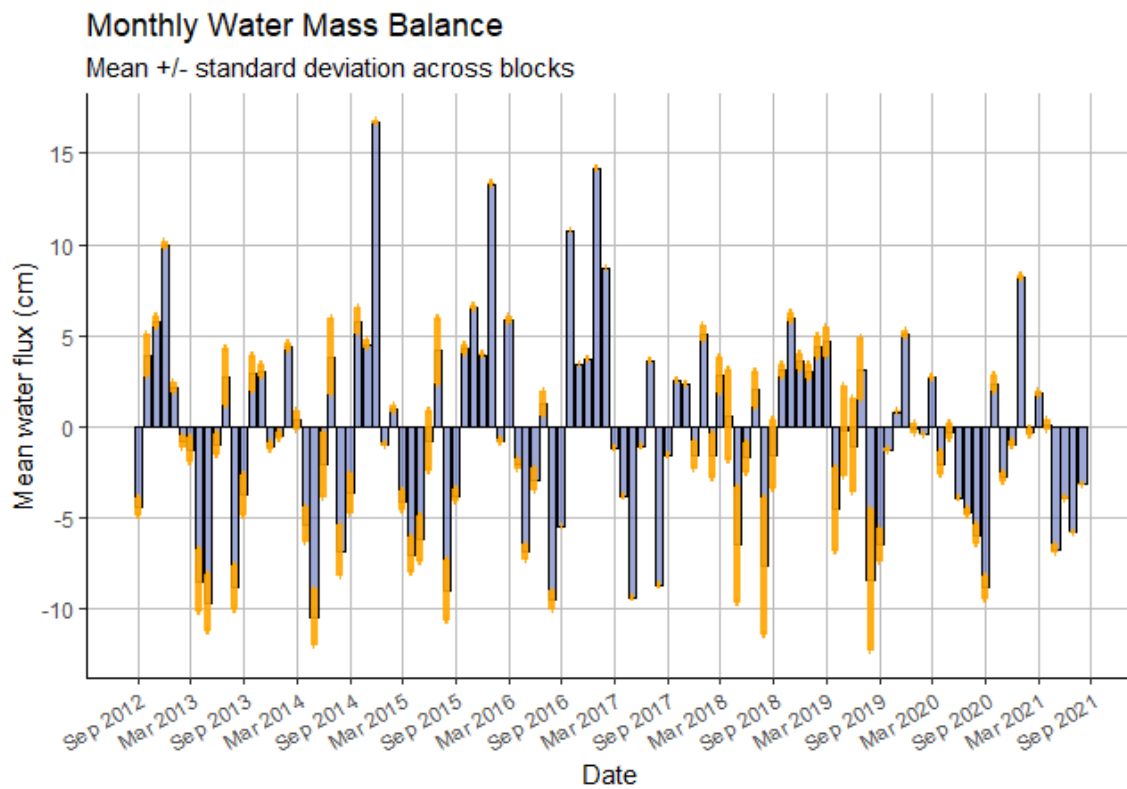
Figure 2-4. Monthly Water Mass Balance. The net water mass balance calculated on a monthly basis. The

net water flux is averaged across the six orchard blocks (blue). Variability in the water mass balance

across the orchard blocks is shown in orange as +/- one standard deviation from the mean. The monthly

water mass balance indicates every year there are months with a positive net water flux (recharge),

regardless of whether the annual net water flux is positive or negative.

Total Average Annual Recharge
from monthly water mass balance
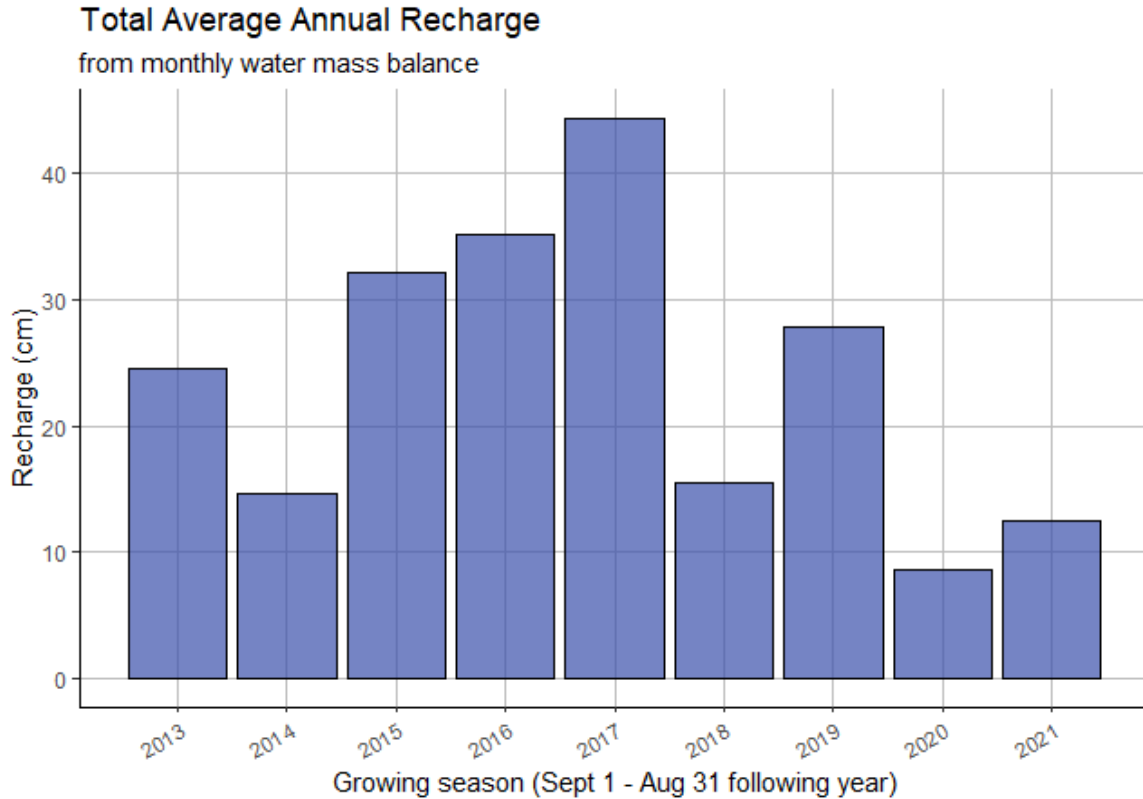
Figure 2-5. Total Annual Recharge from Monthly Water Mass Balance. The monthly water mass balance is used to estimate total recharge during the growing season by summing only months with positive net water flux. While useful for estimating recharge from the water mass balance during net drying years (2013, 2014, 2020, 2021), this method is likely to overestimate recharge.

ET rates estimated for the orchard are likely to introduce at least 10-30% error in the water mass balance (Allen et al. 2011). With average ET >100 cm/year, this introduces an uncertainty of 10-30 cm in the water mass balance. The overall impact is that the absolute magnitude of ET uncertainty is larger than the amount of recharge predicted by the water mass balance (Healy 2010).

Despite uncertainty in ET, the ETc predicted with the crop coefficient was close to actual ET data (ETa) collected via remote sensing satellite. The tree age-adjusted ETc was on average within 34% of the satellite-collected ETa. Satellite-collected ETa is also subject to its own sources of error, expected to be

around 10-20% (Allen et al. 2011). The tree age-adjusted crop coefficient used in this study was particularly successful at fitting the ETc to the ETa. The average difference between ETc and ETa in the youngest block of trees in 2013 (NW; 1 year old) until the time the trees matured at 5 years old was even less than the average difference for the entire orchard (4% as opposed to 6%) (Figure 2-6). It is expected that actual ET at the orchard is lower than the ET predicted with the crop coefficients, because this is calculated as a potential ET under pristine growing conditions (Allen et al. 2005). ETc was on average 6% higher than the ETa.
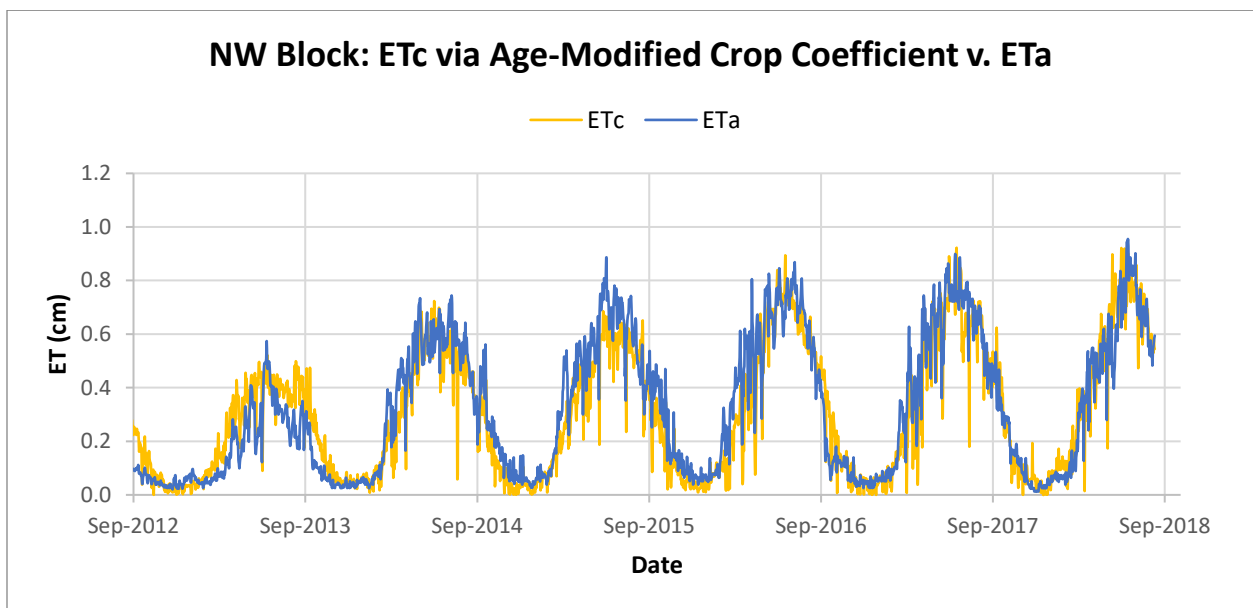
Figure 2-6. ETc vs. ETa for NW Block. *ETc is calculated using the age-adjusted crop coefficient (k_c) multiplied by the reference ET measured at the nearest CIMIS station (ETo). ETa is the actual ET as measured via satellite. The NW block was 1 year old in September 2012. There is less ET when the trees are young. By the time the trees are 5 years old the trees are mature, and ET stabilizes.*

2.5.1.2 N Fluxes

N leaching was estimated for 2013-2021 using fertilizer application rates, harvested yields, as well as estimates of atmospheric deposition, N uptake for tree growth, and mineralization and denitrification in

the soil. (Table 2-3). Fertilizer application rates for mature tree blocks ranged from 186-302 kg/ha (234

kg/ha average) and was based on meeting the N demand for the yield estimated and updated throughout

the growing season (Figure 2-7). On average the yield was 2,275 lbs kernels/acre, equivalent to a N

uptake of 175 kg/ha. The highest yield was in 2020. The yields of the mature tree blocks under HFLC in

2018-2021 were on average 16% more than the yields in 2013-2017, regardless of unusually low yields in

2019 due to crop-damaging weather conditions that spring.
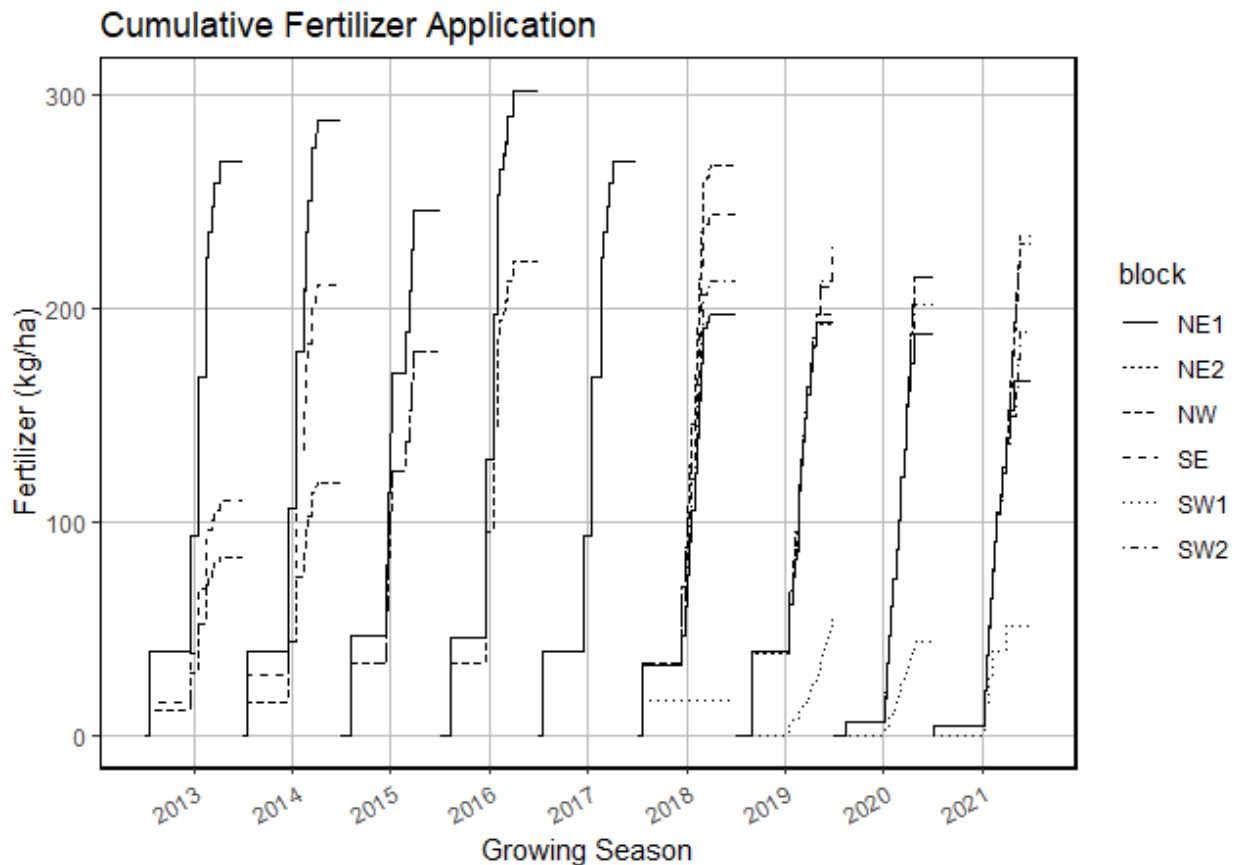
Figure 2-7. Orchard Fertilizer Application Rates. Cumulative fertilizer application throughout the growing season is displayed. Blocks with younger trees require less fertilizer such as in 2013 and 2014. Starting in the 2018 growing season, fertilizer was applied in smaller, more frequent applications, resulting in a less jagged curve. Adaptively managing fertilizer applications throughout the growing season resulted in less fertilizer necessary since the 2018 growing season.

HFLC management resulted in higher kernel yields even though fertilizer application rates under HFLC were on average 15% lower than before in 2013-2017. This is also reflected in the NUE. Using the complete mass balance, the overall average NUE of the mature blocks from 2013-2021 was 80%. With the partial mass balance, NUE_{growth} was 96%. Average NUE of the mature orchard blocks from 2013-2017 was 75% (NUE_{growth} = 88%). Under HFLC from 2018-2021 the average NUE was 85% (NUE_{growth} = 106%). NUE of the young tree blocks was much lower, as low as 27% for the NW block and 31% for SW1 after their first harvests. The increase in both NUE and NUE_{growth} in the mature tree blocks under HFLC was statistically significant with the two-tailed Welch's t-test (p-value < 0.05). In 2020 the NUE was >100% for the NW and SE blocks. Due to the poor growing conditions in 2019, the NUE >100% may be caused by some unused N from 2019 remaining in the root zone being taken up by the roots in 2020. Overall, orchard-wide increases in N efficiency reflect a decrease in N losses from 25% to 15% of the applied N, which translates to a ~40% decrease in N leaching.

Table 2-3. Measured Annual N Mass Balance Summary

	N Mass Balance (average lbs/acre)	*Pre-HFLC*					*HFLC*			
		2013**	*2014*	*2015*	*2016*	*2017**	*2018**	*2019**	*2020**	*2021*
HARVEST	Kernels	2,950	2,189	2,100	2,063	2,312	2,600	1,882	3,133	2,174
		±184	±691	±339	±180	±320	±406	±266	±615	±885
INPUT	Fertilizer	240	217	200	243	240	207	185	182	177
	Atmospheric deposition	18	18	18	18	18	18	18	18	18
	Mineralization (40 kg/ha)	36	36	36	36	36	36	36	36	36
OUTPUT	Crop uptake	201	149	143	140	157	177	128	213	127
	Tree growth	36	46	46	43	41	37	35	35	40
	Denitrification	12	11	10	12	12	10	9	9	9
SUMMARY	NUE_{growth}	0.99	0.90	0.95	0.75	0.83	1.03	0.88	1.36	0.94
	NUE	0.85	0.76	0.78	0.66	0.72	0.86	0.72	1.09	0.76
	GW Losses	45	65	55	101	83	36	66	-22	55

Note: NUE_{growth} is a partial mass balance while NUE is the full mass balance.
*Does not include young block SW1
**Does not include young blocks NW or SE

Nitrate leaching is estimated from the annual mass difference in N inputs and outputs (Figure 2-8). N leaching across the orchard blocks ranged from 145 kg/ha/year to less than zero. The highest N leaching rates were observed in 2016 and the lowest in 2020. An apparent N leaching rate less than zero (observed in the NW and SE blocks in 2020) results from high NUE. In that case the actual N leaching is assumed to be zero. The orchard-wide average N leaching rate from 2013-2021 weighted according to the area of the blocks was 57 kg/ha/year. The average N leaching rate from 2013-2017 was 67 kg/ha/year while under HFLC from 2018-2021 it was a third as much—45 kg/ha/year. Considering the leaching rates from just the mature tree blocks, average leaching rates are approximately 70 kg/ha/year and 34 kg/ha/year before and after switching to HFLC. This mass balance suggests a decrease in N leaching from the orchard of around 33-50%, depending on the tree age.
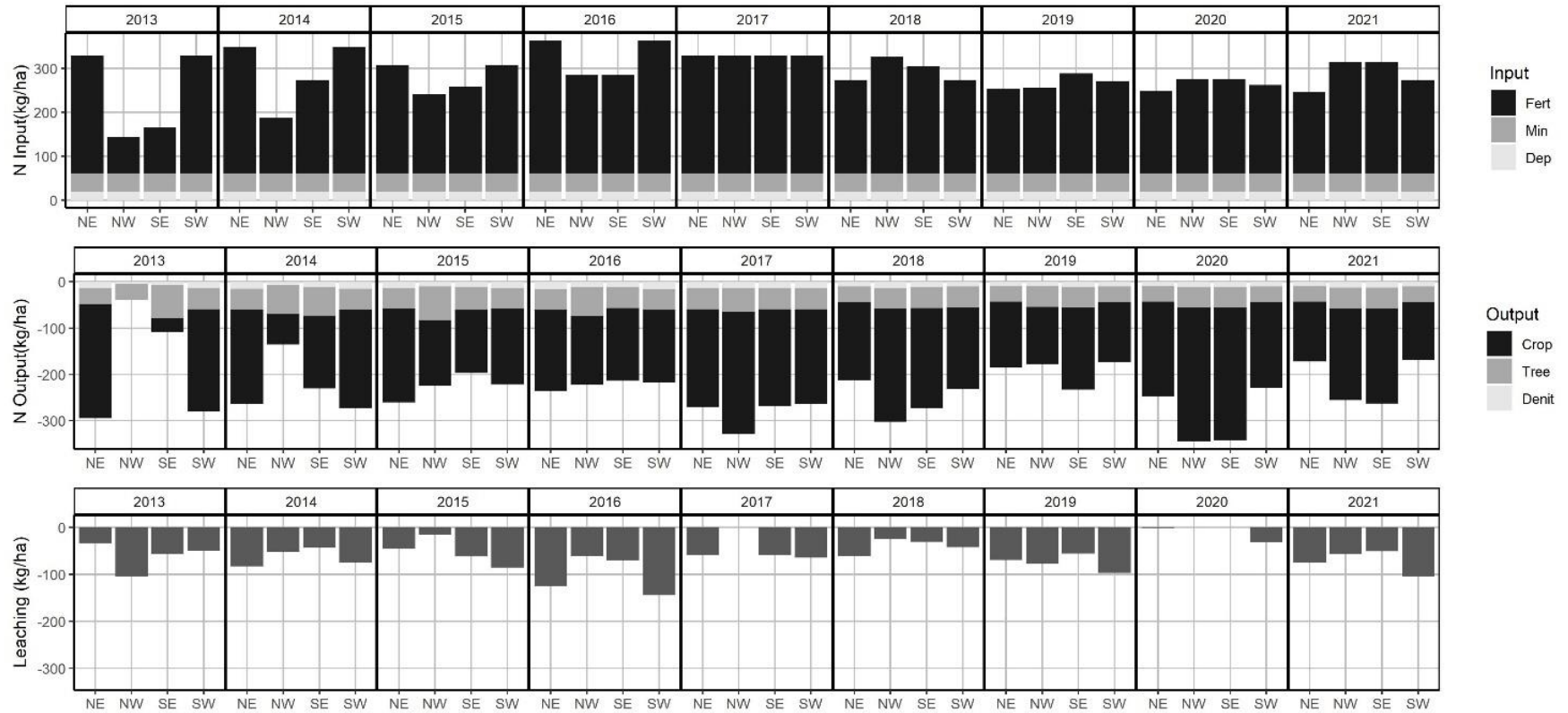
Figure 2-8. N Mass Balance Summary. *The N mass balance inputs are fertilizer (fert), mineralization (min), atmospheric deposition (dep). The outputs*

are N uptake in the harvested crop (crop), N uptake for tree growth (tree), denitrification (denit), and leaching to groundwater. Leaching is calculated

from the difference between the N inputs and outputs. In this figure the NE1 and NE2 blocks are combined, as well as the SW1 and SW2 blocks. Because

the trees were young there was no harvest recorded for SW1 2018-2020.

2.5.2 Model Results

Water and solute mass balance errors for the model runs were less than 1% as reported by HYDRUS.

Simulation runtime is approximately two minutes on a 2.9 GHz processor with 16 GB of RAM. Over the

20 profiles, 440 simulations were performed using 22 parameter sets, for a total runtime of 15 hours. Non-

converging parameter sets were removed, with 16-22 simulations converging per profile.

2.5.2.1 Water Fluxes

Precipitation and irrigation in the model were the same as used in the mass balance, discussed in Section

2.5.1.1 Water Fluxes. Because HYDRUS calculates actual ET based on potential ET and water stress,

modeled ET is less than the potential ET, which was derived from the crop-coefficient and reference ET.

Despite using 50% compensated root water uptake, modeled ETa is less than the satellite-measured ETa.

Overall, the modeled ETa is 92% of the measured ETa (Figure 2-9). However, the modeled ETa is within

the estimated error range of 10-20% for remote sensing energy balance (Allen et al. 2011). If the model

ETa is lower than the real ETa, then the reduced root water and nutrient uptake results in biased high

recharge and N leaching estimates.
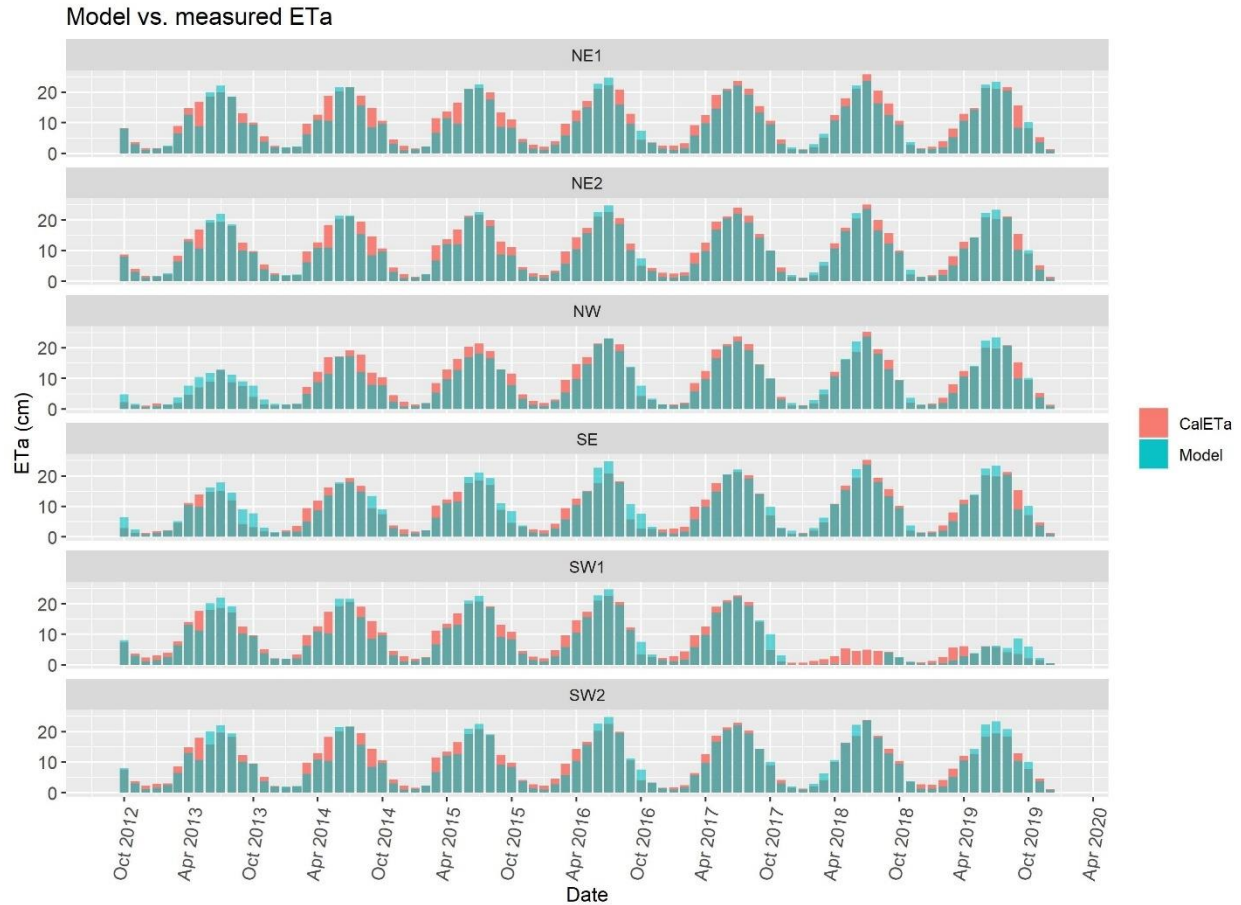
Figure 2-9. Model vs. Measured ETa. *The model reduces the potential ET (ETc) according to water stress, producing the model ETa. This is compared to the satellite-measured ETa across the orchard blocks during the model period. Assuming the satellite measured ETA data is more accurate, the model tends to underestimate ET during the spring and fall, but slightly overestimates ET during the peak month of July.*

Modeled recharge rates are calculated as the water flux just above the water table depth at 7 m. Between 2013 and 2021, modeled recharge rates for the orchard ranged from less than 1 cm/year (2021) to approximately 20 cm/year in 2017 (Figure 2-10). The modeled average recharge rate, evenly weighted across the 20 profiles spanning the orchard, was 7 cm/year. Variability in annual recharge rates between mature orchard blocks within a given year was low (standard deviation = 1.3 cm). Young orchard blocks had higher recharge rates, even during dry years (such as SW1 block in 2019 and 2020). Though

irrigation rates for young trees are lower (in 2019 and 2020 SW1 block received 50-75% of the water received by the other blocks), less efficient water uptake results in more recharge overall. The mass balance model predicted 20-45 cm/year recharge in the SW1 block for the 2018 and 2019 growing seasons. The numerical model predicts similar recharge rates of 20-35 cm/year in the SW1 block, but delayed by a year (2019 and 2020 growing seasons). This is most likely because the mass balance model does not consider changes in storage and in the numerical model the water must physically traverse the 7 m vadose zone to recharge groundwater.
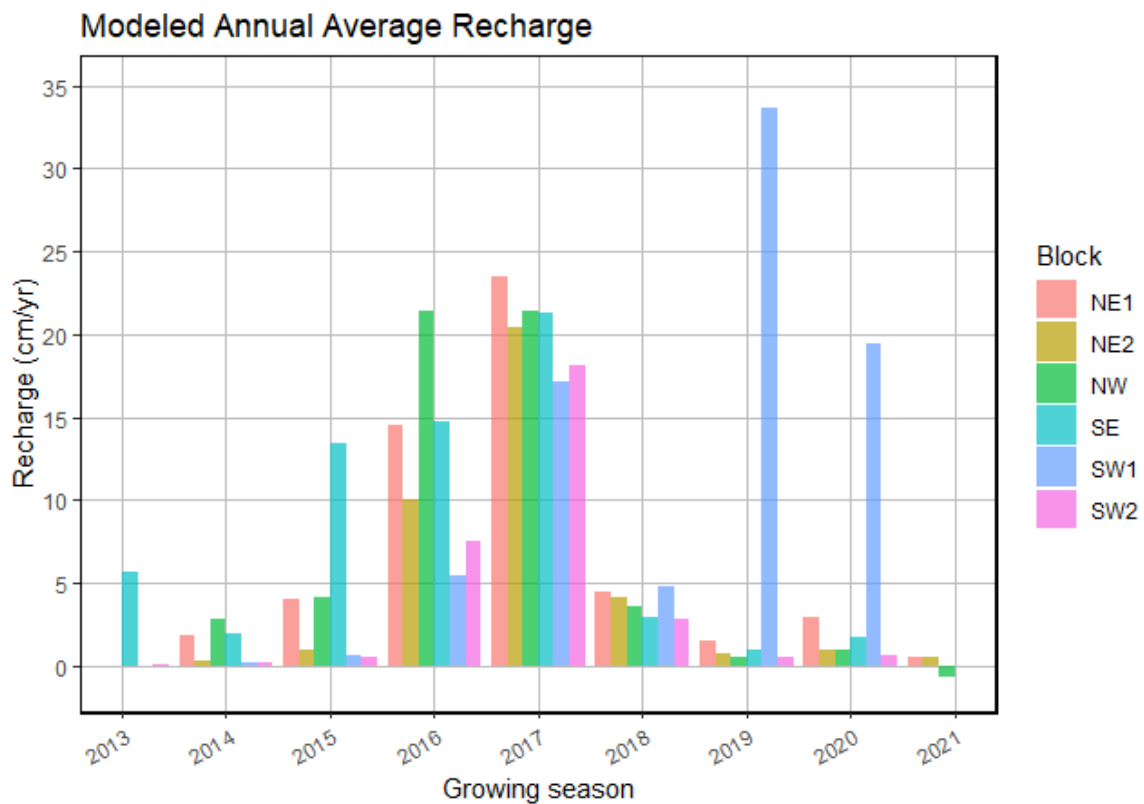
Figure 2-10. Modeled Annual Average Recharge. The model recharge is calculated from the cumulative annual water flux leaving the bottom of the soil profile (7 m depth) in the vadose zone model. Typically, net downward fluxes are predicted in the model, even during exceptionally dry years. Water uptake in young tree blocks is less efficient, resulting in higher recharge rates (SW1 block in 2019 and 2020), despite only receiving 50-75% of irrigation applied to mature tree blocks.

During wet to average years, the highest recharge rates generally occur during April-August and are typically 1-5 cm/month (Figure 2-11). In dry years, the lowest recharge rates occur during this period. During dry years monthly recharge rates are <0.1 cm/month. During the driest periods, profiles in the NW block exhibited small (<0.1 cm/month) upward water fluxes at 7 m depth. Recharge rates in young tree blocks are like a wet year in the mature blocks (1-5 cm/month), regardless of whether it was a wet or dry year.

Hydraulic parameter uncertainty had less impact on the modeled water fluxes than the geologic differences between the profiles. The average coefficient of variation (CV) of annual recharge among the simulations for an individual mature block profile during 2013-2021 was 0.85. The CV of the average annual recharge across the 20 profiles was 1.19, demonstrating that the sediment heterogeneity has a bigger impact on recharge than the hydraulic parameter uncertainty.
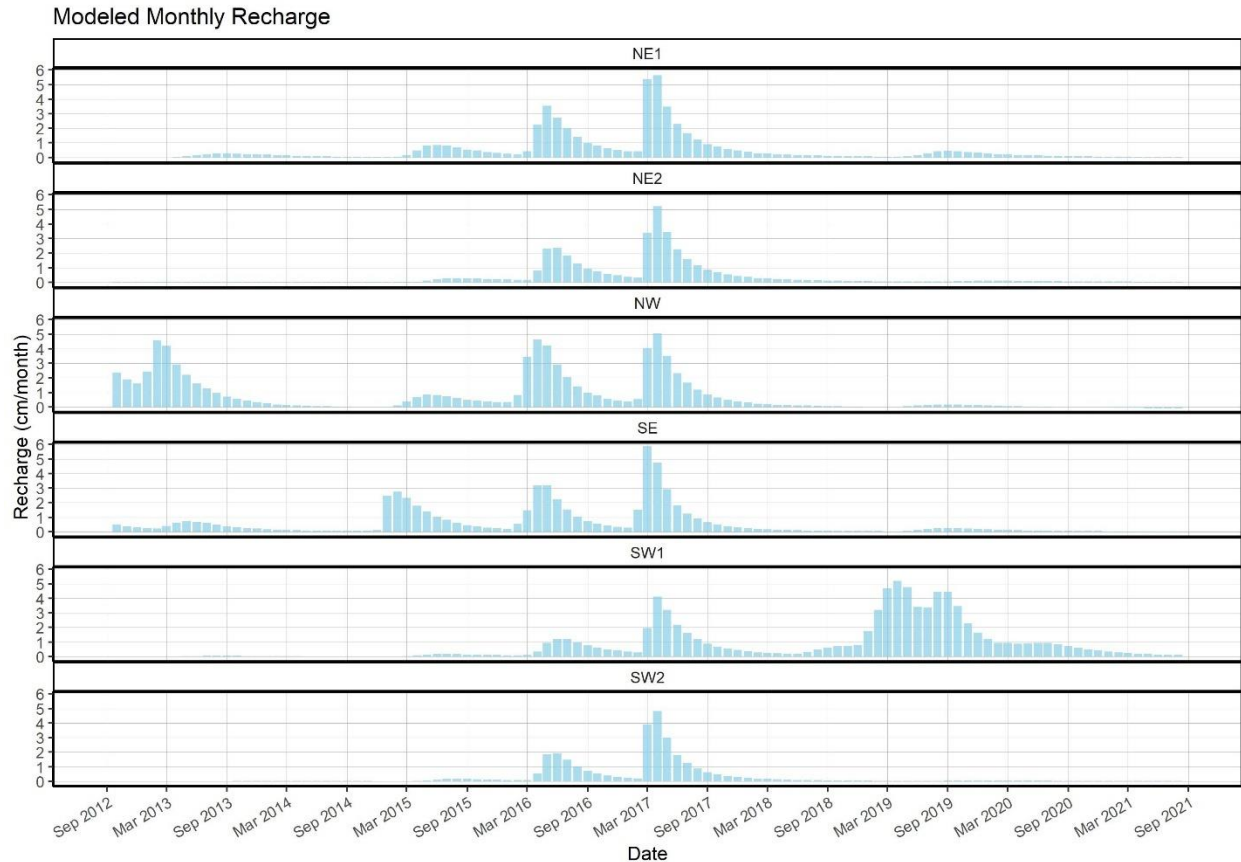
Figure 2-11. Modeled Monthly Recharge. *Modeled monthly recharge is calculated from the cumulative monthly water flux leaving the bottom of the soil profile (7 m depth) in the vadose zone model. During wet years the peak monthly recharge rates are of the same order of magnitude across the orchard. Recharge rates are higher in the NW and SE block in 2013, and in the SW1 block in 2019 because the trees are young and are irrigated less efficiently than the rest of the orchard.*

2.5.2.2 N Fluxes

The nitrate concentration in water flux exiting the bottom of the twenty soil profiles represents the nitrate concentration in groundwater recharge across the orchard (Figure 2-12). It takes 12-20 years for surface forcing to impact the modeled nitrate concentration of porewater arriving at the water table. Variation in delay time is due to differences in the profile geology. Nitrate breakthrough at the bottom of the profile exhibits an oscillating pattern following the period of tree replanting (25 years). Nitrate concentrations

increase up to 80-150 mg/L as trees mature and decrease to 20-50 mg/L after replanting. Efficient irrigation of mature trees leads to lower water fluxes, and, hence, higher nitrate leaching concentrations; meanwhile, young trees with higher water fluxes due to inefficient irrigation, and lower N applications, cause nitrate concentrations roughly half that of mature trees. Modeled nitrate concentrations within the same orchard block vary by up to 50-80 mg/L across profiles at the same timestep (standard deviation = 16.8 mg/L). This simultaneous inter-block variability in nitrate leaching concentration is due to differences in sediment structure between the profiles. The profiles within the same block receive the same water and fertilizer treatments and are otherwise identical. Spatial variability in nitrate concentrations leaching from the vadose zone within a block may be just high as orchard-wide spatial variability in nitrate leaching concentrations.

Over the 90-year simulation period, there were no significant differences between the cumulative N fluxes through the 20 profiles. This is to be expected because the long simulation time results in pseudo steady-state conditions. However, N fluxes over short periods of time (on the order of one to 10 years) varied between profiles depending on the sediment structure of the profile. For example, the steep slope in concentration in profile 7 in the NE2 block (Figure 2-12) demonstrates a quick response to stresses at the surface. The highest N flux rates were also modeled in profile 7. This is explained by the high fraction of coarse sediment in profile 7. More sandy soils were logged in profile 7 compared to the other profiles.

Modeled nitrate concentrations in groundwater recharge are summarized across the orchard for the twenty profiles (Figure 2-13). The orchard average nitrate concentration in recharge increases steadily for 30 years, following a 15-year delay from the beginning of the simulation. The average concentration plateaus at 75 mg/L for the next 25 years (1972-1997). During this period, 90% of the modeled porewater nitrate concentrations at the bottom of the vadose zone are between 30 mg/L and 110 mg/L. Around 10 years after the switch to HFLC management (2027), simulations indicate that

average nitrate concentrations in recharge will begin to decrease. They will continue to decrease for the next 20 years (2027-2047) throughout the remainder of the simulation. At the end of the simulation (the 90th year, 2047) the average nitrate concentration in recharge is 45 mg/L and is still rapidly decreasing. The switch to HFLC management results in a 40% reduction in the concentration of nitrate leaching from the vadose zone over a period of 30 years and more.
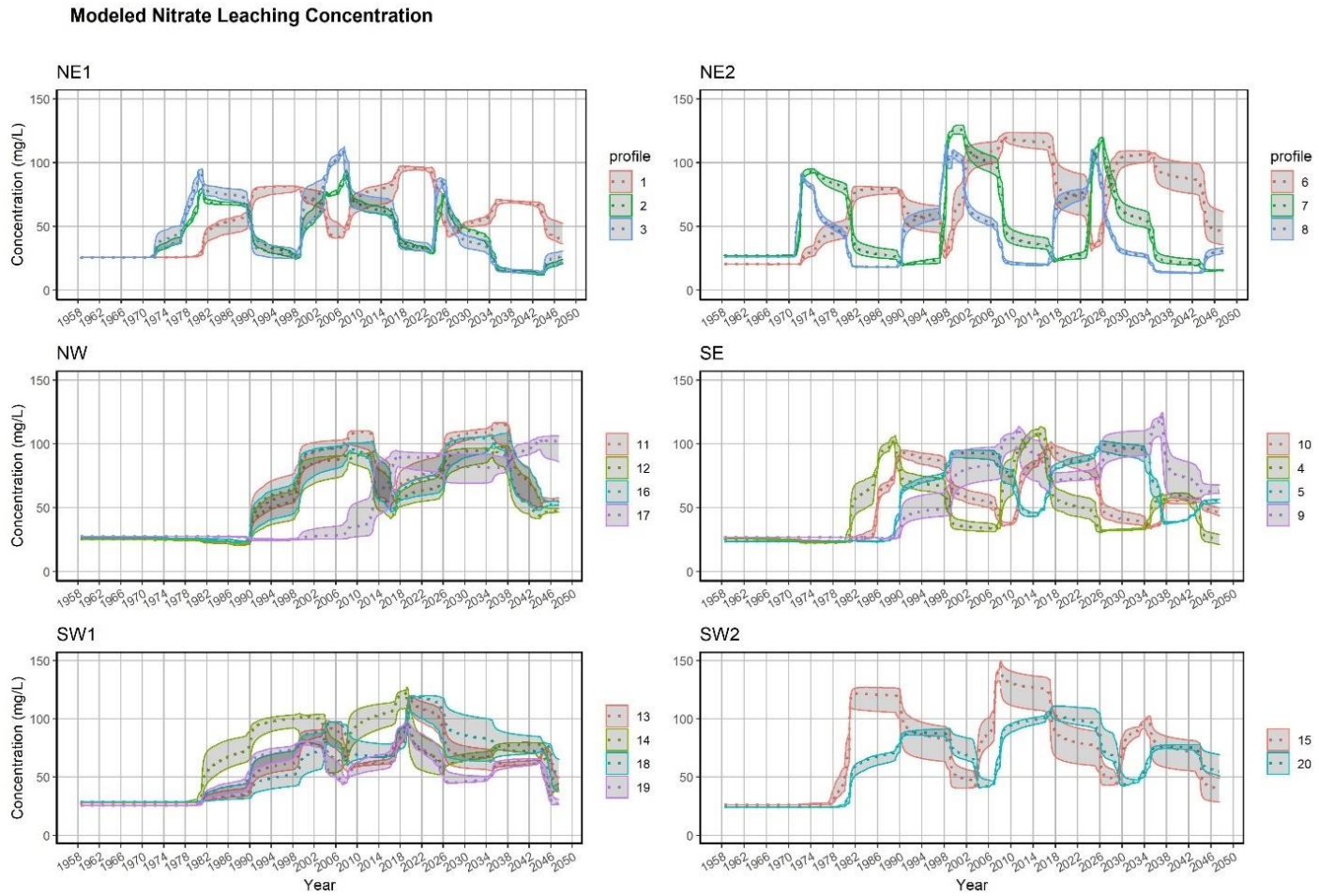
Figure 2-12. Modeled Nitrate Concentrations Leaching from Vadose Zone. *The modeled nitrate leaching concentration is the concentration of nitrate in water leaving the bottom of the vadose zone. The modeled average nitrate concentration across the Monte Carlo simulations with different hydraulic parameter values is presented for the soil profiles as a dotted line. The 90% confidence interval of the simulated values is shaded in gray.*

Modeled Average N Concentration in Recharge
across 20 Profiles
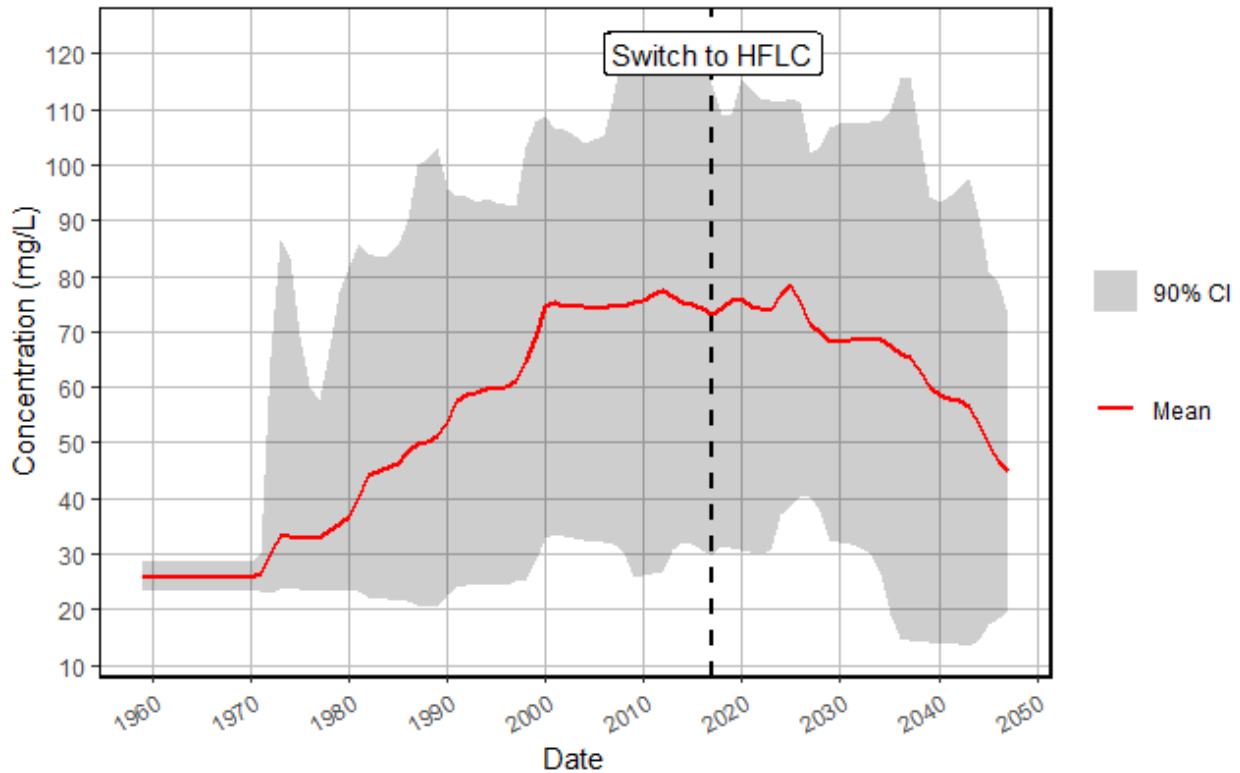
Figure 2-13. Orchard Summary of Modeled Nitrate Concentrations in Groundwater Recharge. The modeled nitrate concentration in groundwater recharge for the twenty profiles and the Monte Carlo simulations is averaged (red line), representing the orchard-wide average nitrate concentration in groundwater recharge. The shaded gray area includes 90% of the range of modeled concentrations. The shaded area mostly represents spatial variability in nitrate leaching, rather than hydraulic parameter uncertainty, which was comparatively small.

The total mass of nitrate leaching to groundwater depends on both the volume of recharge and the nitrate concentration in the recharge. Because leaching rates are closely tied to recharge, leaching rates during dry years are lower than wet years or after a tree replanting. Leaching rates predicted by the model are assessed at the water table (7 m depth). Modeled annual leaching rates at the water table below mature tree blocks range from 1-10 kg/ha/year during dry years to 40-200 kg/ha/year during wet years (Figure 2-

14). Less efficient irrigation of young trees results in a pulse of water flushing accumulated nitrate to the water table. The first year after trees are replanted, N leaching rates at the water table are higher, around 200 kg/ha/year and up to 340 kg/ha/year for some locations. Despite young trees receiving less than half the fertilizer of mature trees, the mass of N leaching under young trees is two or three times the amount of N applied in fertilizer during those first years of planting, which is an indication that an accumulation of excess N in the soil profile is being flushed out. The overall modeled N leaching rate at the water table during 2013-2021 was 50 kg/ha/year. N leaching rates in model years 2002-2017 were selected to represent pre-HFLC conditions, while 2032-2047 represent N leaching after the switch to HFLC. Before HFLC, average N leaching rates were approximately 55 kg/ha/year; after the switch to HFLC the average leaching rate decreased to approximately 40 kg/ha/year. The numerical model suggests that over time, HFLC will result in at least a 28% decrease in N leaching.

Figure 2-14. Modeled Annual N Fluxes. *Cumulative annual N fluxes include inputs: fertilizer plus atmospheric deposition (fert), mineralization (mineral); and outputs: root uptake for tree growth and harvested crop (crop), denitrification (denit), and leaching to groundwater. The leaching flux is modeled directly as the cumulative annual N mass flux out the bottom of the soil profile (7 m depth) and is not the difference between measured inputs and outputs, like in the N mass balance.*

The amount of N leaching to groundwater per month is evaluated at the water table (Figure 2-15). The model predicts N leaching rates at the water table to be the highest from March until June, and to peak in April. These are months where combined precipitation and frequent irrigation lead to higher recharge rates. Monthly N leaching rates for mature blocks during dry years are predicted to be less than 1 kg/ha; however, for young tree blocks or during wet years, monthly N leaching rates can be up to 40-50 kg/ha. The model-predicted average monthly N leaching rate from 2013-2021 is 4.5 kg/ha/month.
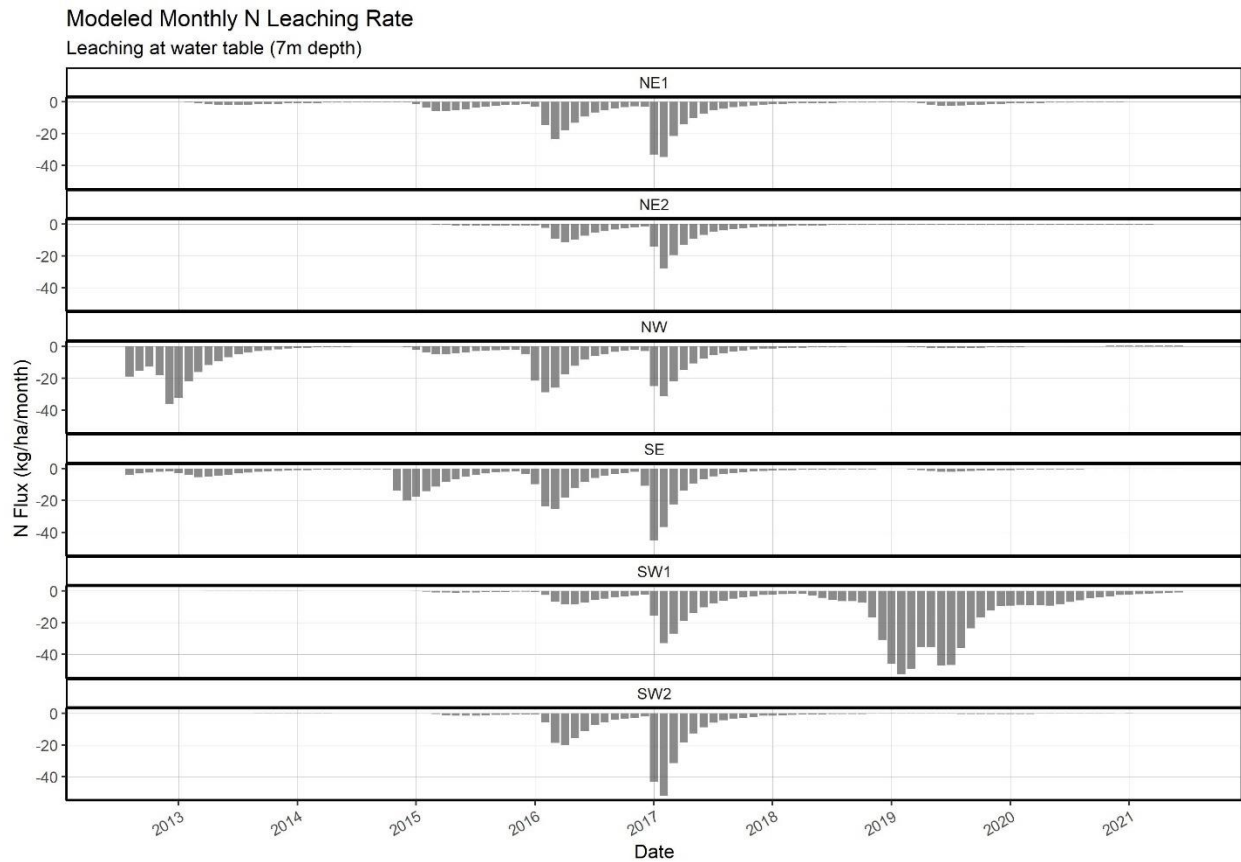
Figure 2-15. Modeled Monthly N Flux at Water Table. Modeled monthly N flux is calculated from the cumulative N mass flux leaving the bottom of the soil profile (7 m depth). The monthly N mass flux closely reflects the shape of the water flux because the average N concentrations across profiles within orchard blocks is less temporally variable than the water flux.

As with recharge, hydraulic parameter uncertainty had less impact on the modeled N fluxes than the geologic differences between the profiles. The average CV of monthly N leaching among the simulations for an individual profile was 0.80. Meanwhile the CV of the modeled monthly N leaching for all simulations across the orchard was 3.8.

Though the model predicts leaching rates directly, NUE was calculated from model N fluxes for comparison with the mass balance results (Figure 2-16). Model NUE was compared before and after the switch to HFLC (Figure 2-17). The modeled average NUE before the switch to HFLC in 2017 was 0.83, and ranged from 0.4 to 1.2. Average NUE after 2018 was 0.90, but has a larger range from 0.35 to 1.34. Low NUE is modeled in profiles located in blocks that are recently replanted, regardless of the sediment profile. The increase in NUE under HFLC was statistically significant with the two-tailed Welch's t-test (p-value < 0.001).
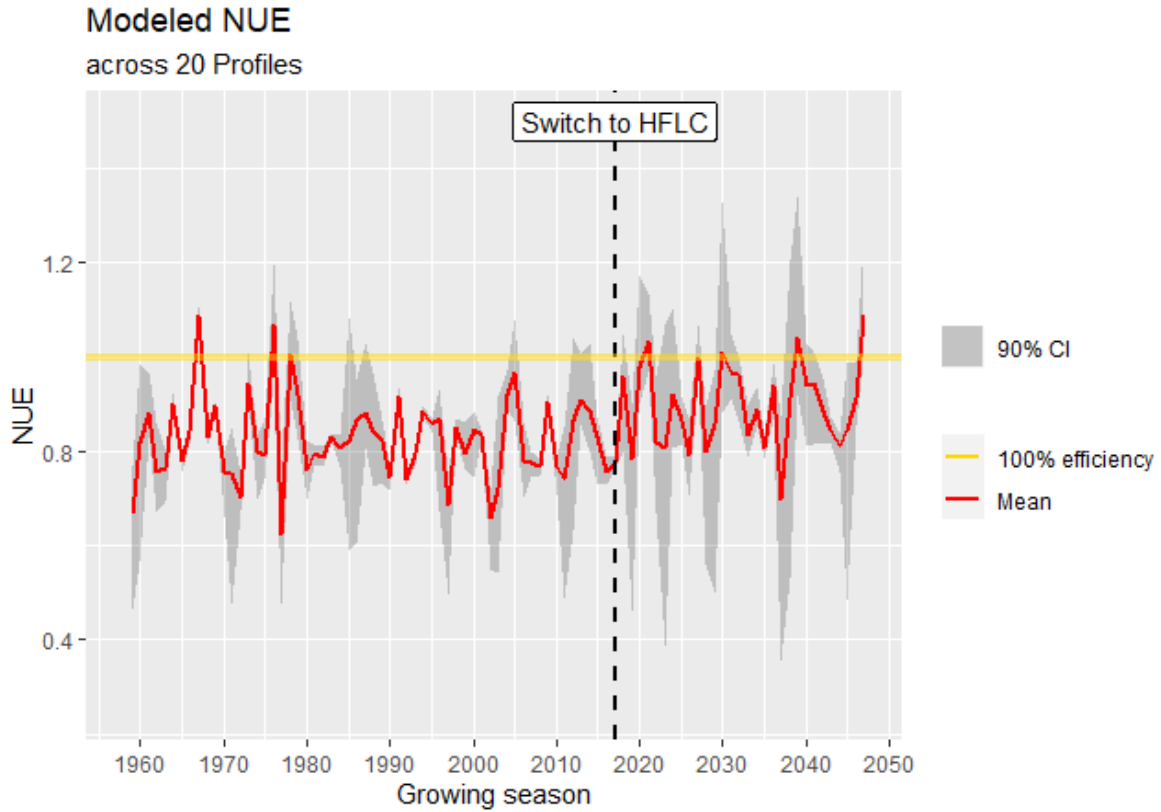
Figure 2-16. Model NUE. *The NUE is calculated from the model as the ratio of modeled N outputs to inputs. The NUE is calculated for each simulation produced at the 20 profiles. The orchard average (red line) and the variability across the orchard (gray area) are produced from the results. In the model, NUE fluctuates mostly in response to tree age (when young trees are planted), and the amount of recharge (climate). After the switch to HFLC the range of NUE is wider, but on average the NUE appears to increase.*
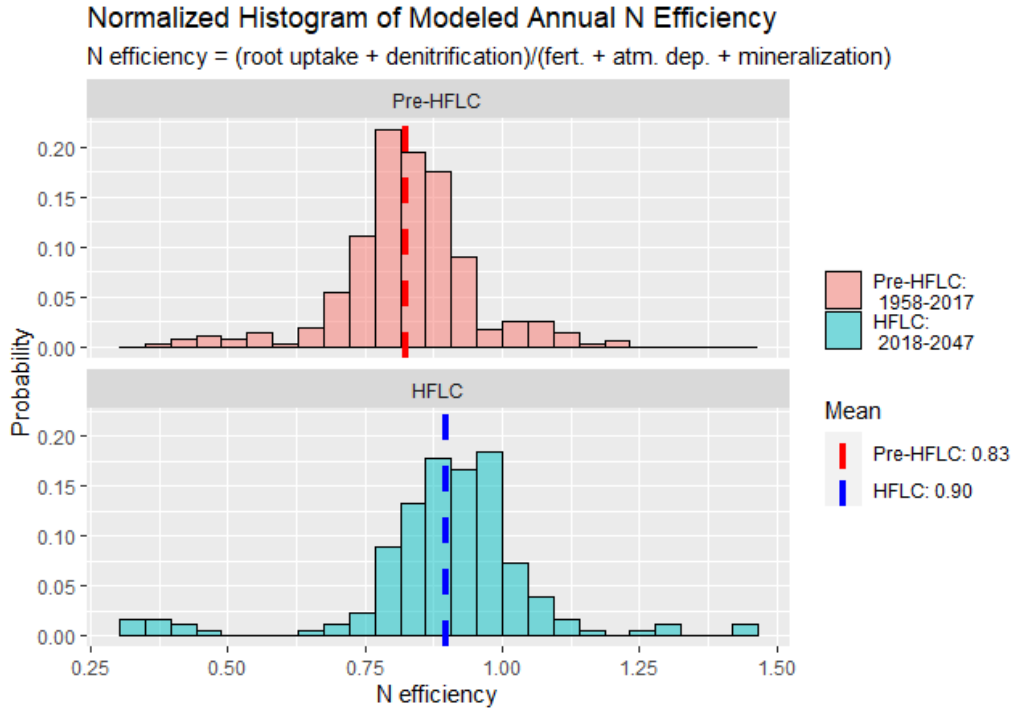
Figure 2-17. Model NUE Response to Nutrient Management. *The probability distribution of the model NUE results calculated before and after the switch to HFLC. There is one NUE calculation per simulation per year, resulting in approximately n=25,960 pre-HFLC datapoints and n=12,760 HFLC datapoints. The increase in the mean NUE under HFLC is statistically significant (p<0.001).*

2.6 Discussion

First the model results from Section 2.5.2 Model Results are discussed in comparison to the water and N mass balance in Section 2.5.1 Mass Balance Results. Then, the impact of switching to HFLC on N leaching from the orchard is discussed.

2.6.1 Mass Balance vs. Simulated Model Fluxes

The mass balance calculated for the orchard blocks produces overall similar recharge rates to those observed in the numerical model. During the wettest year, 2017, the annual recharge rate from the numerical model (20 cm) was within the range estimated by the water mass balance (15-45 cm). The

monthly mass balance recharge rates are more useful for dry years where the annual net water balance is negative, but results in annual recharge estimates often twice as much as the numerical model. Monthly recharge rates under the mass balance are of a similar magnitude to the modeled monthly recharge rates. The mass balance predicts recharge typically during the months of October through April, and sometimes in July. When recharge is predicted (some months the net water balance is negative), it is generally at rates of 3-5 cm/month. The model predicts that the highest recharge rates occur from April-August, typically 1-5 cm/month during wet years. Unlike the mass balance, during dry years the model predicts very little recharge throughout the year (<0.5 cm/month) because the model considers changes in water storage in the soil profile. Recharge rates peak in the month of December and January in the mass balance model, but peak in the month of April in the numerical model. This delay indicates that it takes about 4 months for the winter rain pulse to make it to the bottom of the vadose zone at 7 m depth. If the climate is exceptionally dry, as in 2014 and 2021, there is no pulse following the winter rain and peak recharge rates occur in September and October after the trees have been harvested and irrigation is still active.

Comparison of the ET rate used in HYDRUS and the mass balance to the satellite-measured ETa, showed that the overall ET rates used in this study tended to be less than the satellite-measured ETa by about 8%. ET was more likely to be too low compared to the satellite-measured ETa (by about 20%) during the winter and spring. The effect on the mass balance is increased recharge. ET in June and July tended to be about 3% too high. The method of adding positive monthly water budgets to estimate recharge can quickly compound this error and bias recharge estimates towards overestimation. Uncertainty in satellite-measured ETa is estimated to be 10-20% itself, which limits the interpretability of these comparisons. Decreasing uncertainty in ET by installing on-site sensors in future studies would be useful in refining recharge estimates for both the mass balance and modeling.

Modeled N leaching rates are similar to those expected from mass balance estimates. The average

N leaching rate for the orchard during 2013-2021 is estimated to be 57 kg/ha/year by the mass balance

and 50 kg/ha/year by the model. N leaching rates are slightly lower in the model because the modeled

average NUE are typically slightly higher than the mass balance NUE, even considering the effect of soil

hydraulic parameter uncertainty on NUE (Table 2-4). As in Gurevich et al. (manuscript in preparation), N

leaching rates and therefore the NUE is highly sensitive to uncertainty in the $cRoot_{max}$ parameter. A

$cRoot_{max}$ value of 0.035 mg/cm^2 was used because it reduced the mean absolute error between the mass

balance and modeled NUE (Figure 2-18), and it produces maximum nitrate concentrations in recharge

that are similar to the maximum measured nitrate concentration in shallow groundwater. Groundwater

nitrate concentrations exceeding 100 mg/L and up to 113 mg/L have been consistently measured in the

SW1 block at profile 13. The mass balance results suggest that numerical models of the vadose zone may

be improved with a more refined understanding of $cRoot_{max}$ for almond trees, which most likely varies by

tree variety, age, and growing conditions.

Table 2-4. Orchard Average Modeled v. Mass Balance NUE

	Pre-HFLC					*HFLC*			
	2013**	2014	2015	2016	2017*	2018*	2019*	2020*	2021
Mass Balance	0.85	0.76	0.78	0.66	0.72	0.86	0.72	1.09	0.76
Numerical Model	0.87	0.89	0.83	0.76	0.78	1.00	0.88	0.98	1.03
90% CI:	**0.85-0.89**	**0.76-1.12**	**0.68-0.89**	0.71-0.80	0.75-0.80	0.90-1.07	0.84-0.91	**0.88-1.29**	0.95-1.21

Note: | *Does not include young block SW1
**Does not include young blocks NW or SE
Bold indicates mass balance is within model 90% confidence interval that growing season

Compared to the mass balance, the model predicts slightly higher NUE and lower N leaching

rates overall. While a high root uptake parameter might contribute to this difference, another possibility is

the occurrence of preferential flow paths at the orchard, which are not included in the 1D model, that

might divert nutrients away from the roots in certain areas. Unlike the mass balance which uses harvest

records, the model also does not consider the impact unfavorable growing conditions might have on

nutrient uptake, such as the early spring freeze in 2019, which damaged the blossoms and contributed to the lowest yields during the study period.
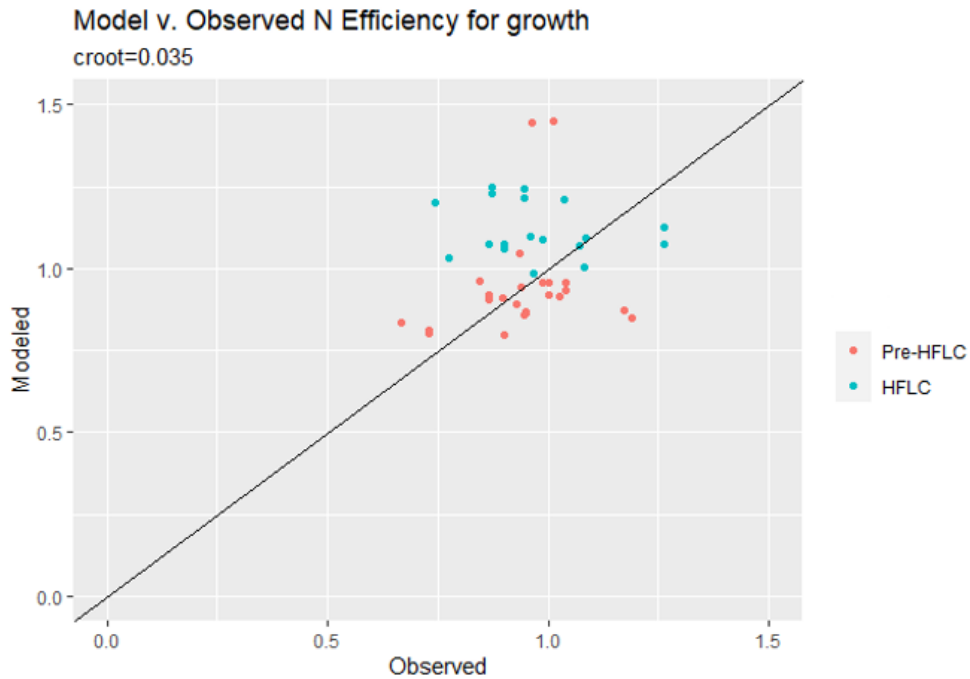
Figure 2-18. Modeled vs. Mass Balance NUE. *NUE_{growth} is compared between the model and mass balance (observed). NUE_{growth} is calculated individually for the blocks which produced a harvest for the years 2013-2021. NUE_{growth} is calculated from only the ratio of N uptake for the crop and tree growth to fertilizer applied. In the mass balance N uptake for the crop is estimated from the N content of the harvested yield per acre plus an estimated N uptake for growth from literature (Brown 2010). HYDRUS calculates the N uptake by the roots, which is sensitive to the $cRoot_{max}$ parameter. The $cRoot_{max}$ parameter was manually adjusted to reduce the sum of the residual between the modeled and observed NUE_{growth}.*

2.6.2 HFLC Impact on N Leaching

HFLC treatments increased NUE at the orchard. The orchard was well-managed before HFLC and already exhibited a high NUE of above 80%, predicted by both the model and mass balance. HFLC is predicted to increase the long-term average NUE by 7% (model) to 10% (mass balance). Because any

deficiency in NUE is assumed to represent N leaching, this improvement translates to a 40% decrease in N loading to groundwater (in both the mass balance and model predictions).

Both the mass balance and model predict that the N leaching rate at the water table will be reduced in response to HFLC; however, the model predicts that it will take several years for groundwater nitrate concentrations to respond to the change in nutrient management. The mass balance predicts that HFLC will reduce N leaching from 67-70 kg/ha/year to 34-45 kg/ha/year, depending on tree age in the orchard. This represents a 33-50% decrease in N loading to groundwater. Baram et al. (2016A) found, using the N mass balance, that N losses at an almond orchard under comparable nutrient management scenarios to have similar but slightly higher leaching rates ranging from 60-100 kg/ha/year, though that study only continued for two years (2014-2015). The model predicts that N leaching rates would decrease from 55 to 40 kg/ha/year. But, because it takes over a decade for nitrate to traverse the vadose zone to groundwater, the model period must span several decades to capture the full impact of a switch in nutrient management. Therefore, it was more useful to compare changes in NUE between the mass balance and model than changes in N leaching rates.

The reduction in annual N leaching rates observed with HFLC is primarily due to a reduction in N leaching during the months of February and March, when recharge rates are higher (Figure 2-19). This study demonstrates that the smaller, more frequent fertilizer applications in HFLC result in less excess N in the root zone, particularly during wet months when recharge rates are higher, and N is more likely to be lost through leaching.

Modeled Monthly N Leaching Rate
20 soil profiles: Last 15 years before HFLC and
15 years after 15 years with HFLC
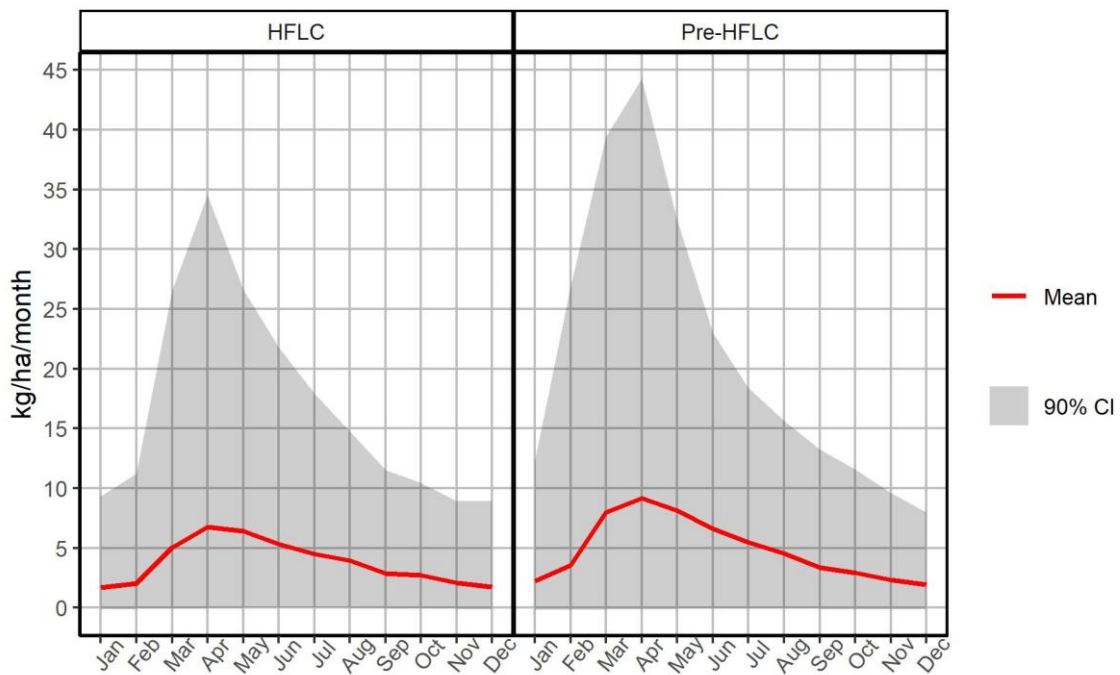
Average reduction in monthly leaching rate by switching to HFLC
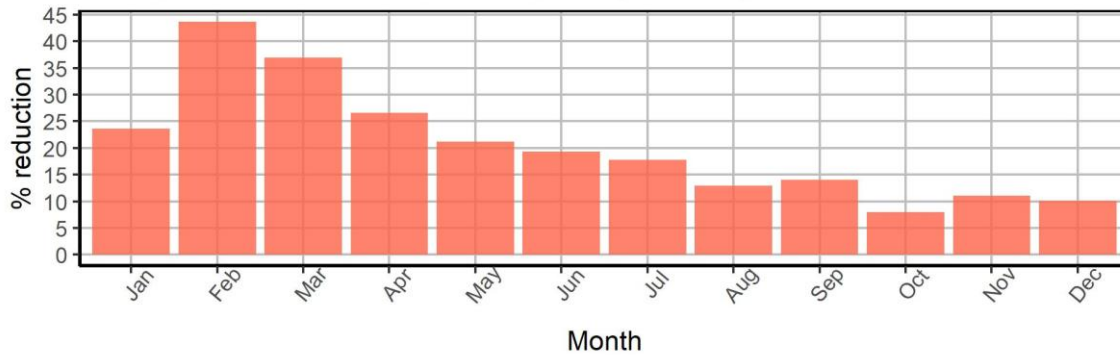
Figure 2-19. HFLC Reduces Modeled Monthly N Leaching Rates. Top: A subset of model years were selected to compare monthly leaching rates before and after switching to HFLC. HFLC (left) is represented by model years 2032-2047, while pre-HFLC (right) is represented by model years 2002-2017). N leaching peaks in the months of March-May. Bottom: HFLC did not equally impact monthly leaching rates. N leaching reduced the most during the months of February, March, and April, times when fertilizer is typically applied, and the soil profile usually has a higher water content.

Under the prior nutrient management practice, the modeled average nitrate concentration in groundwater recharge at the orchard is 75 mg/L. While increases in NUE are observed almost immediately after switching to HFLC, it takes 10 years before leaching nitrate concentrations, and therefore N leaching rates, start to decrease. After 30 years of HFLC, average nitrate concentrations are decreasing rapidly, but are still well above the MCL of 10 mg/L. After 30 years of HFLC, average nitrate concentrations reaching groundwater are about 45 mg/L, which is a 40% reduction from before. If N leaching under HFLC averages 43 kg/ha/year, then 43 cm/year of recharge would be needed to dilute average nitrate concentrations to 10 mg/L. Recharge for the entire orchard during 2013-2021 ranged from 5-20 cm. Under dry climate conditions and efficient irrigation, deficits in recharge needed to dilute nitrate could be made up through artificial recharge sources such as agricultural managed aquifer recharge (Ag-MAR).

2.6.3 Spatial Variability in Nitrate Leaching

As observed in several studies noted previously, this model also predicts high spatial variability in nitrate leaching (Baram et al. 2016; Onsoy et al. 2005; Gurevich et al. 2021). At a given time, modeled nitrate concentrations in groundwater recharge ranged from 30 to 110 mg/L, even within the same orchard block. Since 2017, groundwater samples have been collected regularly from monitoring wells at the same locations as the HYDRUS-1D profiles. Nitrate concentrations measured in the monitoring wells have ranged from 4-113 mg/L. During a given sampling event, the median nitrate concentration measured across the orchard is consistently about 20-30 mg/L. The modeled range in the nitrate concentrations leaching to groundwater is similar to the spatial variability in nitrate measured in shallow groundwater. On average, it appears that nitrate concentrations measured in shallow groundwater wells tend to be lower than the modeled leaching N concentration (75 mg/L). The model suggests lower nitrate leaching rates than the mass balance (Section 2.6.1 Mass Balance vs. Simulated Model Fluxes), but compared to

measured nitrate in groundwater, the model nitrate leaching rates are higher. Significant denitrification below the root zone would contribute to the discrepancy between modeled nitrate concentrations and measured nitrate in groundwater, though prior studies suggest denitrification below the root zone is limited (Harter et al. 2005; Onsoy et al. 2005). Also, due to mixing along the well screens, nitrate concentrations at the water table may not be representative of groundwater samples in which water from near the water table is mixed with older, deeper groundwater. Groundwater modeling could be used to better relate nitrate concentrations at the water table to the mixed groundwater samples collected from the monitoring wells.

As in Gurevich et al. (manuscript in preparation), differences in irrigation efficiency between young and mature trees cause widely fluctuating nitrate concentrations leaving the root zone over time (over a time period of ~25 years). The rate at which the change in nitrate concentration reaches the bottom of the vadose zone depends on the soil hydraulic characteristics of sediment the water passes through. As water passes through a unique progression of heterogeneous soil textures in every soil profile, water and nitrate transport speeds up and slows down at different rates. Interestingly, it was observed that uncertainty in the soil hydraulic parameter values has a negligible impact on overall nitrate fluxes because the spatial variability at the orchard scale is many times greater. The lateral mean lengths of the interbedded deposits are on the order of 50-200 m (Gurevich et al. 2021). As a result, soil profiles separated by even a few meters are likely completely distinct from one another. Thus, the spatial variability in nitrate leaching observed in the 20 profiles across the orchard is likely to be just as high within a 50-200 m radius.

2.7 Conclusion

The challenge in developing efficient nutrient management strategies is quantifying the relationship between the amounts and timing of fertilizer and irrigation applications and N loading to groundwater.

Nitrogen loading to groundwater by agriculture in the Central Valley is tracked by regulators using a simple mass balance. Physics-based models, such as the ones used in this study, can evaluate mass balance estimates while accounting for the impact of geologic heterogeneity on nitrate transport. In this study we developed a vadose zone model which predicts spatial and temporal patterns in nitrate transport to shallow groundwater at the orchard scale. The numerical model is used to quantify the impact HFLC nutrient management will have on N loading to groundwater over the next 30 years. N loading to groundwater in the physics-based model is compared to mass-balance estimates to indicate the accuracy of the simple approach used by farmers and regulators today. The key findings of this study are as follows:

1) During the study period, N loading rates to groundwater predicted at the sub-orchard scale varied between zero to over 150 kg/ha/year using both the numerical model and mass balance approaches. Orchard-average N loading rates during the study period 2013-2021 were also similar using both methods (50 kg/ha/year and 57 kg/ha/year, respectively).

2) Both the numerical model and mass balance predict that HFLC nutrient management reduces nitrate leaching to groundwater by about 40% (+/- 10%).

3) HFLC management increased crop yields, lowered fertilizer applications, and improved NUE right away. But dry climate and efficient irrigation at the orchard results in low recharge rates (7 cm/year). With such low recharge rates, it will take 10 years to see any benefits at the water table, and over 30 years for the deep vadose zone to reach a new steady state.

4) Differences in climate (precipitation) and the management of trees based on their age causes temporal variability in N loading rates. Spatial variability in sediment structure combined with changing N loading rates over time created high spatial variability in N leaching to groundwater, even within orchard blocks under the same fertilizer and irrigation treatments.

This study demonstrates how nutrient management practices adopted by farmers influence the spatial and temporal distribution of nitrate loading to groundwater, and also how farmers can reduce nitrate leaching to groundwater through the timing and adjustment of fertilizer and irrigation applications. This study confirms that when evaluated for several years over multiple management units, changes in N loading using the N mass balance are consistent with predictions of a detailed, physics-based numerical model. This promising finding suggests that the adoption of simple, inexpensive monitoring through N mass balance is an appropriate alternative to intensive field measurements or highly detailed, field-scale numerical models.

2.8 References

Allen, Richard G., Albert J. Clemmens, Charles M. Burt, Ken Solomon, and Tim O'Halloran. 2005. "Prediction Accuracy for Projectwide Evapotranspiration Using Crop Coefficients and Reference Evapotranspiration." *Journal of Irrigation and Drainage Engineering* 131 (1): 24. https://doi.org/10.1061/(ASCE)0733-9437(2005)131:1(24).

Allen, Richard G., Luis S. Pereira, Terry A. Howell, and Marvin E. Jensen. 2011. "Evapotranspiration Information Reporting: I. Factors Governing Measurement Accuracy." *Agricultural Water Management* 98 (6): 899–920. https://doi.org/10.1016/j.agwat.2010.12.015.

Badr, M. A., A. S. Taalab, and W. A. El-Tohamy. 2011. "Nitrogen Application Rate and Fertigation Frequency for Drip-Irrigated Potato." *Australian Journal of Basic and Applied Sciences* 5 (7): 817–25.

Baram, S., V. Couvreur, T. Harter, M. Read, P. H. Brown, J. W. Hopmans, and D. R. Smart. 2016A. "Assessment of Orchard N Losses to Groundwater with a Vadose Zone Monitoring Network." *Agricultural Water Management* 172 (July): 83–95. https://doi.org/10.1016/j.agwat.2016.04.012.

Baram, S., V. Couvreur, T. Harter, M. Read, P.H. Brown, M. Kandelous, D.R. Smart, and J.W. Hopmans. 2016B. "Estimating Nitrate Leaching to Groundwater from Orchards: Comparing Crop Nitrogen Excess, Deep Vadose Zone Data-Driven Estimates, and HYDRUS Modeling." *Vadose Zone Journal* 15 (11): 1–13. https://doi.org/10.2136/vzj2016.07.0061.

Bellvert, Joaquim, Karine Adeline, Shahar Baram, Lars Pierce, Blake L. Sanden, and David R. Smart. 2018. "Monitoring Crop Evapotranspiration and Crop Coefficients over an Almond and Pistachio Orchard Throughout Remote Sensing." *Remote Sensing* 10 (12): 2001. https://doi.org/10.3390/rs10122001.

Botros, Farag E., Yuksel S. Onsoy, Timothy R. Ginn, and Thomas Harter. 2012. "Richards Equation–Based Modeling to Estimate Flow and Nitrate Transport in a Deep Alluvial Vadose Zone." *Vadose Zone Journal* 11 (4): vzj2011.0145. https://doi.org/10.2136/vzj2011.0145.

Brown, Patrick. 2010. "Development of a Nutrient Budget Approach to Fertilizer Management in Almond." Final Report 2008-13 10-0039SA. CDFA Fertilizer Research and Education Program. https://www.cdfa.ca.gov/is/ffldrs/frep/pdfs/completedprojects/10-0039-SA_Brown.pdf.

Brown, Patrick, Sebastian Saa, Saiful Muhammad, and Sat Darshan Khalsa. 2020. "Nitrogen Best Management Practices." Almond Board of California. https://www.almonds.com/sites/default/files/2020-12/ABC_Nitrogen_8.5x11_vmags.pdf.

California Water Boards. 2022. "Groundwater Issue: Groundwater Quality." April 11, 2022. https://www.waterboards.ca.gov/water_issues/programs/groundwater/issue_gq.html.

Carle, Steven. 1999. "T-PROGS: Transition Probability Geostatistical Software." https://www.researchgate.net/profile/Steven-Carle/publication/284548821_T-PROGS_Transition_Probability_Geostatistical_Software_Version_21/links/604127ef4585154e8c77e100/T-PROGS-Transition-Probability-Geostatistical-Software-Version-21.pdf.

Doll, David, and Kenneth Shackel. 2016. "Drought Management for California Almonds." *Crops & Soils* 49 (2): 28–35. https://doi.org/10.2134/cs2016-49-2-9.

Domenico, P. A., and M. D. Mifflin. 1965. "Water from Low-Permeability Sediments and Land Subsidence." *Water Resources Research* 1 (4): 563–76.

Drechsler, Kelley, Allan Fulton, and Isaya Kisekka. 2022. "Crop Coefficients and Water Use of Young Almond Orchards." *Irrigation Science* 40 (3): 379–95. https://doi.org/10.1007/s00271-022-00786-y.

Dubrovsky, N. M., K. R. Burow, G. M. Clark, J. A. M. Gronberg, P. A. Hamilton, K. J. Hitt, D. K. Mueller, M. D. Munn, L. J. Puckett, and B. T. Nolan. 2010. "Nutrients in the Nation's Streams and Groundwater, 1992–2004, Circular 1350." *US Geological Survey, Reston, VA, USA*. https://pubs.usgs.gov/circ/1350/.

EU Nitrogen Expert Panel. 2015. "Nitrogen Use Efficiency (NUE) an Indicator for the Utilization of Nitrogen in Food Systems." Wageningen University, Alterra, Wageningen, Netherlands.

Farneselli, Michela, Paolo Benincasa, Giacomo Tosti, Eric Simonne, Marcello Guiducci, and Francesco Tei. 2015. "High Fertigation Frequency Improves Nitrogen Uptake and Crop Performance in Processing Tomato Grown with High Nitrogen and Water Supply." *Agricultural Water Management* 154 (May): 52–58. https://doi.org/10.1016/j.agwat.2015.03.002.

Faunt, Claudia. 2009. "Groundwater Availability of the Central Valley Aquifer, California." U.S. Geological Survey Professional Paper 1766. https://pubs.usgs.gov/pp/1766/PP_1766.pdf.

———. 2012. "Contours of Corcoran Clay Depth in Feet from Page (1986) for the Central Valley Hydrologic Model (CVHM)." USGS Science Data Catalog. 2012. https://data.usgs.gov/datacatalog/data/USGS:2eedd7e1-0522-465f-9478-c47e5263a46e.

Feddes, R. A., P. J. Kowalik, and H. Zaradny. 1978. *Simulation of Field Water Use and Crop Yield*. Simulation Monographs. Wageningen: Center for agricultural publishing and documentation.

Fetter, C. W. 2001. *Applied Hydrogeology*. 4th ed. Upper Saddle River, N.J: Prentice Hall.

Fetter, Charles Willard, Thomas Boving, and David Kreamer. 2017. *Contaminant Hydrogeology*. Waveland Press.

Fitts, Charles R. 2002. *Groundwater Science*. Amsterdam ; Boston: Academic Press.

Fleckenstein, Jan H., and Graham E. Fogg. 2008. "Efficient Upscaling of Hydraulic Conductivity in Heterogeneous Alluvial Aquifers." *Hydrogeology Journal* 16 (7): 1239–50. https://doi.org/10.1007/s10040-008-0312-3.

Fogg, Graham E. 1986. "Groundwater Flow and Sand Body Interconnectedness in a Thick, Multiple-Aquifer System." *Water Resources Research* 22 (5): 679–94. https://doi.org/10.1029/WR022i005p00679.

Gurevich, Hanna, Shahar Baram, and Thomas Harter. 2021. "Measuring Nitrate Leaching across the Critical Zone at the Field to Farm Scale." *Vadose Zone Journal* 20 (2): e20094. https://doi.org/10.1002/vzj2.20094.

Gurevich, Hanna, Iael Raij-Hoffman, Sat Darshan Khalsa, Patrick Brown, and Thomas Harter. n.d. "The Fate of Surplus N in an Almond Orchard: Mass Balance vs. Model."

Hansen, Birgitte, Lærke Thorling, Jörg Schullehner, Mette Termansen, and Tommy Dalgaard. 2017. "Groundwater Nitrate Response to Sustainable Nitrogen Management." *Scientific Reports* 7 (1): 8566. https://doi.org/10.1038/s41598-017-07147-2.

Harbaugh, Arlen W., Christian D. Langevin, Joseph D. Hughes, Richard G. Niswonger, and Leonard F Konikow. 2017. "MODFLOW-2005: USGS Three-Dimensional Finite-Difference Groundwater Model." U.S. Geological Survey. https://doi.org/10.5066/F7RF5S7G.

Harter, T., and J. R. Lund. 2012. "Addressing Nitrate in California's Drinking Water; Report for the State Water Resources Control Board." *Center for Watershed Sciences, University of California: Davis, CA, USA*. https://groundwaternitrate.ucdavis.edu/files/139110.pdf.

Harter, Thomas, Yuksel S Onsoy, Katrin Heeren, Michelle Denton, Gary Weissmann, Jan W Hopmans, and William R Horwath. 2005. "Deep Vadose Zone Hydrology Demonstrates Fate of Nitrate in Eastern San Joaquin Valley." *California Agriculture* 59 (2): 124–32. https://doi.org/10.3733/ca.v059n02p124.

Healy, Richard W. 2010. *Estimating Groundwater Recharge*. Cambridge university press.

Heath, Ralph C. 1998. *Basic Ground-Water Hydrology*. Vol. 2220. US Department of the Interior, US Geological Survey.

Henri, Christopher Vincent, Thomas Harter, and Efstathios Diamantopoulos. 2020. "On the Conceptual Complexity of Non-Point Source Management: Impact of Spatial Variability." *Hydrology and Earth System Sciences* 24 (3): 1189–1209. https://doi.org/10.5194/hess-24-1189-2020.

Herman, Jon, and Will Usher. 2017. "SALib: An Open-Source Python Library for Sensitivity Analysis." *The Journal of Open Source Software* 2 (9): 97. https://doi.org/10.21105/joss.00097.

Khalsa, Sat Darshan S., David R. Smart, Saiful Muhammad, Christine M. Armstrong, Blake L. Sanden, Benjamin Z. Houlton, and Patrick H. Brown. 2020. "Intensive Fertilizer Use Increases Orchard N Cycling and Lowers Net Global Warming Potential." *Science of The Total Environment* 722 (June): 137889. https://doi.org/10.1016/j.scitotenv.2020.137889.

Kourakos, George, Frank Klein, Andrea Cortis, and Thomas Harter. 2012. "A Groundwater Nonpoint Source Pollution Modeling Framework to Evaluate Long-Term Dynamics of Pollutant Exceedance Probabilities in Wells and Other Discharge Locations." *Water Resources Research* 48 (6). https://doi.org/10.1029/2011WR010813.

Lockhart, K. M., A. M. King, and T. Harter. 2013. "Identifying Sources of Groundwater Nitrate Contamination in a Large Alluvial Groundwater Basin with Highly Diversified Intensive Agricultural Production." *Journal of Contaminant Hydrology* 151 (August): 140–54. https://doi.org/10.1016/j.jconhyd.2013.05.008.

Mann, Michael E., and Peter H. Gleick. 2015. "Climate Change and California Drought in the 21st Century." *Proceedings of the National Academy of Sciences* 112 (13): 3858–59. https://doi.org/10.1073/pnas.1503667112.

Maples, Stephen R., Graham E. Fogg, and Reed M. Maxwell. 2019. "Modeling Managed Aquifer Recharge Processes in a Highly Heterogeneous, Semi-Confined Aquifer System." *Hydrogeology Journal* 27 (8): 2869–88. https://doi.org/10.1007/s10040-019-02033-9.

Marr, Jenny, Devinder Dhillon, David Arrate, Shem Stygar, and Romain Maendly. 2018. "FLOOD-MAR: Using FLood Water For Managed Aquifer Recharge to Support Sustainable Water Resources." White Paper. CA Department of Water Resources. https://cawaterlibrary.net/document/flood-mar-using-flood-water-for-managed-aquifer-recharge-to-support-sustainable-water-resources/.

Meisinger, J. J., and G. W. Randall. 1991. "Estimating Nitrogen Budgets for Soil-Crop Systems." In *Managing Nitrogen for Groundwater Quality and Farm Profitability*, 85–124. John Wiley & Sons, Ltd. https://doi.org/10.2136/1991.managingnitrogen.c5.

Onsoy, Y. S., T. Harter, T. R. Ginn, and W. R. Horwath. 2005. "Spatial Variability and Transport of Nitrate in a Deep Alluvial Vadose Zone." *Vadose Zone Journal* 4 (1): 41–54. https://doi.org/10.2113/4.1.41.

Phillips, Steven, Karen Burow, D.L. Rewis, Jennifer Shelton, and Bryant Jurgens. 2007. "Hydrogeologic Setting and Ground-Water Flow Simulations of the San Joaquin Valley Regional Study Area, California," January, 4–31.

Phillips, Steven P., Diane L. Rewis, and Jonathan A. Traum. 2015. "Hydrologic Model of the Modesto Region, California, 1960-2004." Scientific Investigations 2015–5045. US Department of the Interior, US Geological Survey.

Pollock, D. W. 2016. "User Guide for MODPATH Verison 7–a Particle Tracking Model for MODFLOW. Open-File Report 2016–1086." US Geological Survey, Washington, DC.

Rajput, T. B. S., and Neelam Patel. 2006. "Water and Nitrate Movement in Drip-Irrigated Onion under Fertigation and Irrigation Treatments." *Agricultural Water Management* 79 (3): 293–311. https://doi.org/10.1016/j.agwat.2005.03.009.

Salamon, P., D. Fernàndez-Garcia, and J. J. Gómez-Hernández. 2007. "Modeling Tracer Transport at the MADE Site: The Importance of Heterogeneity." *Water Resources Research* 43 (8). https://doi.org/10.1029/2006WR005522.

Schulze-Makuch, Dirk. 2005. "Longitudinal Dispersivity Data and Implications for Scaling Behavior." *Groundwater* 43 (3): 443–56. https://doi.org/10.1111/j.1745-6584.2005.0051.x.

Selker, John S., James T. McCord, and C. Kent Keller. 1999. *Vadose Zone Processes*. CRC Press.

Silva, Sebastian Saa, Saiful Muhammad, Blake Sanden, Emilio Laca, and Patrick Brown. 2013. "Almond Early-Season Sampling and In-Season Nitrogen Application Maximizes Productivity, Minimizes Loss." *Almond Board of California*, 9.

Simunek, Jirka, Jan Hopmans, and Naftali Lazarovitch. 2010. "A New Compensated Root Water and Nutrient Uptake Model Implemented in HYDRUS Programs," May.

Simunek, Jirka, M. Th Van Genuchten, and M. Sejna. 2013. "The HYDRUS-1D Software Package for Simulating the One-Dimensional Movement of Water, Heat, and Multiple Solutes in Variably-Saturated Media, Version 4.17." *HYDRUS Software Series 3*, 342.

Spalding, R. F., and M. E. Exner. 1993. "Occurrence of Nitrate in Groundwater—A Review." *Journal of Environmental Quality* 22 (3): 392–402. https://doi.org/10.2134/jeq1993.00472425002200030002x.

State Water Resources Control Board. 2017. "GROUNDWATER INFORMATION SHEET: Nitrate." GAMA Program. https://www.waterboards.ca.gov/gama/docs/coc_nitrate.pdf.

Stewart, W. M., D. W. Dibb, A. E. Johnston, and T. J. Smyth. 2005. "The Contribution of Commercial Fertilizer Nutrients to Food Production." *Agronomy Journal* 97 (1): 1–6. https://doi.org/10.2134/agronj2005.0001.

Storlie, Craig A., Philip E. Neary, and James W. Paterson. 1995. "Fertilizing Drip-Irrigated Bell Peppers Grown on Loamy Sand Soil." *HortTechnology* 5 (4): 291–94. https://doi.org/10.21273/HORTTECH.5.4.291.

Syvertsen, J. P., and J. L. Jifon. 2001. "Frequent Fertigation Does Not Affect Citrus Tree Growth, Fruit Yield, Nitrogen Uptake, and Leaching Losses." In *Proc. Fla. State Hort. Soc*, 114:88–93.

Syvertsen, J. P., and S. M. Sax. 1999. "Fertigation Frequency, Wetting Patterns and Nitrate Leaching from Lysimeter-Grown Citrus Trees." In *Proceedings of the Florida State Horticultural Society*, 112:9–14.

Tanachaichoksirikun, Pinit, Uma Seeboonruang, and Graham E. Fogg. 2020. "Improving Groundwater Model in Regional Sedimentary Basin Using Hydraulic Gradients." *KSCE Journal of Civil Engineering* 24 (5): 1655–69. https://doi.org/10.1007/s12205-020-1781-8.

Thompson, Thomas L., Scott A. White, and Michael A. Maurer. 2000. "Development of Best Management Practices for Fertigation of Young Citrus Trees," October. https://repository.arizona.edu/handle/10150/223854.

Thompson, Thomas L., Scott A. White, James Walworth, and Greg J. Sower. 2003. "Fertigation Frequency for Subsurface Drip-Irrigated Broccoli." *Soil Science Society of America Journal* 67 (3): 910–18. https://doi.org/10.2136/sssaj2003.9100.

UNESCO. 2022. *The United Nations World Water Development Report 2022: Groundwater: Making the Invisible Visible*. Paris. https://unesdoc.unesco.org/ark:/48223/pf0000380721.

U.S. Geological Survey. n.d. "National Water Information System Data Avilable on the World Wide Web (Water Data for the Nation)." Accessed May 16, 2022. http://waterdata.usgs.gov/nwis/.

Van Groenigen, J. W., G. L. Velthof, O. Oenema, K. J. Van Groenigen, and C. Van Kessel. 2010. "Towards an Agronomic Assessment of N2O Emissions: A Case Study for Arable Crops." *European Journal of Soil Science* 61 (6): 903–13. https://doi.org/10.1111/j.1365-2389.2009.01217.x.

Vrugt, J. A., M. T. van Wijk, J. W. Hopmans, and J. Šimunek. 2001. "One-, Two-, and Three-Dimensional Root Water Uptake Functions for Transient Modeling." *Water Resources Research* 37 (10): 2457–70. https://doi.org/10.1029/2000WR000027.

Weissmann, G. S., and G. E. Fogg. 1999. "Multi-Scale Alluvial Fan Heterogeneity Modeled with Transition Probability Geostatistics in a Sequence Stratigraphic Framework." *Journal of Hydrology* 226 (1): 48–65. https://doi.org/10.1016/S0022-1694(99)00160-2.

Weissmann, Gary S., Steven F. Carle, and Graham E. Fogg. 1999. "Three-Dimensional Hydrofacies Modeling Based on Soil Surveys and Transition Probability Geostatistics." *Water Resources Research* 35 (6): 1761–70. https://doi.org/10.1029/1999WR900048.

Zhang, Yonggen, and Marcel G. Schaap. 2017. "Weighted Recalibration of the Rosetta Pedotransfer Model with Improved Estimates of Hydraulic Parameter Distributions and Summary Statistics (Rosetta3)." *Journal of Hydrology* 547 (April): 39–53. https://doi.org/10.1016/j.jhydrol.2017.01.004.

Zheng, Chunmiao, and Gordon D. Bennett. 1995. *Applied Contaminant Transport Modeling: Theory and Practice*. New York Albany Paris [etc.]: Van Nostrand Reinhold ITP.

Zheng, Chunmiao, and P. Patrick Wang. 1999. "MT3DMS: A Modular Three-Dimensional Multispecies Transport Model for Simulation of Advection, Dispersion, and Chemical Reactions of Contaminants in Groundwater Systems; Documentation and User's Guide."

CHAPTER 3. Modeled effects of spatially variable geology and leaching from agriculture on nitrate in shallow groundwater wells at the orchard scale.

3.1 Abstract

Agriculture, particularly the application of nitrogen fertilizers, is the leading source of nitrate contamination of groundwater. Long-term solutions to addressing nitrate contamination of groundwater focus on reducing leaching from farms by improving nitrogen use efficiency in agriculture. In this study, a numerical model of groundwater flow and nitrate transport in the unconfined aquifer underlying a 56-ha almond orchard in the Central Valley simulates the shallow groundwater quality response to a 40% reduction in nitrate leaching caused by a change in nitrogen management practices. The groundwater model is integrated with a flow and transport model of the vadose zone. The model was developed to 1) predict how long it will take for nitrate concentrations in the twenty monitoring wells at the orchard to decrease, and 2) isolate the cause of high spatial variability in nitrate concentrations measured in the monitoring wells across the orchard. Since the change in nutrient management in 2017, average nitrate concentrations in the monitoring wells have increased from 20 to 30 mg/L NO3-N in 2021. The groundwater model predicts that despite improved nutrient management, nitrate concentrations at this site will continue to increase up to an average of 50 mg/L NO3-N over the next 30 years. The dry climate in California's Central Valley, combined with high efficiency irrigation, results in low recharge rates (less than 10 cm/year at the orchard) and therefore slow vertical groundwater flow to shallow wells delaying the displacement of legacy nitrate already below the root zone and in shallow groundwater. It may take 40-50 years to measure improvements in shallow groundwater quality. Spatial variability in groundwater nitrate concentrations observed at the orchard scale is found to be primarily caused by nonuniformity in nitrate leaching from the vadose zone. Modeling spatial variability in nitrate leaching from the vadose zone was necessary to reproduce the distribution of nitrate concentrations observed at the orchard

monitoring wells. It was also found that simple models which upscale spatial variability in geologic media and in nitrate leaching are easy to develop and predict the average response well.

3.2 Introduction

Nitrate is the most widespread groundwater contaminant in the world (Spalding and Exner 1993). While nitrate occurs naturally, concentrations above 1 mg/L in groundwater indicate anthropogenic sources (Dubrovsky et al. 2010). Agriculture, particularly the application of nitrogen fertilizers, is the leading source of nitrate contamination of groundwater. The highest groundwater nitrate concentrations in the United States are found in agricultural areas with high fertilizer applications (Dubrovsky et al. 2010). In California's Central Valley, 90% of nitrate loading to groundwater comes from agriculture, with 60% of the nitrate originating as synthetic fertilizers applied to crops (Harter and Lund 2012). Nitrogen fertilizers oxidize into nitrate, which is a mobile contaminant that will leach to groundwater if a surplus is applied. Due to a widespread and prolonged history of agriculture, nitrate concentrations in California exceed the U.S. EPA's drinking water Maximum Contaminant Limit (MCL) of 10 mg/L in over 800 public supply wells (State Water Resources Control Board 2017), and nitrate is estimated to impact 40-50% of domestic wells in the Central Valley (Lockhart et al. 2013). This is alarming because California is dependent upon its groundwater, with about 80% of the population relying partially or entirely on groundwater as a source of drinking water (California Water Boards 2022). Nitrate contamination of groundwater is a serious threat to groundwater-dependent communities, particularly in areas with intensive agriculture.

Addressing nitrate in groundwater requires actions to meet both immediate and future needs. Safe drinking water is immediately supplied by treating contaminated water, mixing it with cleaner water, or finding another water source (from surface water or drilling a new well). This step requires substantial financial and technical resources which are inaccessible to small, rural, disadvantaged communities (T. Harter and Lund 2012). This is a temporary fix while other long-term solutions are implemented. The

long-term solution to protect future groundwater quality is to reduce nitrate leaching by improving nitrogen management practices in agriculture. Nitrogen management practices should lower the amount of surplus fertilizer applied and increase the nitrogen use efficiency (NUE). Denmark followed this approach in the mid-1980s, and a study of groundwater records in the subsequent years has indicated positive outcomes. To address concerns regarding nitrate leaching from agriculture, Denmark enacted policy since 1985 encouraging sustainable management of agriculture and increased NUE. These actions are thought to have contributed to improvements observed in shallow groundwater quality over the next 30 years (Hansen et al. 2017).

This study develops a field-scale numerical groundwater model of the relationship between nitrate leaching from an almond orchard in the Central Valley, California, and nitrate concentrations in the underlying shallow groundwater. The model is used to predict orchard-scale groundwater-quality impacts of switching to nutrient management practices which increase NUE and decrease nitrate leaching. Of particular concern is the amount of time it will take to see a reduction in groundwater nitrate concentrations. While Hansen et al. (2017) noted evidence of widespread improvements within 30 years in Denmark, the timescale will be dependent upon the groundwater ages in the wells sampled. The groundwater model is also used to estimate the groundwater ages and recharge source areas for twenty (20) monitoring wells installed at the orchard.

Groundwater samples collected from the 20 monitoring wells since 2017 reveal that nitrate concentrations in shallow groundwater across the orchard vary spatially by over an order of magnitude (Gurevich et al. 2021). The spatial variability in groundwater nitrate concentrations is high despite consistent water and nutrient management practices across the orchard. This study also evaluates potential causes of spatial variability in groundwater nitrate concentrations measured in shallow groundwater wells at the orchard. Potential causes evaluated include spatial variability in nitrate leaching from the orchard,

and spatial variability in the aquifer geologic media. Prior studies have found high spatial and temporal variability in nitrate leaching from the vadose zone at the field scale (See Chapter 2, Baram et al. 2016; Onsoy et al. 2005). Interlayered coarse and fine alluvial sediments at the orchard create aquifer heterogeneity that causes non-uniform groundwater flow. Alluvial fan geomorphology is common in much of the Central Valley aquifer (Faunt 2009). Spatial variability in nitrate leaching and aquifer heterogeneity are present at both the field and regional scales. Spatial variability in nitrate leaching at the regional scale is created by a patchwork of land uses with different crop types and leaching rates (T. Harter and Lund 2012). Aquifer heterogeneity is observed at the scale of centimeters (especially vertically) to hundreds of meters (Gurevich et al. 2021; Weissmann and Fogg 1999). Groundwater modeling at the regional scale found that nonuniformity in nitrate leaching impacts the variability of nitrate concentrations between wells more than aquifer heterogeneity (Kourakos et al. 2012). However, this has not been evaluated before at the field or orchard scale.

3.3 Study Area

The study site is a 56-ha (140-acre) commercial almond orchard located near Modesto in Stanislaus County, California (Figure 3-20). The study site has historically been used for agriculture and has been an almond orchard for more than 30 years. From aerial photographs, the southeastern portion of the site appears to have been used to grow alfalfa or hay in the mid-1990s until 2010. The study site is currently surrounded by other almond orchards and a walnut orchard to the east. Historically, the surrounding land uses have included almond orchards, vineyards, and a turkey farm to the east.

Based on groundwater elevations collected from the twenty on-site monitoring wells, groundwater generally flows from the north or northeast towards the south or southwest. The water table is at a depth of approximately 7 m. The water table elevation fluctuates by less than one meter throughout the year. In 2017, the twenty (20) shallow groundwater monitoring wells were installed across the

orchard. The monitoring well screens are 7 m-long and bridge the water table from a depth of approximately 7m below the ground surface (bgs) to 14 m bgs. Since 2017, groundwater samples have been collected four to seven times per year and analyzed for nitrate. Nitrate concentrations measured in the monitoring wells range from 4-113 mg/L. The median nitrate concentration measured across the orchard is above the MCL, about 20-30 mg/L. While the groundwater nitrate concentrations vary spatially across the orchard, the nitrate concentrations in individual wells change slowly over time. For example, the nitrate concentration in monitoring well MW13 is consistently the highest measured in the orchard, over 70 mg/L since September 2019. Meanwhile, monitoring well MW9 is in the middle of the orchard and has some of the lowest nitrate concentrations, consistently below the MCL of 10 mg/L.
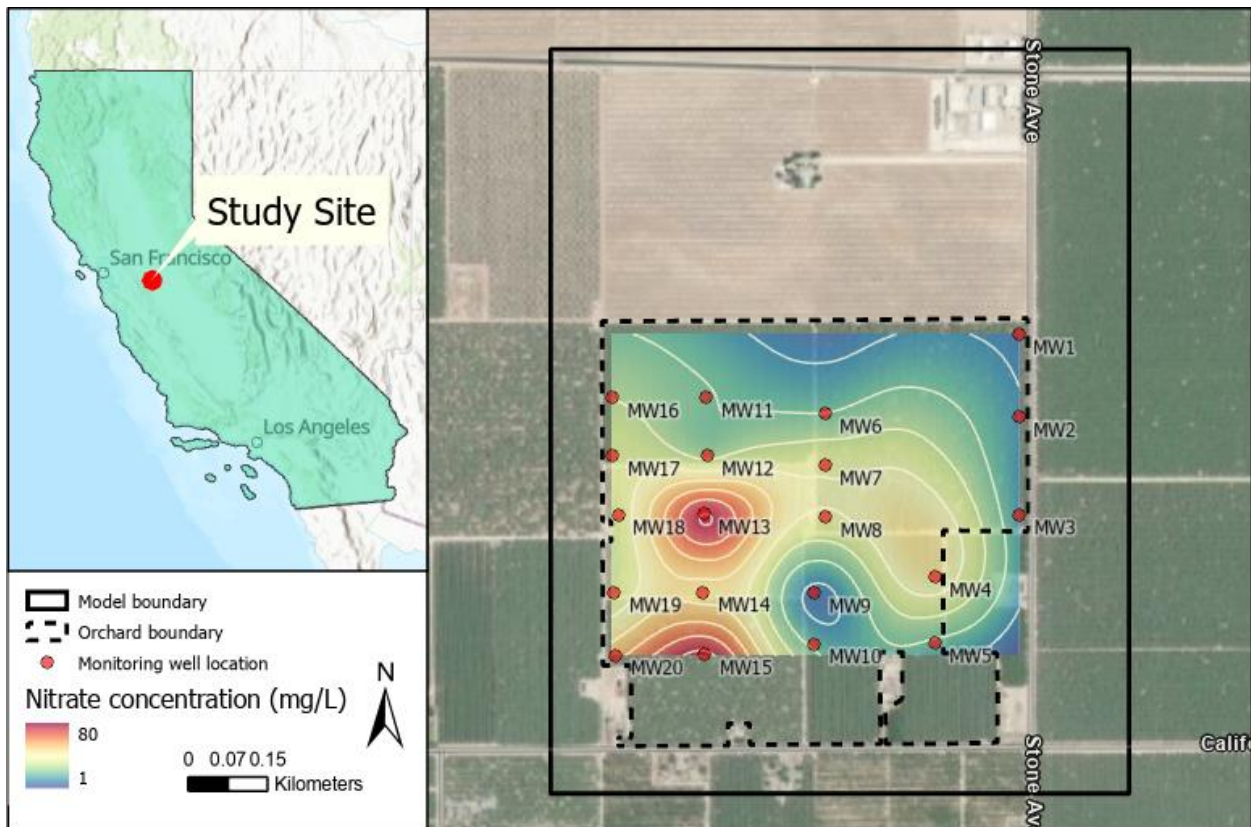
Figure 3-20. Orchard Location Map. *Nitrate concentrations measured in monitoring wells at the orchard in September 2021 are interpolated (spline interpolation) between the monitoring wells. There is high*

spatial variability in nitrate in the shallow groundwater at the orchard, ranging from less than 10 mg/L to

over 80 mg/L (see Appendix).

The geology at the orchard is characterized in prior work described in Gurevich et al. (2021). The orchard is located on alluvial fan deposits of the Tuolumne River, which is located approximately 3.4 km (2 miles) to the south. The sediments are heterogeneous, interbedded coarse channel sands and fine floodplain deposits.

In 2017, the orchard switched to high frequency, low concentration (HFLC) nutrient management practices. A numerical model of the vadose zone was developed to evaluate the response in nitrate leaching at the orchard to the new nutrient management practice (see Chapter 2). Both the vadose zone model and nitrogen mass balance estimates predicted that HFLC increases the NUE and decreases nitrate leaching from the orchard. But changes in groundwater would be delayed by at least 10 years, the amount of time it takes for nitrate to travel from the surface to the water table. The vadose zone model also predicted spatial variability in nitrate leaching, caused by a combination of soil heterogeneity in the unsaturated zone and variable root water and nitrogen uptake.

3.4 Methods

A groundwater flow model was developed for the shallow, unconfined alluvial aquifer underlying the almond orchard, plus areas upgradient. Heterogeneous alluvial sediments in the aquifer are represented using a geostatistical model. Backwards particle tracking is used to estimate the representative groundwater age and source areas of twenty shallow monitoring wells bridging the water table. Nitrate transport is simulated using a numerical solution to the advection-dispersion equation. The influence of uncertainty in hydraulic parameters of the sediments and the geology on groundwater flow and nitrate transport to the monitoring wells is evaluated stochastically. Last, model scenarios were developed to

evaluate the impact of aquifer heterogeneity vs. vadose zone nitrate leaching spatial variability on the spatial variability of nitrate concentrations in groundwater.

3.4.1 Geologic Model

A detailed representation of the porous media through which groundwater flows was previously developed for the shallow unconfined aquifer underlying the orchard (Gurevich et al. 2021) and is described in the following section. The geologic model was developed by first classifying observed soil textures into a set of hydrofacies. Then geostatistical properties of the hydrofacies are calculated using the Transition Probability Geostatistical Software (T-ProGS) by (Carle 1999). Finally, stochastic simulations of the geology are created which honor the calculated geostatistical properties and observed data.

Sediments within the shallow aquifer at the orchard are alluvial fan deposits including interbedded coarse channel sands and fine floodplain deposits. The alluvial deposits form lenses that are laterally discontinuous, even at the orchard scale. As a result, the shallow aquifer is unconfined to semi-confined. A regionally continuous fine-grained layer is the Corcoran Clay, a lacustrine deposit which in the vicinity of the site is estimated to be at a depth of roughly 30-40 m and a thickness of 6 m or more (Faunt 2012). The Corcoran Clay acts as a confining layer separating the upper unconfined to semi-confined aquifer from the underlying confined aquifer. The geologic model includes the alluvial deposits overlying the Corcoran Clay to an estimated depth of 40 m.

The interbedded alluvium is characterized by the juxtaposition of soil textures observable at different scales. Soil cores collected at the 20 monitoring well locations were logged to a total depth of 7m in 30-cm increments. A total of 19 soil textures were described, ranging from clay and loamy mixes to coarse sand. Within the 30-cm logged increments, textural heterogeneity was observed at an even finer centimeter-scale that is not captured in the geologic model. The 19 soil textures observed in the soil cores

were grouped into four facies representing floodplain deposits (clay and silt) and channel sands (fine sand and coarse sand).

Geostatistical properties of the facies that define the geologic model include the proportions of the different facies, mean length, and the transition probability. Facies proportions based on the soil logs were 34% clay, 32% silt, 24% fine sand, and 0.092% coarse sand. Mean lengths in the vertical direction were calculated using the soil log data in T-ProGS. In the horizontal direction, mean lengths were determined using soil maps (Weissmann et al. 1999). The transition probability matrix generated in T-ProGS recognizes cross-correlation between facies and represents the chance that a facies transitions into another in each direction. Then T-ProGS uses Markov chains to generate a stochastic realization of the geology onto the model grid that adheres to observed data at the monitoring well locations and is also consistent with specified facies proportions and transition probabilities. Individual realizations are random and equally probable without additional conditioning information.

3.4.2 Groundwater Flow Model Development

A groundwater model of the orchard and upgradient areas was developed in MODFLOW-2005 (Harbaugh et al. 2017). MODFLOW-2005 is a finite difference model that numerically solves the 3D groundwater flow Equation (3-1).

$$\frac{\partial}{\partial x}\left(K_x h \frac{\partial h}{\partial x}\right) + \frac{\partial}{\partial y}\left(K_y h \frac{\partial h}{\partial y}\right) + \frac{\partial}{\partial z}\left(K_z h \frac{\partial h}{\partial z}\right) + W = S_y \frac{\partial h}{\partial t} \qquad (3\text{-}1)$$

The groundwater flow equation solves for changes in potentiometric head (h) in the x, y, and z directions over time (t) in an unconfined aquifer. The hydraulic conductivity (K) in the x, y, and z directions has a proportional influence on the groundwater flow and is a property of the porous media. Sinks and sources of water are represented as W. The specific yield of the porous media is S_y, which is the amount of water

that can drain from the pores by gravity. The hydraulic parameters of the porous media are parameterized for the four facies in the geologic model.

The finite difference model grid encompasses the 56-ha (140-acre) orchard and is 1404 m long, 1092 m wide, and 40 m deep. It is oriented north-south and is longer in the direction of groundwater flow to include upgradient areas from the monitoring wells. Water levels measured in monitoring wells since 2017 suggest groundwater flow generally comes from the north-northwest or the north-northeast and varies seasonally. The upgradient area includes 600 m to the north of the site, which is occupied by another almond orchard and a huller/sheller facility. Source areas of the monitoring wells were expected to be generally less than 600 m away based on initial testing using a steady-state model of a much larger area. The model width is the orchard width plus a 100 m buffer on either side. MODFLOW cell dimensions are 12m in the lateral and transverse directions and 0.32 m in the vertical and match the cell dimensions of the geologic model. The cell size used is as small as possible to reduce numerical dispersion in the transport model and to capture the detail of the geologic heterogeneity. The vertical resolution is similar to the soil logging interval (30 cm) and is the highest level of detail possible given the soil profile data. The lateral cell size is also limited to increase the number of cells between monitoring wells, some of which are separated by less than 100m. The resulting model has 1.3 million cells and 125 layers, 117 rows, and 91 columns.

A transient model was developed for a 60-year simulation period from 1987-2047. The groundwater flow model has six stress periods per year and monthly timesteps. The first 30 years from 1987-2017 model groundwater conditions under prior nutrient management practices at the orchard. Nutrient management practice at the orchard changed in September 2017 to HFLC (start of the 2018 growing season), which increased the nutrient use efficiency of the orchard and reduced nitrate leaching

to groundwater. The last 30 years from the modeling period (2017-2047) predict how shallow groundwater will respond to this change in management practice.

3.4.2.1 Boundary Conditions

Boundary conditions in this model are informed by a regional groundwater flow model, data from local groundwater wells, and a vadose zone model developed for the orchard. Boundary conditions constrain groundwater head and fluxes through the top, sides, and bottom of the model. The top is a flux boundary representing recharge, the sides are a constant head boundary consistent with local seasonal and historic groundwater levels, and the bottom is a flux boundary.

3.4.2.1.1 Recharge

Water flux through the top of the model is recharge predicted by the vadose zone model (Figure 3-21). Recharge is applied to the layer containing the water table through the RCH package in MODFLOW. The vadose zone model represents climate conditions from orchard growing seasons 2013-2021 (growing season starts September of the previous year) repeated as a cycle every nine years. Recharge predicted by the vadose zone model is based on orchard-specific irrigation data which is responsive to ET and precipitation. For this reason, recharge is considered to represent conditions for the efficiently irrigated orchard over the past decade well, but the recharge does not account for trends in historic climate. Recharge is predicted at twenty 1D soil profiles at locations corresponding to the monitoring wells. Recharge rates for the whole area are interpolated between the 20 points using nearest neighbor interpolation.

There is annual, seasonal, as well as spatial variability in recharge rates. Annually, recharge rates respond to total precipitation. Water years 2016 and 2017 received above average rainfall while 2015 and 2019 were about average, and the other years were well below average. Recharge rates in 2016 and 2017 are around 10-20 cm/year for the orchard, while less than 5 cm/year of recharge is predicted during the

dry years. Seasonally, most recharge occurs during the months April-August, and recharge rates are low

throughout the year during dry years. Spatially, recharge varies slightly due to differences in the sediment

structure of the soil profiles. Recharge variability is higher when young trees are present. Young trees less

than 3 years old have higher recharge rates than mature trees' because the water demand is lower and

irrigation is less efficient. In blocks with young trees, recharge rates were similar to the recharge rate in a

mature block during a wet year.
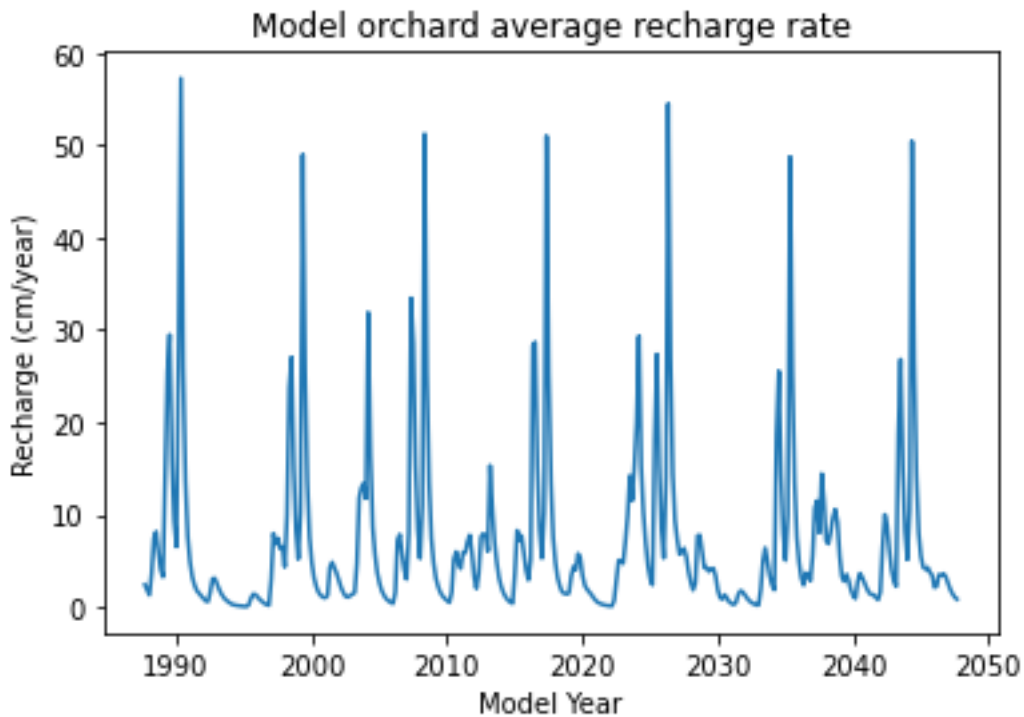
Figure 3-21. Orchard Average Recharge Rate. Recharge rates are interpolated from 20 1D vadose zone

models (Chapter 2) to the entire orchard. The orchard average recharge rate ranges from <5 cm/year to

almost 60 cm/year. The seven high recharge rates correspond to the 2017 wet year in the 9-year repeated

climate model.

3.4.2.1.2 Consistency with Regional Flow

The model domain is part of a larger regional groundwater system spanning from the Sierra foothills to the east to the San Joaquin River to the west. Lateral and bottom groundwater fluxes in the orchard model were matched to fluxes in a regional flow model as well as regional and on-site groundwater data. Use of the regional flow model is limited because its representation of gradients, water table, and recharge rates at the orchard are not consistent with observations. In those cases, local data is used to improve shortcomings of the regional model.

A groundwater model of the Modesto region, called the MERSTAN model, was developed and calibrated by the USGS in 2015. The MERSTAN model is a transient flow model for 1960-2004. The orchard is represented by only a few cells in the 400m-square grid of the MERSTAN model. In the MERSTAN model, the direction of groundwater flow in the vicinity of the orchard is generally east to west and the water table is at a depth of 2 m. However, groundwater elevations measured in 2004 at wells located near the orchard (CA Department of Water Resources Water Data Library; https://wdl.water.ca.gov/WaterDataLibrary/) suggest that the local groundwater flow was north to south. Water level measurements in 2004 reveal the water table was at a depth of about 6.8m. Water levels collected at the on-site monitoring wells regularly since 2017 suggest groundwater flow at the orchard is from the north-northwest, north, or north-northeast, and flows towards the south-southeast, south, or south-southwest. The average water table depth measured on-site since 2017 has been 6.7m. Considering this information, the constant head boundary was developed using groundwater elevation data collected from wells at or near the orchard in variance from the regional model.

Constant Head Boundary

Constant head boundaries around the edges of the groundwater model are used to control the lateral and vertical head gradients as well as water table within the flow model. Lateral gradient magnitude and

direction in the model was based on annual average groundwater conditions calculated from groundwater elevations collected at the twenty on-site monitoring wells during the 2018-2021 water years.

Groundwater elevations were collected roughly every seven weeks, resulting in approximately seven monitoring events per year. Groundwater elevations fluctuate by less than 1m between summer/winter and between years during those three years. This results in little change in magnitude of the groundwater gradient, though the direction changes seasonally. Generally, the gradient in late summer (post-harvest) to early winter is from the north-northwest and in the late winter-spring from the north-northeast. This may be because of local groundwater pumping outside the orchard during the growing season, and/or a seasonal influence of the nearby Tuolumne River on groundwater.

The groundwater elevations measured at the twenty wells were resampled to the same six bimonthly events (January, March, May, July, September, November) using linear interpolation. Then groundwater elevations were averaged by month at each well to produce a timeseries representing groundwater elevations at the wells throughout an average year (for the period 2018-2021). For each bimonthly event, the head gradient direction and magnitude in the unconfined aquifer was calculated by fitting the average groundwater elevations to Equation 3-2 using the *lm* function in the R stats package (Fitts 2002).

$$Ax + By + C = h^2 \qquad\qquad (3\text{-}2)$$

Where constants A, B, and C define the head, h, gradient direction and magnitude in the x, y plane. Equation 3-2 is used to predict the bimonthly varying head along the north, south, east and west boundaries of the groundwater model. The average lateral gradient magnitude in the average groundwater elevation model is 0.04% and the average heading of groundwater flow is 194 degrees, which are consistent with observations at the orchard.

Water table measurements collected outside but near the orchard have fluctuated over time with an overall declining trend since the 1980s. Historic groundwater elevations were used to adjust the water table in the constant head boundary because of its strong influence over the water table in the groundwater model. There are four shallow groundwater wells in the vicinity of the orchard with extended records of historic groundwater elevation observations in the DWR Water Data Library (Table 3-5).

Table 3-5. Local Groundwater Wells

Local Well Name	Type	Screened interval (ft bgs)	Coordinates	Location relative to orchard	Data availability
Gisler 236	Irrigation	144-236	37.6554, -121.0723	2.9 km NNE	1991-2021
Warnock 46	Irrigation	<240	37.6429, -121.1085	1.8 km NNW	1963-2021
Paradise 235	Irrigation	96-132	37.6141, -121.0578	2.6 km SE	1991-2021
Young 76	Irrigation	12-152	37.6180, -121.0942	0.6 km S	1963-2021

The local well names are Gisler 236, Warnock 46, Paradise 235, and Young 76 and they are located to the north-northeast, north-northwest, southeast, and south of the model boundary, respectively. Warnock 46 and Young 76 records extend to 1963 and Gisler 236 and Paradise 235 records date back to 1991. Groundwater elevations were collected from these wells annually or semi-annually (Figure 3-22). Historically, the highest groundwater elevations occurred between 1963-1980. Since then, average groundwater levels have decreased by approximately 2 m.
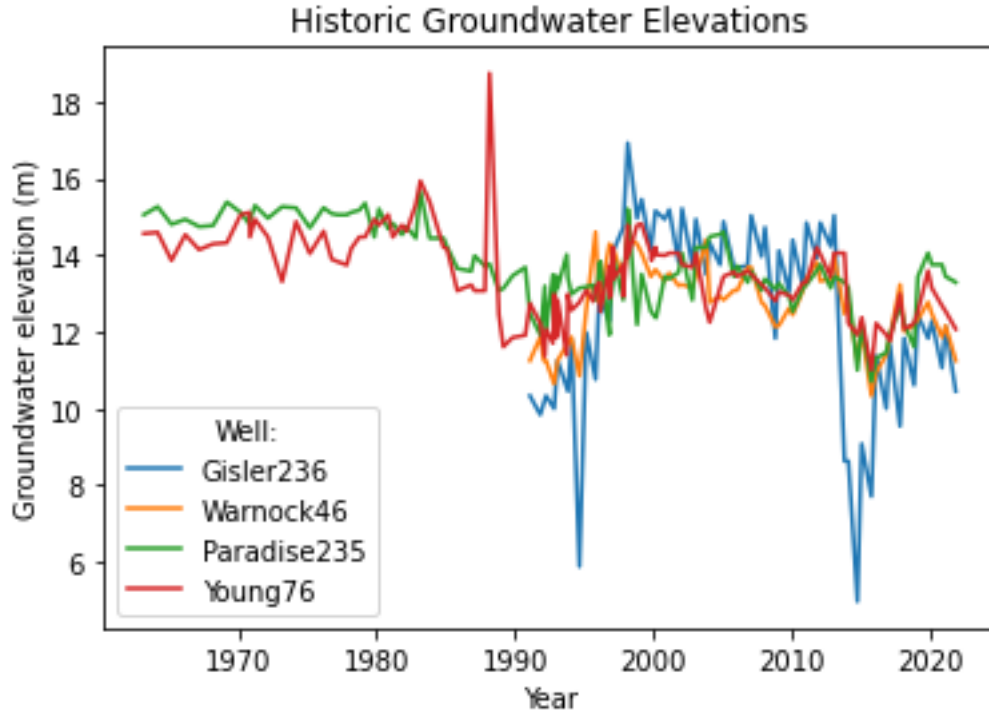
Figure 3-22. Historic Groundwater Elevations in Local Wells. *Groundwater elevations in four irrigation wells near the orchard downloaded from the DWR Water Data Library, used as a proxy for the historic water table elevation at the orchard. Declining groundwater levels are noticeable during the 1986-1992 and 2011-2017 droughts.*

Groundwater elevations from the wells in Table 3-5 were linearly interpolated and resampled to a bimonthly frequency, and then averaged into a single timeseries. The water table in the constant head boundary was adjusted based on the average historic groundwater elevation according to Equation 3-3.

$$h_{chb}(sp) = h_{avg} + \left[C * \frac{recharge_{avg}(sp)}{70cm/year} + R * (h_{hist}(sp) - 12.9m) + k \right] \qquad (3\text{-}3)$$

Where $h_{chb}(sp)$ is the water table head in the constant head boundary in a specific row or column at a given stress period, h_{avg} is the 2017-2022 average head predicted at the model boundary,

$recharge_{avg}(sp)$ is the orchard average recharge rate in cm/year for a given stress period (Section 3.4.2.1.1 **Recharge**), 70 cm/year is the recharge in the regional model in 2004, $h_{hist}(sp)$ is the regional average groundwater elevation for a given stress period based on the wells surrounding the orchard, 12.9 m is the average groundwater elevation at the orchard between 2017 and 2022, and $C, R,$ and k are constants. Constants C and k have units of length (m) and R is unitless.

The purpose of Equation 3-3 is to proportionally adjust the water table along the model boundaries in response to the recharge rate at the orchard and the surrounding groundwater elevations. As a result, the water table is higher with increased recharge and when surrounding groundwater elevations are also high, and vice versa. $C, R,$ and k are constants which were manually adjusted to achieve the best fit between the modeled and observed groundwater elevations.

The resulting dataset is a timeseries of modeled water table along the north, south, east, and west boundaries of the model. When modeling the future (2022-2047), data from 2013-2021 was cycled to match the repetition of climate data used in the orchard vadose zone model. The water table height along the boundary becomes the constant head value in the model layer which spans elevations intersecting the water table. Unsaturated conditions above the water table are represented as inactive (dry) model cells.

Vertical Head Gradient

Potentiometric head below the water table can be described by the vertical head gradient. The vertical head gradient across the entire model thickness is approximated by the proportion of water flux through the bottom of the model and the effective vertical hydraulic conductivity as in Darcy's Law (Equation 3-4).

$$\nabla h_z(sp) = \frac{q_z(sp)}{k_z} \tag{3-4}$$

Where q_z is the specific discharge through the bottom of the model for a specific stress period, k_z is the vertical effective hydraulic conductivity, and ∇h_z is the resulting vertical head gradient for that stress period. The vertical effective hydraulic conductivity is calculated as the weighted harmonic mean of the vertical hydraulic conductivity of the four parameterized hydrofacies in the geologic model. The specific discharge through the bottom of the model is based on the regional model and the recharge rate, discussed in the following section. The resulting vertical head gradient is applied to cells in the constant head boundary that are below the water table. The average vertical gradient is about 0.5% and in the downward direction. Using this method, when recharge rates are low, the vertical gradient is low (<0.1%); when recharge rates are high, the vertical gradient can be >1%. This method does not explicitly consider the seasonal effects of groundwater pumping on vertical gradient within the model area; see the following section for a discussion of groundwater pumping in the model area.

Bottom Flux

Groundwater fluxes through the bottom of the model is the flux suggested by the regional model in 2004 plus groundwater pumping rates. This is because according to well completion reports, the average depth of domestic and production wells in the area is just below 40 m depth, the bottom of the model (Table 3-6). In 2004 the estimated average pumping rate in the vicinity of the orchard was 19.5 cm/year in the regional model. The flux rate out through the bottom of the orchard model corresponds to the bottom flux out of layer 7 of the regional model, and is 30.9 cm/year in 2004. The total bottom flux including pumping suggested by the regional model under 2004 conditions is 50.4 cm/year. The regional model estimates recharge rates of 70 cm/year in the orchard vicinity in 2004, while the orchard average recharge in the vadose zone model rates range from less than 5 cm/year up to about 60 cm/year (Figure 3-21). The bottom flux of 50.4 cm/year was proportionally adjusted for each stress period based on the ratio of the

vadose zone model orchard average recharge for that stress period compared to the regional model's recharge rate of 70 cm/year.

Table 3-6. Well Statistics in Well Completion Report Map Application: Section M03S08E33

Well Type	Number in model area	Minimum depth (ft)	Maximum depth (ft)	Average depth (ft)
Domestic	9	106	185	152
Irrigation	3	203	210	203
Public	0	-	-	-

Effective Hydraulic Conductivity

Hydraulic conductivity in the regional model is mapped at a coarser resolution compared to the facies representation in the orchard groundwater model. For consistency, the effective horizontal hydraulic conductivity in the groundwater model was matched to that of the regional flow model. This ensures that lateral flow behaves similarly in response to changes in the gradient and water table as in the regional model. The effective horizontal hydraulic conductivity was calculated by taking the arithmetic average of the horizontal hydraulic conductivity in the regional model cells that intersect the orchard model. The effective horizontal hydraulic conductivity based on the regional model was approximately 27 m/day. Slug tests were conducted in the twenty monitoring wells located at the orchard using bailers and dataloggers. Analysis of the slug test data returned an effective hydraulic conductivity of 16-18 m/day. The effective horizontal hydraulic conductivity in the groundwater model was thus limited to a range of 16-29 m/day. The effective horizontal hydraulic conductivity is calculated as the arithmetic mean of the parameterized horizontal hydraulic conductivity values weighted by the hydrofacies proportions. Parameterization of the model is described in Section 3.4.2.2 Parameterization and Stochastic Simulation.

3.4.2.2 Parameterization and Stochastic Simulation

Hydraulic properties of the aquifer were parameterized according to the four hydrofacies in the geologic model. Parameters include the horizontal and vertical hydraulic conductivity, the specific storage, specific yield, and porosity. Porosity is relevant to the transport and particle tracking models but not the groundwater flow model (see Sections 3.4.3 Nitrate Transport Model and 3.4.4 Particle Tracking). The vertical hydraulic conductivity used was the horizontal hydraulic conductivity with a 1:10 anisotropy ratio. Parameter ranges (Table 3-7) were estimated from literature based on the sediment type represented in the hydrofacies (Fetter 2001; Heath 1998; Domenico and Mifflin 1965). Saturated hydraulic conductivity in the vadose zone model ranges from 0.15-450 m/day across the 19 soil textures. Hydraulic conductivity in the four hydrofacies spans a similar range; though, the hydraulic conductivity for clay soil types in the groundwater model reaches lower values. Because the aquifer is predominantly unconfined, the model is not anticipated to be sensitive to specific storage, and one set of representative values was selected. Unique parameter combinations of horizontal hydraulic conductivity, specific yield, and porosity were randomly generated from the parameter ranges, assuming a uniform probability distribution, using Latin hypercube sampling (Herman and Usher 2017). Parameter combinations were thrown out if the weighted arithmetic mean of the horizontal hydraulic conductivity was not within desired effective hydraulic conductivity range of 16-29 m/day. Model runs were performed with the unique, randomly generated parameter sets to evaluate the impact of parameter uncertainty on model results. Additionally, model runs were performed with several unique T-ProGS-generated geology realizations, which change the location within the model of the hydrofacies deposits, but maintains the stratigraphy observed along the well screens. By using the same hydraulic parameter values with different geology realizations, these model runs were used to evaluate the impact of geologic uncertainty on model results.

Table 3-7. Hydraulic Parameter Value Estimated Ranges

	Hydrofacies			
	Coarse sand	*Fine sand*	*Mud*	*Clay*
Horizontal hydraulic conductivity (m/d)	120-500	17-120	0.15-1.7	1e-3 – 0.15
Vertical hydraulic conductivity			$k_v = k_h/10$	
Specific yield	0.2-0.3	0.2-0.3	0.03-0.2	0-0.05
Specific storage (m^{-1})	7.53e-6	1.04e-5	1.36e-5	1.47e-5
Porosity	0.2-0.5	0.2-0.5	0.2-0.5	0.2-0.5

3.4.3 Nitrate Transport Model

Nitrate transport was modeled using the program MT3DMS in conjunction with the flow field predicted by MODFLOW-2005. MT3DMS numerically solves the advection-dispersion equation (Equation 3-5). (Zheng and Wang 1999). The advection-dispersion equation assumes mass transport follows Fick's law in that the diffusion and dispersion are proportional to the concentration gradient. In Fickian dispersion, the variance of the plume (second moment) is proportional to the travel distance or time (Fetter et al. 2017).

$$\frac{\partial(\theta C)}{\partial t} = \frac{\partial}{\partial x_i}\left(\frac{\theta D_{ij}\partial C}{\partial x_j}\right) - \frac{\partial}{\partial x_i}(\theta v_i C) + q_s C_s \tag{3-5}$$

Where $x_{i,j}$ is a distance along the cartesian coordinate axes, t is time, θ is the porosity, v_i is the linear pore velocity, C is the solute concentration, D_{ij} is the hydrodynamic dispersion tensor, q_s is inflow or outflow to the aquifer from sources or sinks, and C_s is the solute concentration in the source or sink flux. In this model chemical reactions were ignored. Denitrification is anticipated to be negligible in oxic groundwater conditions anticipated in the shallow aquifer. Parameterization of the porosity is described in Section 3.4.2.2 Parameterization and Stochastic Simulation.

The hydrodynamic dispersion tensor combines the effects of molecular diffusion and mechanical dispersion through the porous media. Because diffusion dominates in the clay-rich portions of the aquifer, it was not neglected; the effective molecular diffusion coefficient was generally estimated as 10^{-9} m^2/s, or 8.64×10^{-5} m^2/day (Fetter et al. 2017). Advection dominates in the sandy portions of the aquifer. The longitudinal and transverse dispersivity combined with the average linear pore velocity represent advection-driven mechanical dispersion. The longitudinal dispersivity was estimated via an empirical power law equation (Equation 3-6) presented in Schulze-Makuch (2005), a method also used in a regional nitrate transport model for the Modesto area (Bastani and Harter 2020).

$$\alpha_L = c(L)^m \qquad\qquad (3\text{-}6)$$

Where α_L is the longitudinal dispersivity, parameters c and m are empirically derived based on the geologic medium, and L is the characteristic flow distance. Parameter values for a geologic medium composed of unconsolidated alluvial sediments were used, $c = 0.085$, $m = 0.81$ (Schulze-Makush 2005), which is also consistent with Bastani and Harter (2020). The characteristic flow distance used in this model was the mean length of the fine sand hydrofacies (200 m), because it occupies a significant portion of the model area and has a higher conductivity, and therefore accepts a large proportion of the groundwater flow in the model. The resulting longitudinal dispersivity is 6 m. The transverse horizontal and transverse vertical dispersivity are a ratio of 1:10 and 1:100 to the longitudinal dispersivity, respectively.

MT3DMS solved the advection-dispersion equation using the implicit standard finite-difference method, which has the advantage of being mass conservative, but can be subject to numerical dispersion errors (Zheng and Wang 1999). Other particle-tracking based Lagrangian solution methods available in MT3DMS were not used because, unlike the implicit finite-difference method with the Generalized Conjugate Gradient solver, these methods require stability constraints on the timestep length. With the

fine grid spacing used in the geologic model (cell thickness of 0.32 m), stability constraints make the timesteps computationally prohibitively short. However, the grid spacing is essentially as fine as possible within computational limits. Given the selected grid discretization and dispersivity, the grid Peclet numbers are low (2 in the horizontal direction and about 5 in the vertical), and therefore numerical dispersion error from the standard finite-difference method is anticipated to be negligible (Zheng and Wang 1999; Zheng and Bennett 1995).

3.4.3.1 Nitrate Sources and Sinks

Sources of nitrate in the model are nitrate in groundwater recharge and nitrate in lateral groundwater flow (through the constant head boundary). The constant head boundary in the flow model serves as a nitrate sink where groundwater flows laterally out of the model. Cells along the bottom layer of the model are also sinks. A timeseries of nitrate concentrations in groundwater recharge are created using a HYDRUS-based model of water flux and nitrate transport through the vadose zone (Figure 3-23). The initial concentration of nitrate in the groundwater, as well as the nitrate concentration of incoming groundwater, is based on groundwater samples collected from wells at the orchard and from wells outside the orchard in the local area. Chemical reaction sinks/sources of nitrate are not considered in the groundwater transport model, though denitrification and nitrogen mineralization are included in the vadose zone model. Due to oxic conditions in shallow groundwater, denitrification rates are anticipated to be negligible.

Leaching nitrate concentrations from the vadose zone were previously modelled in HYDRUS using fertilizer application data for orchard growing season 2013-2021. At the beginning of the 2018 growing season (September 2017), the grower switched nutrient management practices to HFLC fertigation. The vadose zone model creates a timeseries of nitrate concentrations for 1957-2047 representing leaching from the almond orchard under pre-HFLC nutrient management prior to September

2017, and HFLC nutrient management after September 2017. The vadose zone model suggests it takes approximately 15 years for forcing at the surface to impact nitrate concentrations at the water table, and several years more to stabilize. For this reason, a 30-year buffer was implemented; the groundwater transport model starts with the leaching nitrate concentrations in 1987. The vadose zone model also showed that an increase in NUE following the switch to HFLC results in a decrease in nitrate leaching over time. Note that there is also a delay of approximately 15 years from the switch to HFLC in September 2017 to decreasing average nitrate leaching concentrations in recharge at the water table. Average recharge nitrate concentrations range from 45-80 mg/L and are generally increasing before HFLC and decreasing after HFLC. The average recharge nitrate concentration fluctuates around 75-80 mg/L between the years 2000 and 2035. Average recharge nitrate concentrations are predicted to start decreasing rapidly beginning around 2035 and are still decreasing at the end of the simulation in 2047.

Spatial variability in leaching nitrate concentrations is produced in the vadose zone model. As with the vadose zone model recharge rates (Section 3.4.2.1.1 **Recharge**), recharge nitrate concentrations are simulated at twenty 1D soil profiles at locations corresponding to the monitoring wells. Nitrate concentrations in recharge across the entire model area are interpolated between the 20 locations using nearest neighbor interpolation. In a given stress period, leaching nitrate concentrations modeled across the orchard range from around 20 mg/L to 110 mg/L. The minimum leaching nitrate concentration modeled occurs after 2035 and is 12 mg/L (still above the MCL of 10 mg/L).

Temporal variability in leaching nitrate concentrations is also produced in the vadose zone model. Nitrate concentrations are predicted to follow an oscillating pattern which has a period consistent with the tree replanting frequency (25 years was used). Because mature trees are irrigated more efficiently than young trees, the highest leaching concentrations occur when the trees are mature (up to 80-150 mg/L), and the concentrations decrease to 20-50 mg/L after replanting (see Figure 2-11).
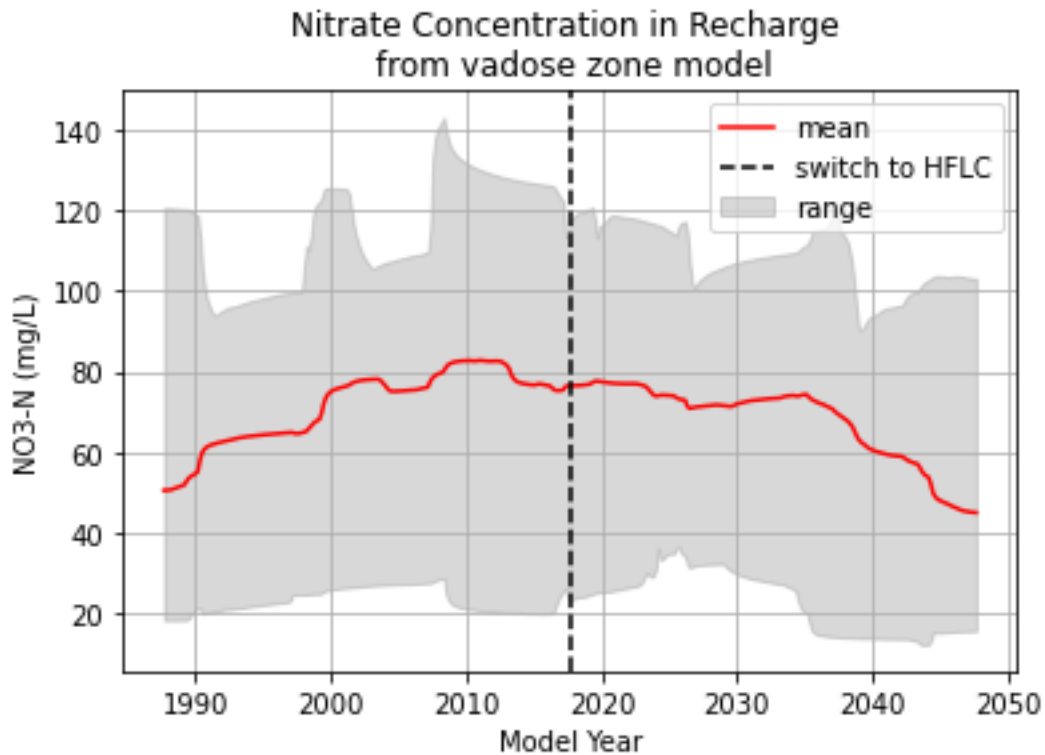
Figure 3-23. Nitrate Concentrations in Recharge. *Nitrate concentration in groundwater recharge is*
interpolated from 20 1D vadose zone models (Chapter 2) to the entire orchard. The orchard average
nitrate concentration in recharge (red) is around 75-80 mg/L before the switch to HFLC. After the switch
to HFLC, average nitrate concentrations in recharge slowly decline after a delay of about 10-15 years.
Spatial variability in nitrate leaching is represented by the range (gray).

The initial concentration of nitrate in groundwater, as well as the nitrate concentration of

incoming groundwater via lateral flow, was set at 4 mg/L. The vadose zone model does not predict nitrate

concentrations leaching from the orchard less than 10 mg/L; however, nitrate concentrations less than 10

mg/L have been measured in the twenty monitoring wells since 2015. The lowest nitrate concentrations

measured in the twenty monitoring wells generally range from 4-10 mg/L and are found at MW1 and

MW2 in the most upgradient, north-eastern portion of the orchard, and MW9 located in the middle of the orchard in the SE block. The minimum concentration of nitrate detected in the twenty monitoring wells at the orchard since 2015 is approximately 4 mg/L (3.49 mg/L at MW2 in May 2018). This indicates that the nitrate concentration of groundwater flowing towards the orchard along the north and east orchard boundaries is likely to be less than 10 mg/L. In 2006, the nitrate concentration in the shallow USGS well at the south-eastern boundary of the orchard was 13.2 mg/L. The nitrate concentration in the mid USGS well (screen depth of 55 m) in 2006 was 4.38 mg/L. Groundwater in a 55 m-deep well is likely to be much older than groundwater measured in the shallow 14 m-deep orchard wells. The nitrate concentration measured in the mid USGS well in 2006 is likely to represent nitrate concentrations from more than 30 years ago (the start of the groundwater model) and is therefore used as the initial nitrate concentration. For these reasons, both the initial nitrate concentration (in 1987) and the lateral groundwater flow nitrate concentration were set to 4 mg/L.

In MT3DMS, the boundary condition was such that incoming groundwater flow through the constant head boundary was a fixed concentration of 4 mg/L. The outflow concentration through cells representing sinks (which may be constant-head cells or cells in the bottom layer) is simply the concentration in outflow predicted by the model at that location.

3.4.3.2 Calculating Modeled Monitoring Well Concentrations

The nitrate transport model produces a timeseries of modeled nitrate concentrations for every model cell which are then converted into a modeled monitoring well concentration. Modeled monitoring well concentrations are compared to the concentrations measured in groundwater samples collected from the twenty orchard monitoring wells. The monitoring wells have a 7 m-long screen which intersects heterogeneous sediment deposits. Groundwater flux through high conductivity sediments (coarse sand and fine sand) is higher than low conductivity sediments (mud and clay). During sampling events, several

well volumes are pumped before sample collection; therefore, the higher flux portions of the well screen comprise a higher portion of sample volumes. A representative monitoring well concentration is calculated by weighting the nitrate concentration in the model cells intersecting the monitoring well screen by the proportion of the groundwater flux contributed to the well. The groundwater flux through the well screen is divided proportionally based on the horizontal hydraulic conductivity of the intersecting model cells by solving a system of equations (Equation 3-7).

$$
\begin{pmatrix}
1 & 1 & 1 & 1 \\
-\dfrac{1}{k_1 A_1} & \dfrac{1}{k_2 A_2} & 0 & 0 \\
0 & -\dfrac{1}{k_2 A_2} & \dfrac{1}{k_3 A_3} & 0 \\
0 & 0 & -\dfrac{1}{k_3 A_3} & \dfrac{1}{k_4 A_4}
\end{pmatrix}
\begin{pmatrix}
Q_1 \\ Q_2 \\ Q_3 \\ Q_4
\end{pmatrix}
=
\begin{pmatrix}
Q_{total} \\ 0 \\ 0 \\ 0
\end{pmatrix}
\tag{3-7}
$$

Where Q_{total} is one unit flux through the well screen, Q_1 through Q_4 are the fraction of the flux attributable to the four hydrofacies, k_1 through k_4 are the horizontal hydraulic conductivities of the four hydrofacies, and A_1 through A_4 are the fraction of the screen length intersecting each of the four hydrofacies.

3.4.4 Particle Tracking

The source area and groundwater age for the monitoring wells are predicted by tracking particles through the groundwater flow field with MODPATH (Pollock 2016). MODPATH uses MODFLOW outputs to compute particle paths through the model. In MODPATH, particles move advectively according to the average linear velocity vectors ($v_{x,y,z}$) calculated with Equation 3-8 as the particle crosses each cell face.

$$
v_{x,y,z} = \frac{q_{x,y,z}}{n}
\tag{3-8}
$$

Where $q_{x,y,z}$ is the volumetric flow rate across the cell face divided by the face's cross-sectional area (specific discharge), and n is the porosity of the porous media. Parameterization of the porosity is described in Section 3.4.2.2 Parameterization and Stochastic Simulation. Ten particles are released around the surface of a 1 m-diameter cylinder in each cell intersecting the monitoring well screen. The monitoring well screens are located at 7 to 14 m below the ground surface, resulting in 220 particles per well. Particles are backtracked to an endpoint where the particle reaches the water table. This represents where and when the particle recharged to groundwater. The horizontal distance from the endpoint to the monitoring well is a representation of the source area travel distance and the difference in time from the start to the end is the travel time, or groundwater age. Particles that intersect the top of the well screen are generally younger and travel shorter distances to the well than particles captured at the bottom of the well screen. The result is a range of groundwater ages and a source area predicted for each well. A single representative groundwater age and source area distance is calculated for each well from the distribution of particles using the flux-weighted average along the well screen, as described in Section 3.4.3.2 Calculating Modeled Monitoring Well Concentrations.

3.4.5 Model Scenarios

Model scenarios (Table 3-8) were developed to evaluate the impact of aquifer heterogeneity vs. nitrate leaching spatial variability on the spatial variability of nitrate concentrations in groundwater. Scenario 1 uses a heterogeneous geologic model combined with the spatially variable nitrate leaching from the vadose zone model. Scenario 2 uses a homogeneous geologic model in which all model cells have the same set of effective hydraulic parameter values (Fleckenstein and Fogg 2008). In Scenario 3 and 4, the nitrate concentration in recharge is averaged across the whole orchard. Scenario 3 uses the heterogeneous geologic model and Scenario 4 uses the homogeneous geologic model.

Table 3-8. Model Scenarios

	Spatially variable nitrate source	*Average nitrate source*
Heterogeneous geology	Scenario 1	Scenario 3
Homogeneous geology	Scenario 2	Scenario 4

3.5 Results

3.5.1 Groundwater Flow Model Performance

3.5.1.1 Groundwater Head

The flow model was calibrated to observed water levels in the twenty orchard monitoring wells. Because the model is conceptualized with four constant head boundaries, and because the effective hydraulic conductivity was not allowed to vary significantly between the parameter sets, hydraulic parameters such as conductivity and porosity have little influence over the modeled water levels. Modeled water levels are mostly controlled by the constant head boundaries. Parameters used to relate recharge and regional water levels to the constant head boundaries were manually adjusted to fit observed water levels collected between 2017 and 2022. Parameters $C, R,$ and k were found to produce a good fit with the observed data with values of 0.035 m, 0.7 (unitless), and 0.7 m, respectively (Figure 3-24). These parameters appear in Equation 3-3 and are used to relate average groundwater levels at the orchard to observed regional groundwater levels and modeled orchard recharge rates for the purpose of adjusting the constant head boundaries. Manual calibration was used because due to the limited amount of observed data compared to the length of the model, an automated adjustment based on reducing residuals (in UCODE) did not visually produce a good fit with observed data. Generally, residuals are less than 1 m from the observed head, with a mean absolute error of approximately 0.5 m (Figure 3-25). The residual plot indicates something is unaccounted for in the model, especially in 2020-2022. The model tends to overestimate heads compared to the 2020-2022 observations; however, the model does capture increasing and decreasing trends in water levels well (Figure 3-24). Similar trends are observed in the twenty monitoring

wells. Monitoring well MW6 and MW20 are presented in Figure 3-24 and demonstrate these similarities.

MW6 is located in the NE1 block and is in the middle of the model, near the northern boundary of the
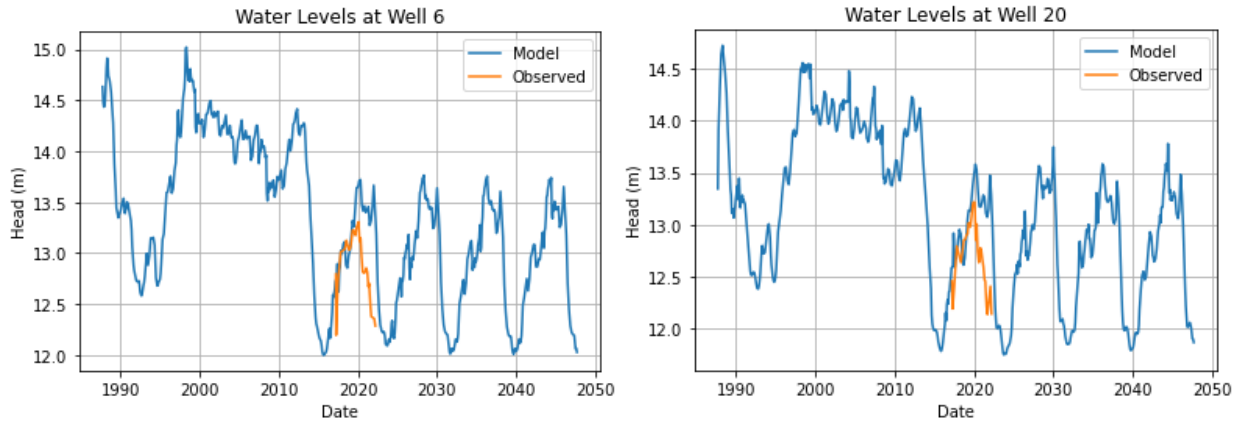
orchard. MW20 is in the southwest corner of the orchard near the western model boundary in block SW2.

Because the water levels in the model are strongly influenced by the regional water levels, there may be

effects from local pumping, regional changes in water levels, and nearby stream interactions that are

unaccounted for in the model.

Figure 3-24. Orchard Modeled vs. Observed Water Table Elevation. Modeled groundwater elevations

(blue) with the orchard-scale model are close to the observed values (orange) during the data collection

period from 2017-2021. The repeating pattern from 2021 to the end of the model is because the 2013-2021

climate and regional water levels are repeated for the future.
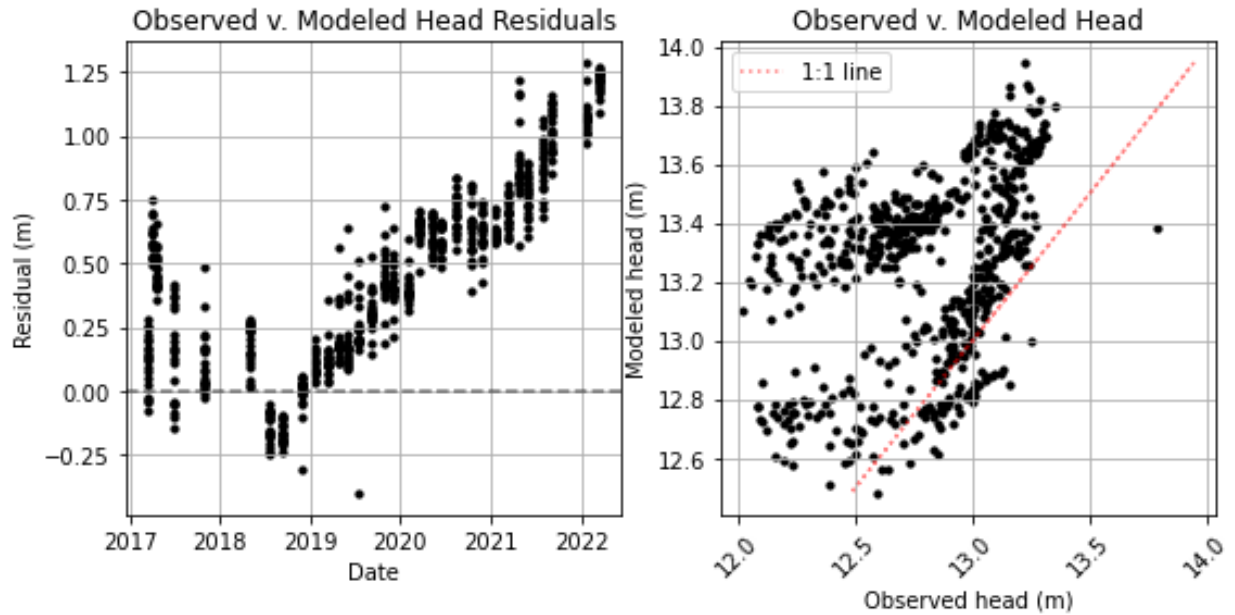
Figure 3-25. Orchard Model Residual Plots. *Left: Residuals between the observed and modeled groundwater head in the twenty monitoring wells. Right: Observed v. modeled heads in the monitoring wells. Most residuals are less than 1 m. There is a pattern of increasing residuals towards the end of the observation period (group of points in the upper left corner), indicating there is a process impacting groundwater flow near the orchard that is not captured in the groundwater flow model. Modeled heads and residuals plot above the dashed lines, indicating the model tends to overestimate heads.*

In addition to the head residuals, the modeled gradient was compared to the groundwater gradient observed in the monitoring wells. The gradient is characterized by its magnitude and direction. The magnitude influences the speed of groundwater flow to the wells and is important in the outcome of transport simulations. The model represents the observed gradient well and there is no obvious trend or clustering in the residuals (Figure 3-26). Gradient direction controls the position of the source area relative to the well. The modeled gradient heading somewhat represents the average observed heading; however, the modeled heading tends to be too far southwest at times when the observed gradient was more in a direction towards the south or southeast (Figure 3-26). Because the monitoring well source

areas are mostly within the orchard or just beyond in neighboring orchards, matching the model gradient direction to the observed gradient is not as important as the gradient magnitude. Additionally, since groundwater storage is not being calculated in this model, the trend in the groundwater head residuals does not indicate a significant impact to the transport model results.
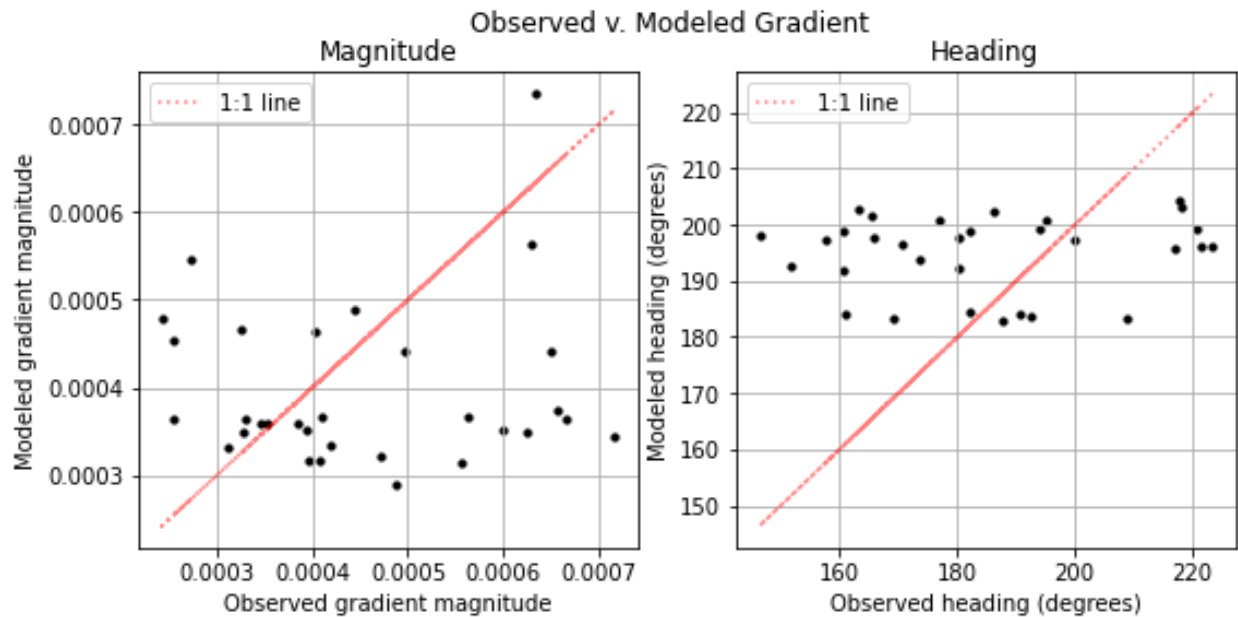
Figure 3-26. Orchard Model vs. Observed Gradient Plots. Observed gradient is calculated from groundwater elevation at twenty monitoring wells over 32 monitoring events. Left: Observed gradient magnitude is compared to the modeled gradient. Right: Observed gradient direction is compared to the model gradient direction.

Water mass balance errors during the model runs were less than 1%, with an average mass balance error of less than 0.1%. Though there is a shallow lateral hydraulic gradient, the high effective horizontal conductivity results in more lateral groundwater flow than vertical (Table 3-9; Figure 3-27). The averaged water budget indicates that the mass balance was overall slightly drying during the 60-year simulation period. The average recharge over the whole simulation period is only 7 cm/year. Inclusion of

the geologic heterogeneity in the groundwater model produces an irregular flow field as the water passes through coarse and fine sediments (Figure 3-28). Fast, lateral flow dominates in the coarse deposits and slow, vertical flow dominates in the fine deposits (Figure 3-29).

Table 3-9. Model Averaged Water Budget

Water Budget (m³/day)	Average Inflow	Average Outflow
Constant Head	676	760
Bottom flux	0	224
Recharge	295	0
Total:	971	984
ΔStorage	26	12
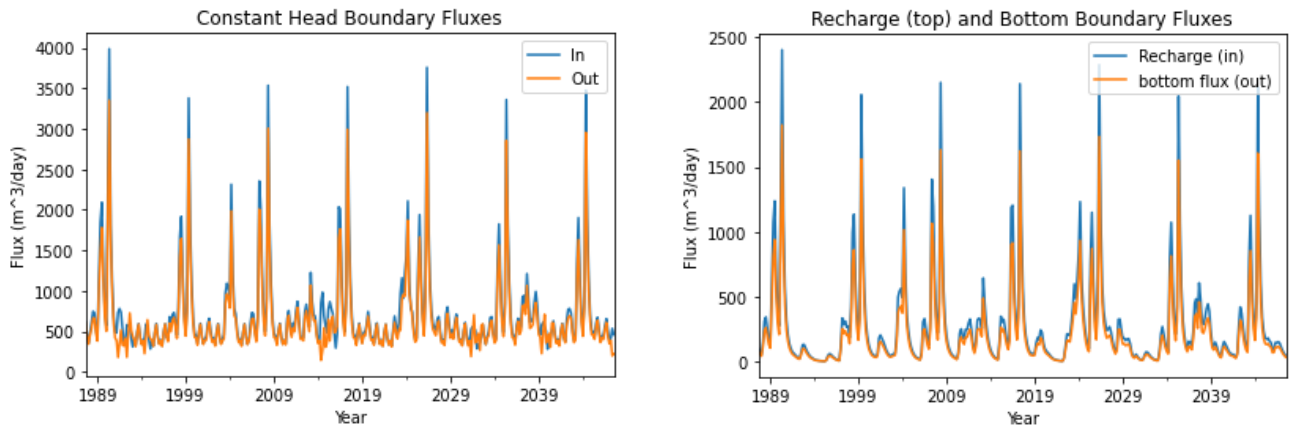
Figure 3-27. Modeled Groundwater Fluxes. *Left: Lateral groundwater flux through the four sides (constant head boundaries) of the model. Right: Vertical groundwater flux in through the top (recharge) and out through the bottom of the model.*
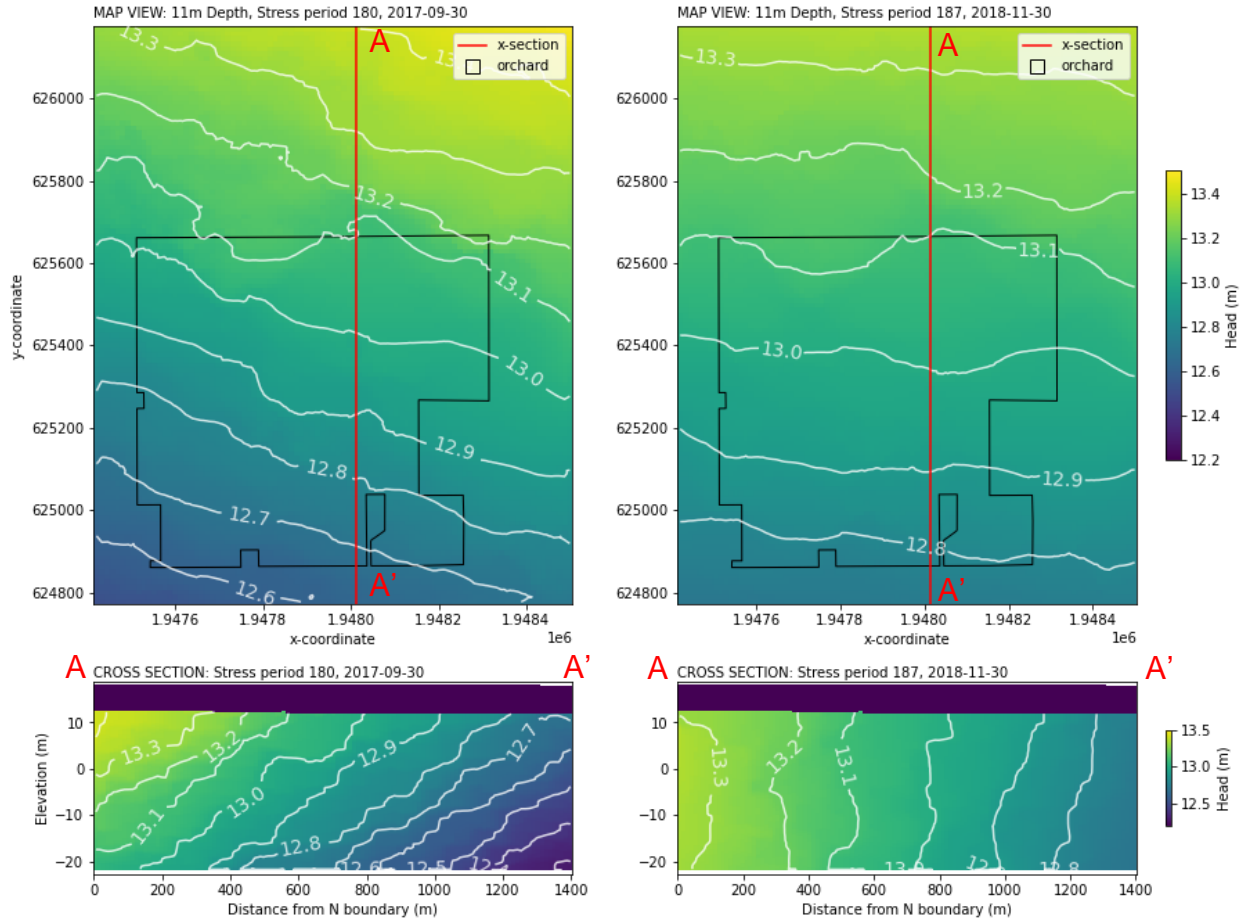
Figure 3-28. Modeled Groundwater Head Contours with Heterogeneous Geology. *Top: map view of groundwater head at 11m depth (4m into the saturated aquifer). Bottom: cross section view of groundwater head from north to south through the middle of the model area. Left side: modeled heads in September 2017. Groundwater flow is from the northeast with a stronger vertical gradient. Right side: modeled heads in November 2018. Groundwater flow is from the north with a weak vertical gradient.*
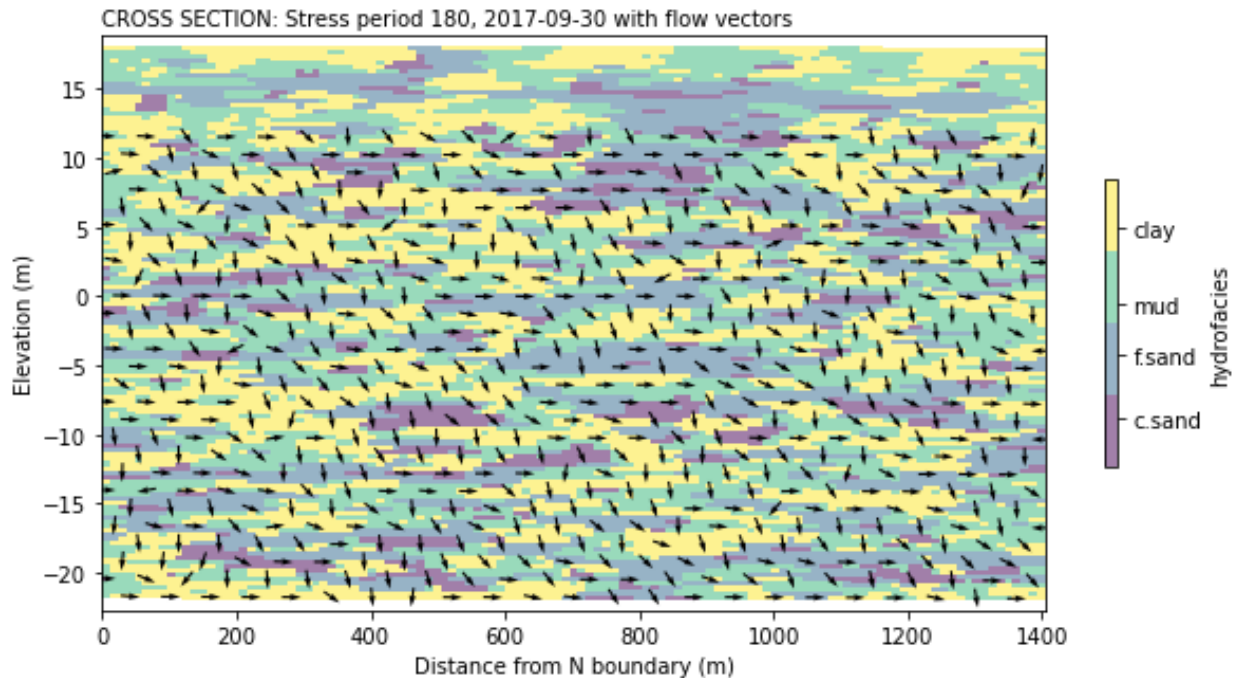
Figure 3-29. Modeled Groundwater Flow Vectors Cross Section. Cross section from north to south through the middle of one realization of the geologic model. Flow vectors from the groundwater model are superimposed. Changes in flow direction are mostly caused by groundwater passing through different geologic units. The geologic model includes four hydrofacies: coarse sand (c. sand), fine sand (f.sand), mud, and clay.

3.5.1.2 Vertical Head Gradient

The vertical head gradient was validated against data from a cluster of multilevel USGS monitoring wells located near the southeast corner of the orchard at the intersection of California Ave and Stone Ave (Table 3-10). Based on groundwater elevations measured between 2004 and 2006, the shallow vertical gradient (up to a depth of ~50 m) ranges from zero or slightly upward, to 1-2% downward. The vertical gradient was estimated by comparing groundwater elevations measured simultaneously in wells screened at a shallow level (12 m depth) and mid-level (55 m depth). The average vertical gradient based off the USGS well groundwater elevation measurements was about 0.5%, close to the estimate of vertical

gradient used in the model. The average vertical gradient in the model is about 0.5% downward and about 90% of the time the model vertical gradient is between 0.03% and 2.5% downward.

Table 3-10. On-Site USGS Well Cluster

USGS Well ID	Coordinates	Location relative to orchard	Data availability	Screened interval (ft bgs)	Vertical gradient (%)		
					min	max	avg
373726121051001				30-34.8	-0.07 (up)	1.48	0.46
373726121051002	37.6241, -121.0861	Adjoining to SE	2004-2006	179-183	-	-	-
373726121051003				274-279.5	1.4	5.2	3.5

Vertical groundwater flow depends on both the vertical head gradient and the vertical hydraulic conductivity per Darcy's Law (4). The vertical anisotropy ratio between the horizontal hydraulic conductivity and the vertical hydraulic conductivity used in the model was 1:10. There is research suggesting that the standard 1:10 ratio used in many models may underestimate actual anisotropy, and anisotropy may range from 1:10 to $1:10^5$ with a ratio of $1:10^3$ perhaps being more common (Fogg 1986; Tanachaichoksirikun et al. 2020). In this study, model convergence errors were encountered if anisotropy ratios much higher than 1:10 were used. It is speculated that the convergence errors occurred because recharge was applied evenly across model cells intersecting the water table at the rate indicated by the vadose zone model. A uniform recharge rate was used for all cells nearest to the corresponding vadose zone model profile, which is a simplification of spatial variability that is likely to exist within a block. Within a local area of heterogeneous sediments, recharge rates are more likely to be higher in cells with higher hydraulic conductivity (sand) than low hydraulic conductivity (clay). A very high anisotropy in the model, particularly in areas with clay, limits the flow of water through the cell and would contribute to model convergence errors. This is a side effect of not using integrated 3D vadose zone and groundwater models. However, the high-resolution geologic model with juxtaposed hydrofacies is an explicit representation of anisotropy in the model (Weissmann and Fogg 1999; Maples et al. 2019).

3.5.1.3 Bottom Flux

In the regional model, domestic pumping was considered to have negligible impact in the model area, and pumping for irrigation was estimated using the FARM package for MODFLOW (Phillips et al. 2015). Most irrigation water used this area is imported surface water supplied by the Modesto Irrigation District via a canal distribution system. The Farm Process estimates groundwater pumping in the region as the difference between surface water supply and land use demand. For the last year of the regional model, 2004, the estimated pumping rate per square meter in the vicinity of the orchard was 19.5 cm/year. The flux rate out through the bottom of the orchard model corresponds to the bottom flux out of layer 7 of the regional model, and is 30.9 cm/year in 2004.

The total bottom flux including pumping suggested by the regional model under 2004 conditions is 50.4 cm/year; however, recharge estimates were also much higher than current estimates. The regional model estimates recharge rates of 70 cm/year in the orchard vicinity in 2004, while recharge estimates for 2013-2021 in the vadose zone model of the orchard are much lower, ranging from less than 5 cm/year to around 20 cm/year. Historically, higher recharge rates at the orchard are likely because flood irrigation methods were previously used before switching to drip and micro-sprinkler irrigation (a change which occurred prior to 2013). The impacts of a prior management practice were not evaluated as part of this model. With lower recharge rates, the bottom flux is likely to be lower as well. The bottom flux of 50.4 cm/year was proportionally adjusted for each stress period based on the vadose zone model orchard average recharge for that stress period. The bottom flux was adjusted solely based on vadose zone model recharge rates and did not consider seasonal or historic impacts caused by changes in groundwater pumping rates. This is not anticipated to have a significant impact on modeled groundwater flow to the monitoring wells because of the low pumping rates anticipated in the model domain. However, the impact

that neglecting seasonal pumping would have on model results is to lower vertical gradients during the summer and therefore cause slightly longer travel times.

3.5.2 Monitoring Well Source Areas and Groundwater Age

Particle tracking results were assessed to approximate the monitoring well source areas and groundwater age distributions. Based on the particle tracking results, the flux-weighted average groundwater age in the wells is around 30-40 years (Table 3-11). The source areas for the monitoring wells are on average a distance of 150-180 m away. Particles released along the length of the well screen create groundwater age and source area distributions which represent groundwater mixing along the well screen. The groundwater age distribution is bimodal, with a fraction of water near the top of the well screen representing ages of 3-5 years, and the rest of the groundwater in the well generally 45-50 years old (Figure 3-30). The source area distance distributions span from less than 20 m to over 600 m from the well, with shorter distances being more frequent. These distributions represent around 70-90% of groundwater flow in the wells, with the other 10-30% of groundwater coming from the fine sediment deposits (slow flow and ages >60 years) or originating outside the model domain.
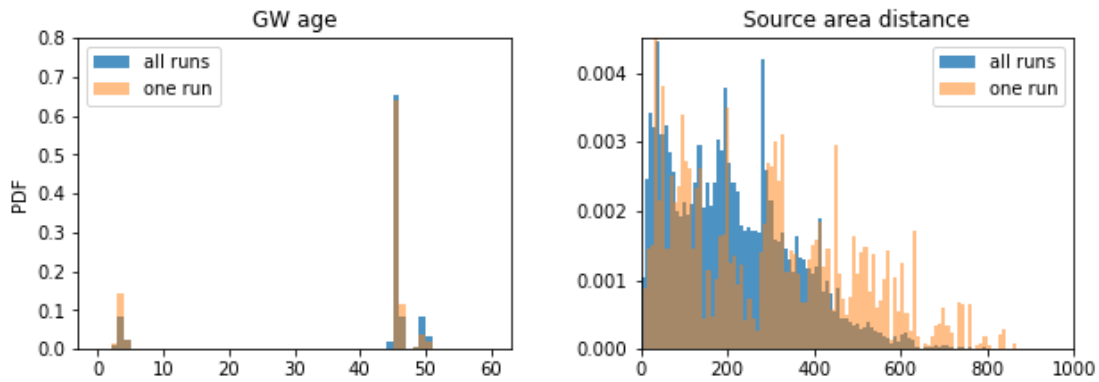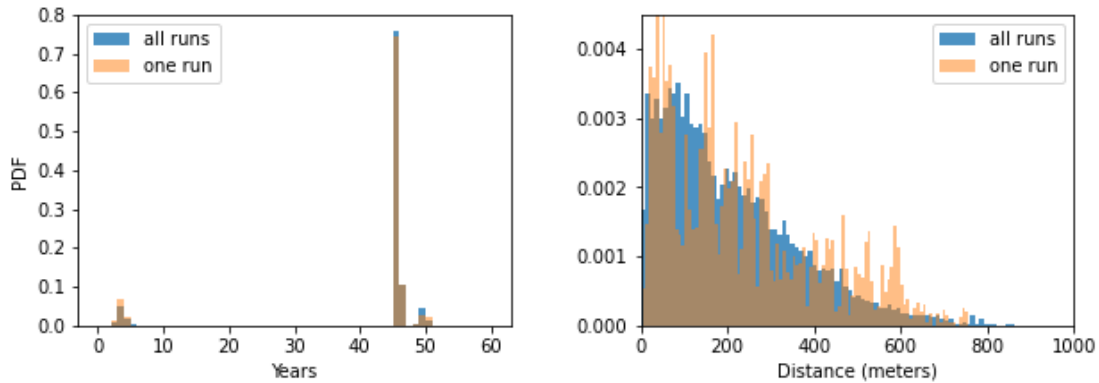
Figure 3-30. Particle Tracking Results. *Monte Carlo simulations performed with the heterogeneous geologic model (Scenario 1) using (A) 26 different combinations of hydraulic parameters with one geology realization, or (B) 26 different geology realizations with one combination of hydraulic parameters. The probability distribution of groundwater ages in the monitoring wells and the source area distance from the well is displayed for all 26 simulations and twenty wells (blue). The probability distribution of just one selected simulation (orange) produces similar pdfs (but less smooth) to all runs, indicating uncertainty in the hydraulic parameters or the heterogeneous geology does not have a significant impact on groundwater travel to the monitoring wells.*

The particle tracking results can be compared to a simple estimate of the groundwater ages. Using an average of 33% porosity and 7 cm/year recharge rates, the average vertical pore water velocity can be estimated as 21 cm/year. With this, the groundwater ages for a well screened from the water table up to 7 m into the aquifer would span one to 33 years. Groundwater ages predicted by the model are older because recharge rates as well as vertical hydraulic gradients are generally very low. The median of the orchard average recharge rate is only 4 cm/year. Thus, most vertical groundwater flow occurs in bursts in response to brief periods where the recharge rates are higher.

The impact of sources of uncertainty on the modeled groundwater ages and source area distances were evaluated separately. The sources of uncertainty evaluated were uncertainty in hydraulic parameter values and the locations of the heterogeneous sediment deposits. Varying the hydraulic parameter values while using the same geology simulation does not produce a significantly different distribution of groundwater ages or distances than varying the geology simulation while keeping the same hydraulic parameters (Figure 3-30 and Figure 3-31). Additionally, performing a single model run (i.e., not considering sources of uncertainty) was found to create nearly identical distributions for groundwater age, and similar distributions (but not as smooth) for source area distance. This suggests that given our conceptual model, uncertainty in the hydraulic parameters or geology has an insignificant impact on the groundwater travel times and source areas for the monitoring wells.

Table 3-11. Modeled Monitoring Well Source Area Distance and Groundwater Age

MW ID	Parameter uncertainty runs N=26			Geologic uncertainty runs N=26		
	Avg. age (years)	Avg. distance (m)	Flow fraction	Avg. age (years)	Avg. distance (m)	Flow fraction
1	32	82	0.70	42	63	0.91
2	35	105	0.80	39	143	0.85
3	26	122	0.60	37	218	0.84
4	33	198	0.73	33	191	0.96
5	34	153	0.77	39	231	0.94
6	25	146	0.83	37	246	0.94
7	28	189	0.77	41	282	0.96
8	31	221	0.78	42	291	0.97
9	33	221	0.81	32	168	0.98
10	20	122	0.43	44	284	0.95
11	18	112	0.38	40	122	0.87
12	33	232	0.71	41	141	0.89
13	34	103	0.75	40	130	0.82
14	20	88	0.59	37	176	0.95
15	21	157	0.72	29	198	0.87
16	34	185	0.74	38	240	0.94
17	29	143	0.66	43	222	0.85
18	20	62	0.59	39	139	0.84
19	24	112	0.72	37	123	0.84
20	28	147	0.61	39	113	0.87
Average	28	145	0.69	38	186	0.90
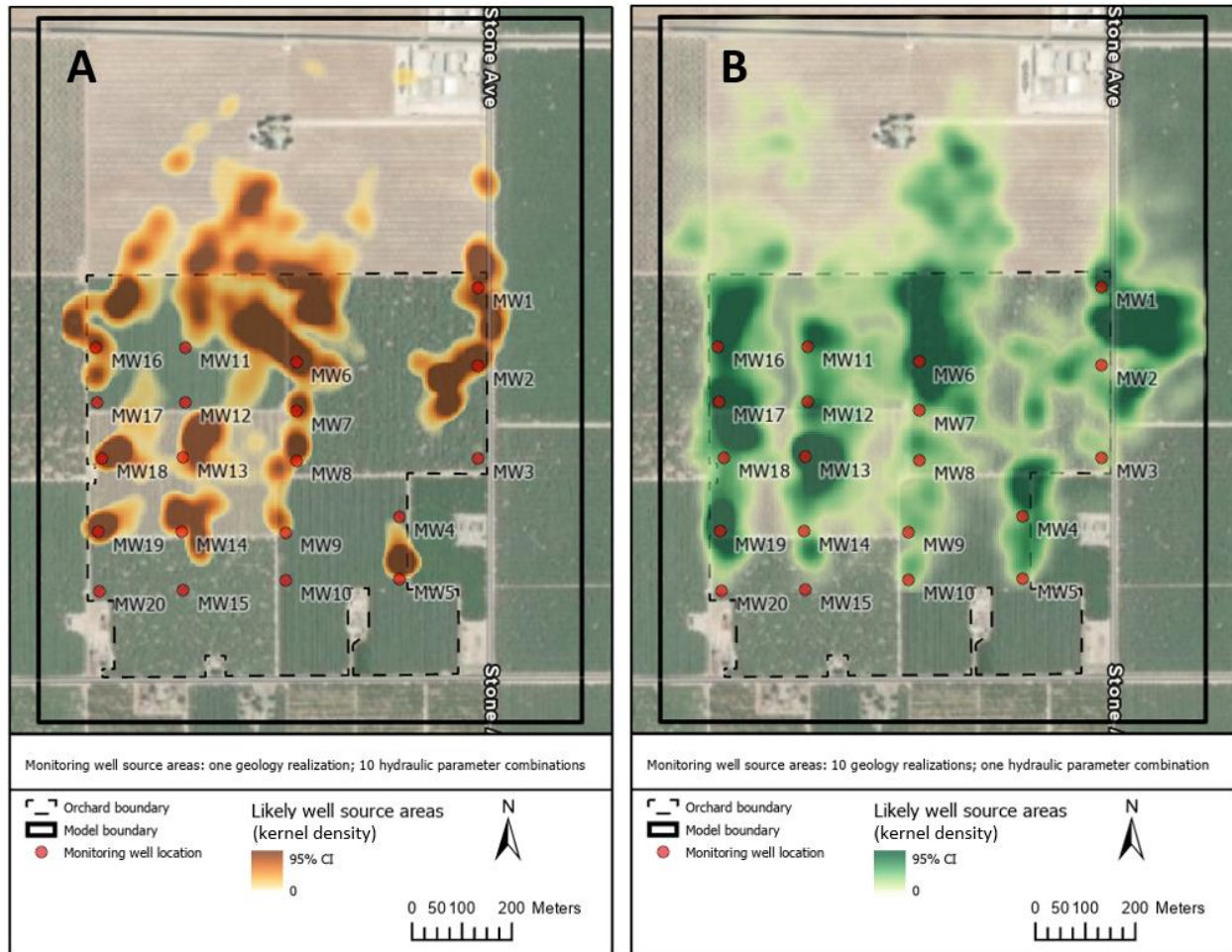
Figure 3-31. Modeled Monitoring Well Source Areas. Source areas predicted from particle backtracking to the water table. Kernel density shows locations at the water table likely to correspond to a source area for one of the twenty monitoring wells. A. Source areas predicted using one geology realization and 10 hydraulic parameter Monte Carlo simulations. B. Source areas predicted using 10 geology realizations and one set of hydraulic parameters.
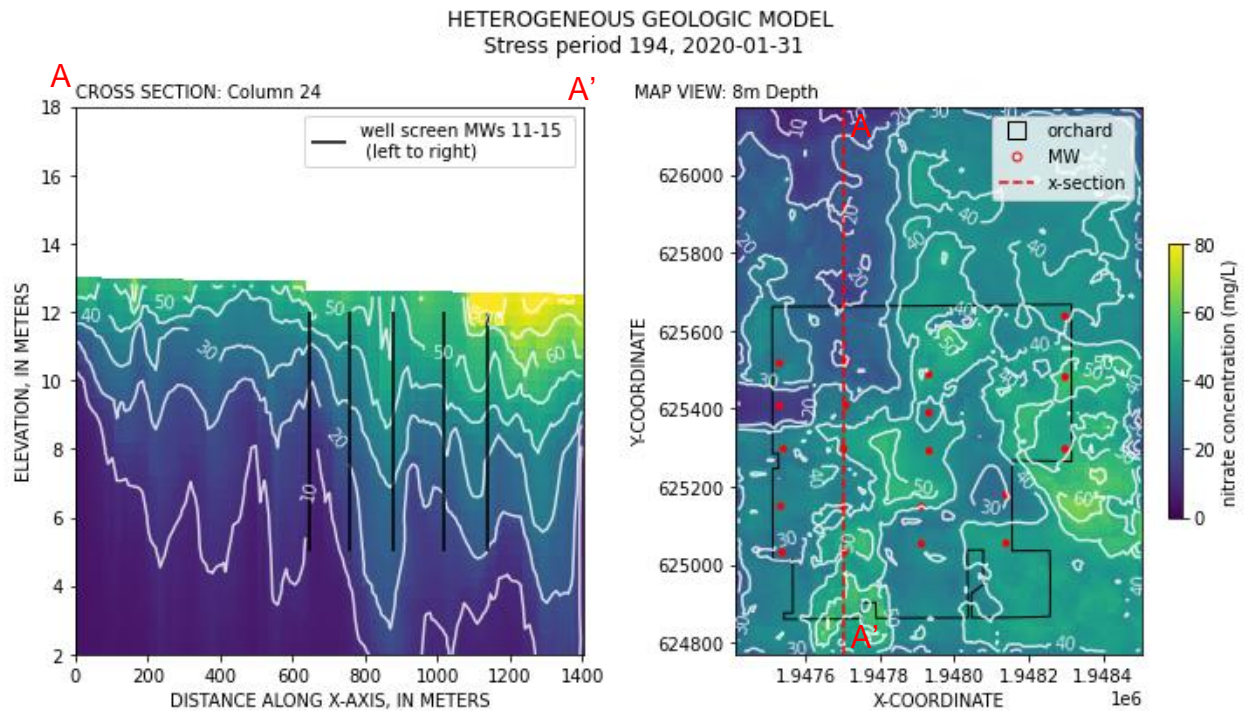
3.5.3 Modeled Nitrate Concentrations

Cumulative nitrate mass balance errors for the transport model were less than 0.01%. Runtime for the 60-year simulation in MT3DMS is approximately 26 hours. Ten runs were performed with different hydraulic parameters while maintaining the same geology. Another ten runs were performed with a

constant set of hydraulic parameters while varying the heterogeneous geology. One model run was conducted for each of the four scenarios in Table 3-8. A total of 24 model runs performed, with a computer processor time of approximately 25 days. Maps of the modeled groundwater nitrate concentrations across the orchard are presented in Figure 3-32 - Figure 3-35. The modeled monitoring well breakthrough curves are presented in Figure 3-36.

Modeled nitrate concentrations in the groundwater aquifer range from approximately 4 mg/L (the ambient concentration) to 120 mg/L. In the models with average nitrate in recharge, the maximum modeled nitrate concentrations in groundwater are lower, around 80 mg/L. Within the portion of the aquifer screened by the wells (approximately 7-14 m depth), 99% of the modeled nitrate concentrations are less than 100 mg/L. The range of nitrate concentrations in the groundwater model is consistent with the monitoring well observations (see Appendix).

Persistent nitrate "hot spots" that have been observed at the orchard are also recreated by the model. The hot spots appear in the versions of the model that use spatially variable nitrate concentrations in recharge. A hot spot has been observed in the vicinity of MW13 in the SW1 block since 2018, with concentrations typically exceeding 50 mg/L, up to 113 mg/L. In the homogeneous model with spatially variable nitrate in recharge, a hot spot with nitrate concentrations >80 mg/L appears in the vicinity of MW8-9 around 2004 and persists until 2033 (around 30 years). During this time, the hot spot migrates laterally roughly 100 m to the southwest and dissipates between MW10 and MW13, once it reaches a depth of about 13 m. The hotspot dissipates as it is pushed down (displaced) by recharge with lower nitrate concentrations during period of higher recharge rates. Development of the hotspot can be traced back to a period of elevated nitrate concentrations in the recharge inputs between 1997 and 2004 at MW7 and MW8. It is worth noting that the vadose zone model previously indicated that these elevated nitrate concentrations in recharge are the result of overlying almond tree growth at the surface for 10-20 years

prior to 1997. This suggests that the hotspot observed near MW13 is potentially the result of high local

nitrate concentrations leaching from the vadose zone, most likely within a few dozen meters upgradient

(north to northeast) of MW13. Depending on how long ago the hotspot developed, it may persist for

another 25 years under similar recharge rates.

Figure 3-32. Modeled Groundwater Nitrate Concentrations Scenario 1. Heterogeneous geology with

spatially variable nitrate in groundwater recharge. Modeled nitrate concentrations in January 2020. Left:

cross section view from north to south through the northwest (NW) and southwest blocks (SW1 and SW2) of

the orchard, passing through monitoring wells MW11-MW15. The black lines represent the well screen.

Fingering in nitrate plume is due to heterogeneous geology. Right: map view at a shallow depth near the

top of the well screens.
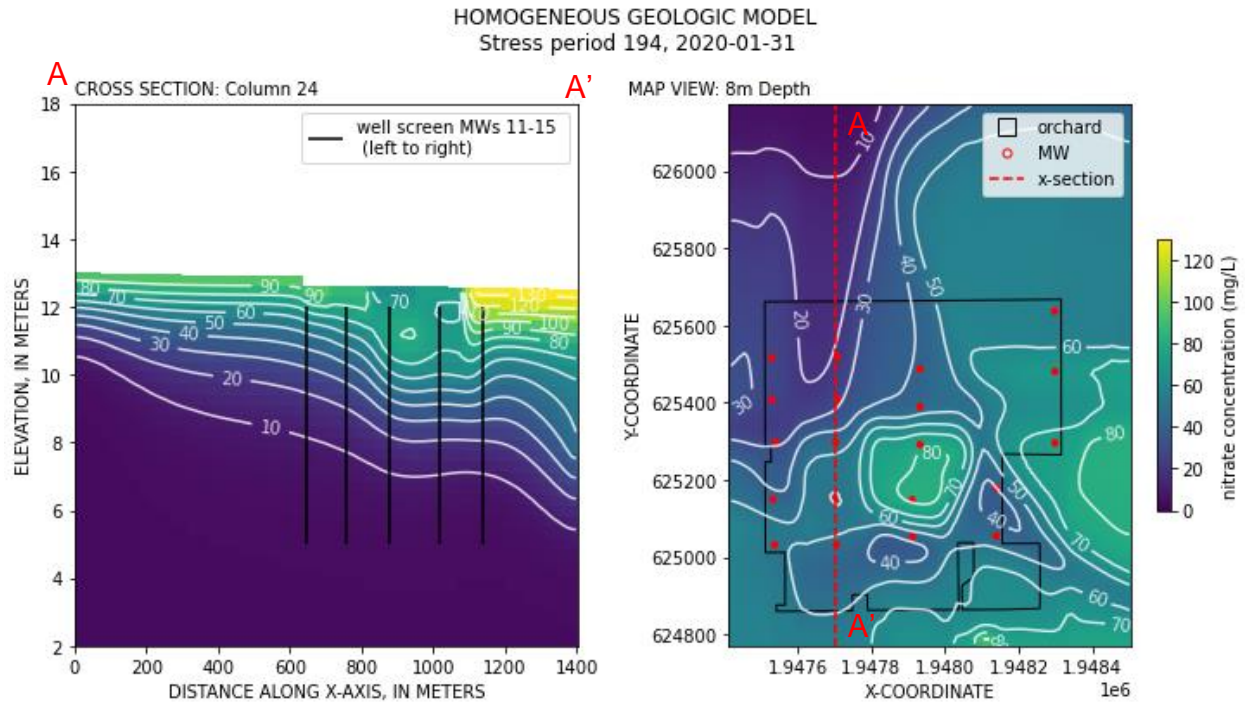
Figure 3-33. Modeled Groundwater Nitrate Concentrations Scenario 2. *Same as Figure 3-32 except the model uses a homogeneous geologic model with the spatially variable nitrate concentrations in recharge. Left: Cross section view shows no fingering, nitrate has not advanced downward as much as Scenario 1. Right: Nitrate hotspot around MW8 and MW9 (70-80 mg/L in center of orchard) was caused by high nitrate in recharge around MW7 and MW8.*

Figure 3-34. Modeled Groundwater Nitrate Concentrations Scenario 3. *Same as Figure 3-32 except the*

model uses orchard-average nitrate concentrations in recharge with a heterogeneous geologic model.

Left: Cross section view shows fingering, nitrate has advanced downward more quickly than in Scenario 1.

Right: Map view shows higher nitrate concentrations in shallow groundwater compared to Scenario 1.

HOMOGENEOUS GEOLOGIC MODEL & AVERAGED NITRATE IN RECHARGE
Stress period 194, 2020-01-31
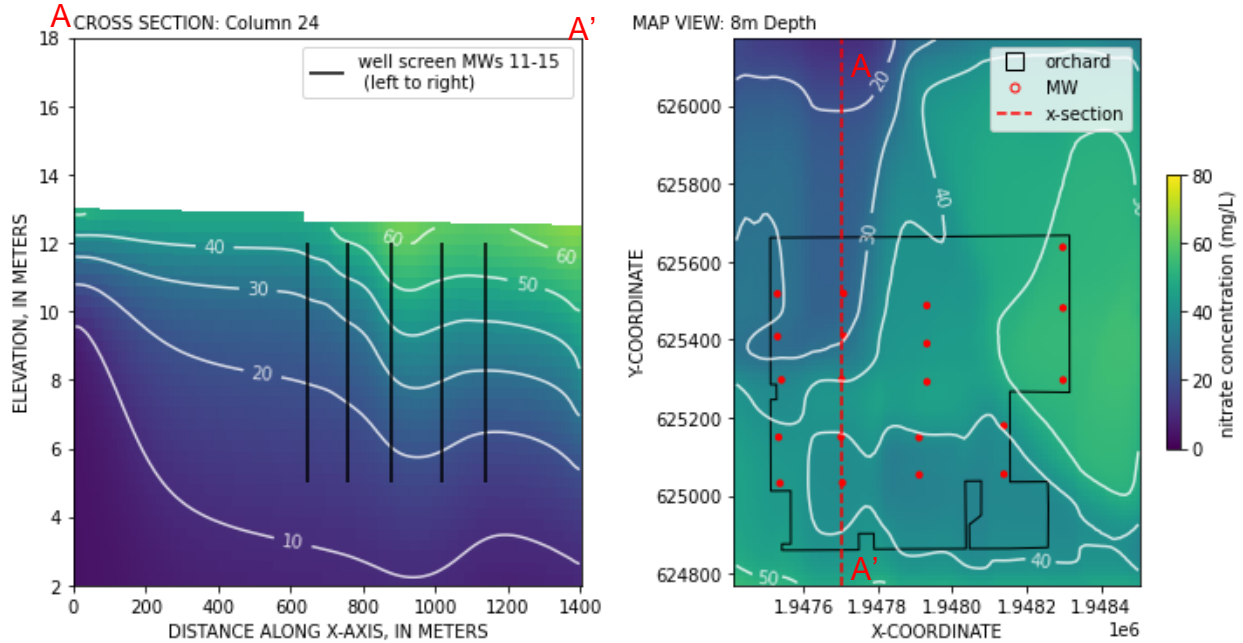
Figure 3-35. Modeled Groundwater Nitrate Concentrations Scenario 4. The model uses orchard-average nitrate concentrations in recharge and a homogeneous geologic model. Left: Cross section view shows no fingering, but nitrate has advanced downward at about the same rate as Scenario 1. Right: Map view shows little spatial variability in nitrate concentrations in shallow groundwater compared to the other scenarios.

Comparing cross sections of the nitrate plume demonstrates the impact of including geologic heterogeneity in the model (Figure 3-32 and Figure 3-35). The heterogeneous geologic model creates preferential flow paths, which become visible through fingering in the nitrate contaminant front. The effect is explicitly modeled macrodispersion. Macrodispersion is field-scale mechanical dispersion created by groundwater flow through a heterogeneous velocity field (Fetter et al. 2017). The heterogeneous velocity field in the groundwater model is created by the varying hydraulic conductivity of the four hydrofacies in the geologic model. As a result, in some locations, the nitrate plume has spread downward more quickly than in the homogeneous model within the same amount of time. For example,

in Figure 3-32, after roughly 30 years the front of nitrate concentrations exceeding 10 mg/L has spread roughly 2 m deeper in the heterogeneous model than in the homogeneous model in Figure 3-33. At other locations, the nitrate plume does not advance downward as quickly as in the homogeneous model. For example, in the heterogeneous model (Figure 3-32), the front of nitrate concentrations exceeding 40 mg/L has not spread as deep as in the homogeneous model in the area to the north of MW11 in the NW block (Figure 3-33). This is possibly because nearby preferential pathways provide routes for high local concentrations of nitrate near the surface to disperse. Also, as a result of increased dispersion, later concentrations modeled in the heterogeneous model are slightly lower because the mass becomes more spread out.

Figure 3-34 and Figure 3-35 show the impact of using an average nitrate concentration in recharge instead of the spatially variable nitrate as modeled in Figure 3-32 and Figure 3-33. Because of the lateral uniformity in the plume, it advances downwards more quickly than when the nitrate in the recharge is spatially variable. When combined with the homogeneous geology (Scenario 4), the plume of nitrate >10 mg/L extends down just about as far as the irregular front of the heterogeneous geologic model with the spatially variable nitrate in recharge (Scenario 1). When the average nitrate in recharge is used with the heterogeneous geologic model (Scenario 3), elevated nitrate concentrations penetrate the aquifer deepest and most quickly out of all the models.

3.5.3.1 Nitrate in Monitoring Wells

Monitoring well concentrations are modeled as the nitrate in the model cells intersecting the well screen weighted by the water flux passing through those cells. Breakthrough curves were prepared for the twenty monitoring wells and are presented in Figure 3-36. For the Monte Carlo simulation results, which correspond to model Scenario 1, the average modeled nitrate concentration in groundwater is presented

along with the maximum and minimum concentrations. Additionally, the results for Scenarios 2, 3, and 4 are presented in addition to measured nitrate concentrations collected between 2017 and 2021.

The breakthrough curves are remarkably similar whether considering the effects of either hydraulic parameter uncertainty or geologic uncertainty on the nitrate concentrations in the wells. The average uncertainty range in nitrate concentrations is about 7 mg/L when considering different hydraulic parameters, and 8 mg/L when considering different heterogeneous geology. This corresponds to an uncertainty of about ± 4 mg/L or $\pm 16\%$ in the predicted nitrate concentrations due to uncertainty in the hydraulic parameter values and the heterogeneous geology. In addition to the uncertainty ranges being similar, the shape of the breakthrough curves at individual wells is about the same regardless of the source of uncertainty considered. This means that the sources of uncertainty considered do not have a significant impact on the predicted nitrate concentrations in the monitoring wells.

Modeled nitrate breakthrough curves at the individual wells are unique, even within the same orchard blocks where the tree age, and water and fertilizer treatments are the same. While there is a general trend of increasing nitrate concentrations throughout the simulation, individual wells have a unique signature of bumps and dips in the breakthrough curve. These patterns are present whether heterogeneous or homogeneous geology is used in the model. This is interpreted to mean that the spatial variability in the nitrate inputs (in recharge) create most of the spatial variability in nitrate concentrations. As mentioned in the previous Section 3.5.3 Modeled Nitrate Concentrations discussing the nitrate plume maps, the effect of modeled geologic heterogeneity is the creation of preferential flow paths and added macrodispersion. The effects of preferential flow are visible in the breakthrough curves as earlier breakthroughs compared to the homogeneous model. Due to increased dispersion of mass, after the early breakthrough has passed, nitrate concentrations in the heterogeneous models are also typically lower than in the homogeneous model.
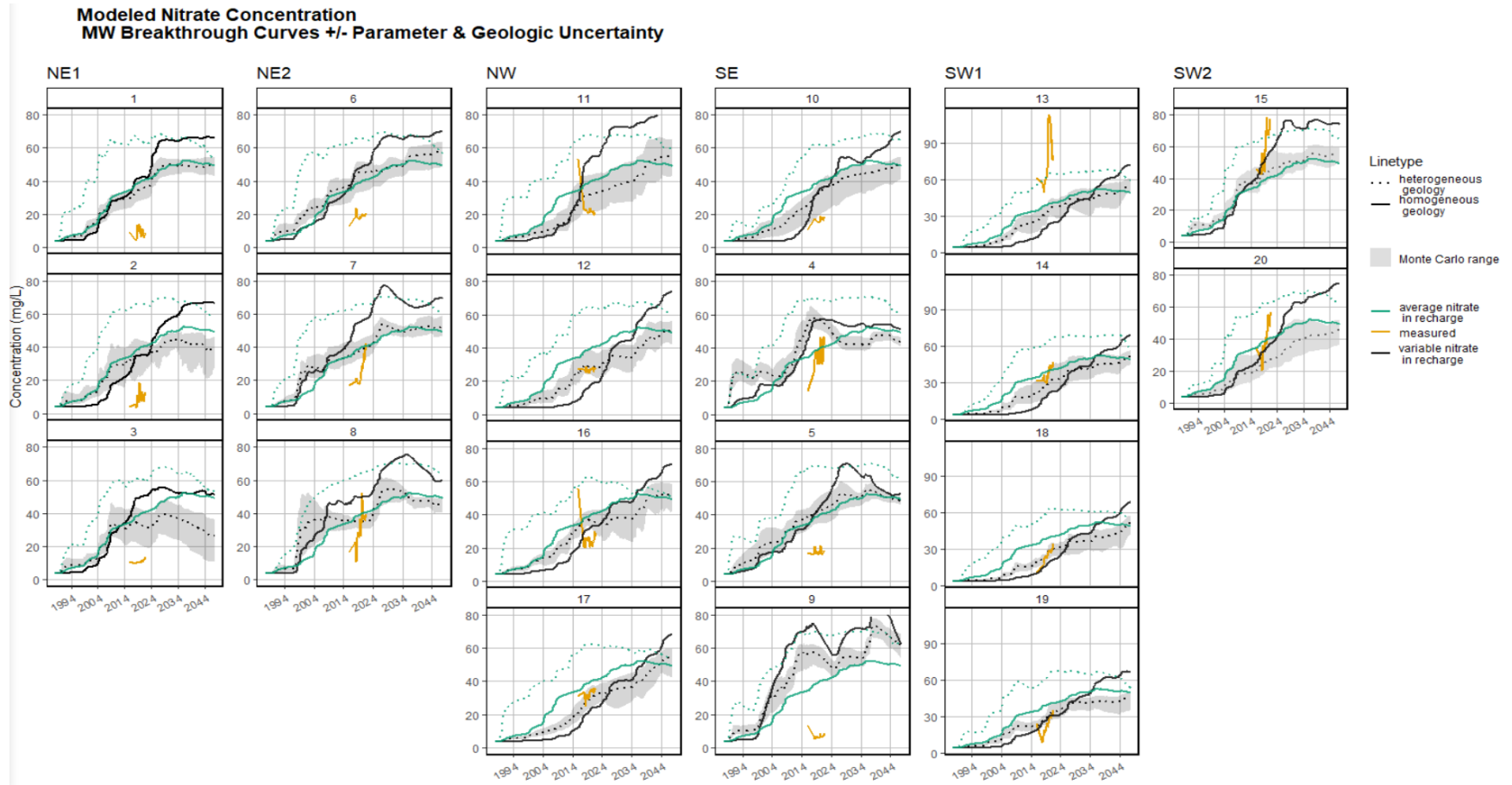
Figure 3-36. Modeled Nitrate Concentrations in Monitoring Wells. *Modeled nitrate concentrations in twenty monitoring wells are organized in columns by orchard block. Within the blocks, tree age and orchard management (fertilizer and irrigation) are the same. Scenario 1: dotted black line with gray area for Monte Carlo simulations. Scenario 2: solid black line. Scenario 3: dotted green line (no Monte Carlo simulations). Scenario 4: solid green line. Measured nitrate concentration in monitoring well: solid orange line.*

The observed nitrate concentrations are compared to nitrate predicted in the four model scenarios at the individual wells (Figure 3-36). Observed nitrate fits well for one or more of the models, such as MW12 and MW17 in the NW block and MW14, MW18, and MW19 in the SW1 block. At wells in the NE1 and, to a lesser extent, NE2 block, as well as MW5 and MW9 in the SE block, the modeled nitrate is higher than the observed nitrate. Recharge rates and nitrate concentrations were not modeled for conditions in the adjacent orchards. The recharge rate and nitrate concentration used in the model is from the nearest vadose zone model profile (monitoring well location) at the study site orchard. The adjacent orchards are not planted on the same schedule as the study site orchard and the trees are different ages. Wells in the NE1 block are the most upgradient and are likely to have source areas in the adjacent orchard. Modeled nitrate in MW13 in the SW1 block was lower than the observed nitrate.

While the transport model was created from the best available data for the orchard, differences between the modeled and observed nitrate concentrations in the well indicate there are additional sources of nitrate variability at scales smaller than the modeled block and field scale. A source of nitrate variability within the blocks that is not included in the model is possibly nutrient uptake variability from tree to tree. While nitrate concentrations in recharge in the model ranged from 10-150 mg/L, a broader range of nitrate concentrations up to 700 mg/L has been observed in porewater collected from below the root zone in the orchard. This indicates that the actual source variability is likely higher than the modeled variability.

At the orchard scale, predictions across the twenty wells are aggregated and compared to orchard average observations. Concentrations across all monitoring wells and model runs are summarized in one breakthrough curve presented in Figure 3-37 and Figure 3-38. Figure 3-37 displays the average concentration in the monitoring wells predicted in Scenario 1, which is likely to be the most realistic model. The range of concentrations across the twenty wells in a given year is shown to compare the

spatial variability created by the different scenarios tested in Figure 3-38. In Figure 3-37, the overall trend for modeled nitrate concentrations in the monitoring wells is to steadily increase from the starting concentration of 4 mg/L to an average of 50 mg/L at the end of the simulation in 2047. Mid-way through the simulation, around the present day (2017-2021), the modeled nitrate concentrations range from around 15-65 mg/L with an average between 30-40 mg/L. The range of measured nitrate concentrations is around 4-113 mg/L; 90% of the measured concentrations are within about 8-65 mg/L. The heterogeneous geologic model with spatial variability in recharge (Scenario 1) successfully recreates much of the spatial variability observed in groundwater nitrate concentrations.
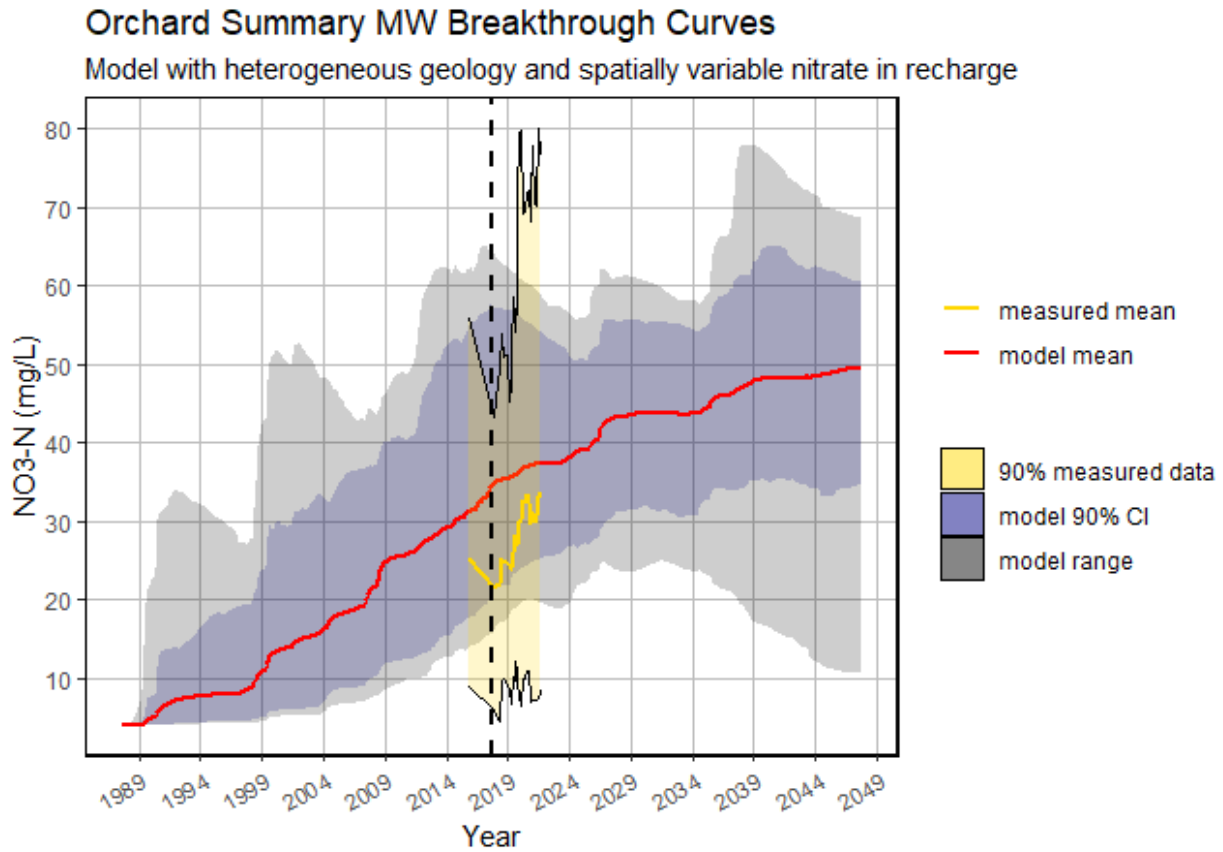
Figure 3-37. Orchard-Scale Summary of Modeled Nitrate in Monitoring Wells; Scenario 1. *Averaged modeled nitrate concentration across 20 monitoring wells (red line). Model range (gray) represent spatial*

variability in nitrate concentrations across the orchard more so than uncertainty in the geologic model or the hydraulic parameter values. Spatial variability in model Scenario 1 (gray) is close to the measured spatial variability (shaded yellow). Average measured concentrations (yellow line) are slightly lower than modeled nitrate (red line) but are within 90% of modeled concentrations (blue).

In addition to recreating much of the measured spatial variability in nitrate, average modeled nitrate concentrations are also close to average measured concentrations. For Scenario 1, the average modeled nitrate concentrations across the 20 wells and 25 model runs (N=500) are typically within 10 mg/L (average difference of 6 mg/L) of the average measured nitrate concentrations. The modeled concentrations in all four scenarios slightly but consistently overestimate the orchard average nitrate concentrations. However, the models also capture the general trend of increasing concentrations by about 2 mg/L per year observed in the measured data between 2017 and 2021. Much earlier breakthrough was observed in Scenario 3, resulting in modeled concentrations much higher than the observations. So, while at individual wells the modeled concentrations may appear to differ from the observations, aggregated across 20 wells at the orchard scale, model Scenario 1 decently represents the observations.
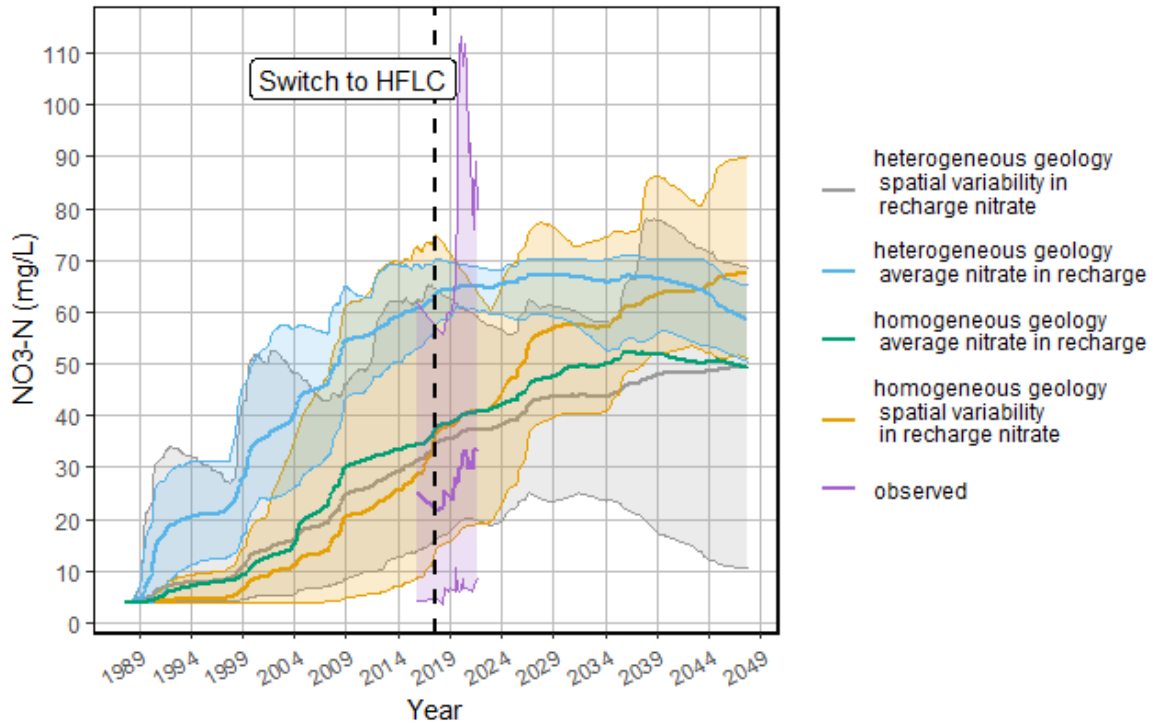
Figure 3-38. Effect of Modeled Spatial Variability on Nitrate in Shallow Groundwater Wells at the Orchard Scale. *Scenario 1: gray. Scenario 2: orange. Scenario 3: blue. Scenario 4: green. Observed nitrate concentrations: purple. Scenario 4 is a simple model to develop and produces average nitrate concentrations similar to the most complex model (Scenario 1), but does not capture spatial variability in shallow groundwater nitrate concentrations caused by spatial variability in nitrate leaching from the vadose zone.*

In Figure 3-38, model Scenarios 1 and 2 (gray and orange) produce the same spatial variability in groundwater nitrate concentrations, regardless of the geologic model used. This is interpreted to mean that heterogeneous geology is not the primary source of spatial variability in groundwater nitrate concentrations. Meanwhile, Scenario 4, the model with the least spatial variability, produces average nitrate concentrations very similar to Scenario 1, the model with the most spatial variability. However,

Scenario 4 only predicts average concentrations at the orchard, and does not predict a distribution of nitrate concentrations. Lastly, Scenario 3 predicted concentrations significantly higher than the other models. Nitrate concentrations predicted in the wells in Scenario 3 are on average 20 mg/L higher Scenario 1. The range of nitrate concentrations is also narrower; on average the range is about 18 mg/L, demonstrating lower spatial variability. Thus, while modeling heterogeneous geology will result in some spatially variable nitrate concentrations in groundwater, most of the spatial variability observed at the orchard in the monitoring wells is understood to result from spatial variability in nitrate in the recharge.

3.5.3.2 Modeled Nitrate Compared to Regional Concentrations

Modeled nitrate concentrations in the orchard monitoring wells were compared to measured regional groundwater nitrate concentrations. A historic record of regional groundwater nitrate concentrations is downloaded from the USGS database of measurements collected from shallow groundwater wells in Stanislaus County (U.S. Geological Survey n.d.). Since 1947, regional shallow groundwater nitrate concentrations have been more likely to be less than 10 mg/L. There appears to be an increasing trend in shallow nitrate concentrations over time (Figure 3-39). The measured and modeled orchard-average nitrate concentrations fit in among the range of regional nitrate concentrations. However, nitrate concentrations in the orchard are on the high end compared to shallow groundwater in the region.
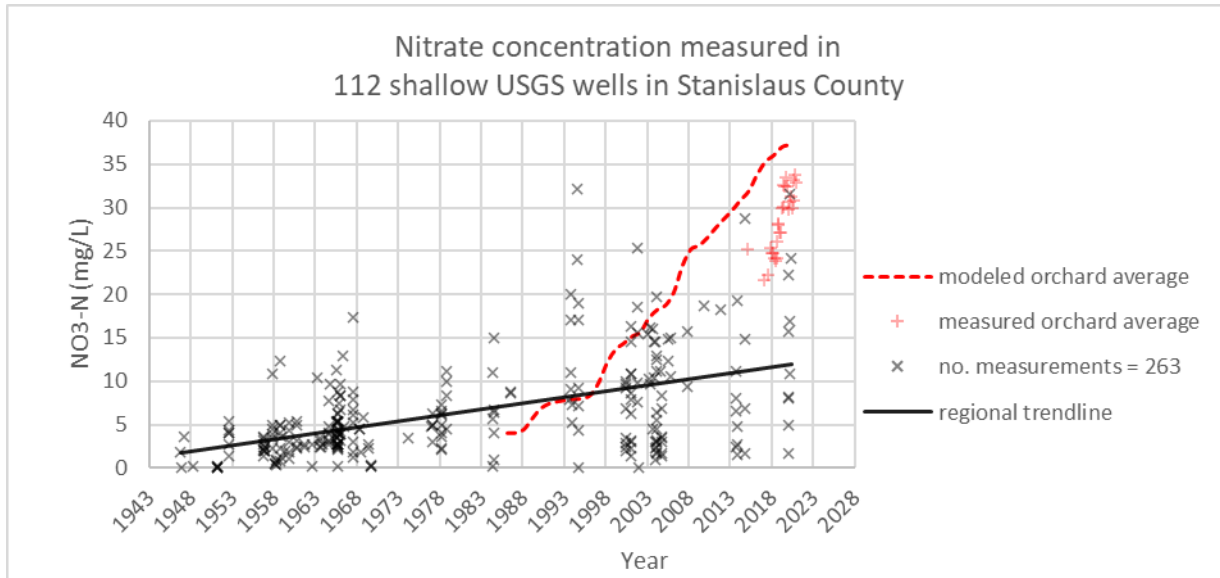
Figure 3-39. Historic Record of Nitrate Concentrations in Groundwater in Stanislaus County. *Nitrate concentrations measured in shallow groundwater wells from USGS since 1947. USGS measurements are fit with a linear trendline. Nitrate concentrations measured in the twenty monitoring wells are averaged and plotted as one red plus for each sampling event. Modeled orchard-averaged nitrate is plotted as a red dashed line.*

3.6 Discussion

3.6.1 Impact of HFLC on Shallow Groundwater Quality

Nitrate loading from the almond orchard is predicted to decrease by about 40% in response to HFLC; however, average nitrate concentrations in shallow groundwater wells at the orchard are predicted to continue to rise for the next 30 years under the current management and climate. Average nitrate concentrations predicted in the monitoring wells at the end of the simulation in 2047 is 50 mg/L. It is unlikely that average nitrate concentrations in the wells would continue to increase beyond the maximum average nitrate concentration in recharge predicted by the vadose zone model, which is 60-80 mg/L.

- 114 -

Based on the vadose zone model results in Chapter 2, nitrate transport from the surface through the vadose zone takes around 10 years. Due to this delay, improvements in water quality due to HFLC will gradually start to appear at the water table around 2027. Purely advective particle tracking predicts that this water then travels 150-180 m through the aquifer to reach the wells, a process that takes on average 30-40 years, with only 10% of the water in the well younger than 10 years. It may take until 2060 or 2070 to see consistent improvements in shallow groundwater quality due to HFLC at the orchard scale. It will take decades longer for the impacts on groundwater quality to be fully realized.

Shallow groundwater flow is slow because of the low hydraulic gradient. In particular, the vertical gradient at the orchard is low. Groundwater flow models in other parts of the basin suggest the opposite historically, in which higher pumping for agriculture and higher recharge through added irrigation return flows has shifted natural flow patterns and increased vertical flow (Phillips et al. 2007). This orchard is different from these other parts of the basin for two reasons. First, there is little groundwater pumping in the vicinity of the orchard; irrigation water is mostly surface water supplied via canal, and there are only a few dwellings in the rural model area which would have a domestic well. Second, the recharge rates are low. High recharge rates create stronger vertical gradients as incoming water pushes downward. The orchard recharge rate in the model is based on data collected between 2013-2021, which includes several years with exceptionally low precipitation. The median orchard recharge is only 4 cm/year, which is a result of efficient irrigation practices and dry climate during the data collection period. In order to see improvements in shallow groundwater quality sooner than 40-50 years from now, recharge rates at the orchard would need to be raised, without simultaneously increasing the mass of nitrate leaching from the root zone.

Since future climate in California is likely to remain dry (Mann and Gleick 2015), increased recharge can only reliably happen through changes in farm management. Less efficient irrigation would

increase recharge rates but would also use more water during the growing season when it's most valuable, and may also increase nitrate leaching. Another solution to increase recharge is through on-farm recharge projects during the winter; a time when water is more plentiful, and fertilizer is not being applied. In addition to accelerating improvements in groundwater quality, on-farm recharge projects are promoted as a way to help replenish stressed groundwater resources (Marr et al. 2018). Groundwater modeling of Modesto at the regional scale has also found that a combination of improved nutrient management practices and winter recharge projects could reverse increasing trends in nitrate in wells within 10 years and result in improved groundwater quality overall (Bastani and Harter 2019). Bastani and Harter (2019) predicted that by reducing nitrate leaching rates to 30 kg/ha/year within well source areas and increasing recharge by an additional 30-90 cm/year with winter recharge projects, groundwater quality in public supply wells would significantly improve within 20 years.

Increased recharge rates would not only speed up groundwater flow to the wells – it would also accelerate transport in the vadose zone. This would temporarily increase leaching rates as nitrate in the soil profile is flushed out. In the long term, the increased recharge would dilute nitrate leaching to a lower concentration. In Chapter 2, the vadose zone model estimated that HFLC resulted in leaching rates of approximately 43 kg/ha/year. Increasing the average recharge rate by 40 cm/year would provide a volume of water sufficient to dilute leaching nitrate to an average concentration below 10 mg/L. In a simplified piston flow estimate, doubling recharge rates would halve the nitrate transport time. A tenfold increase in recharge would potentially improve shallow groundwater quality within as little as 5 years. Given the soil heterogeneity, the assumption of uniform flow in the piston flow model means this should be taken as a rough estimate. The soil heterogeneity may cause significant tailing in the nitrate breakthrough curve, which would reduce the pace of groundwater quality improvements. Future modeling efforts should evaluate recharge rates needed to reduce the nitrate concentrations in a desired faction of groundwater

wells below the MCL. Future modeling should also consider whether tailing in nitrate transport due to soil heterogeneity will cause significant delay in achieving water quality goals below the MCL. These efforts should include shallow domestic wells with small source areas and fast groundwater travel times, as well as deep public supply wells with large source areas and slower travel times.

3.6.2 The Role of Spatial Variability at the Orchard Scale

By testing model scenarios that include combinations of spatial variability in geologic media and in recharge nitrate concentrations, this study found that these sources of variability impact modeled well concentrations differently. Spatial variability in recharge nitrate concentrations caused most of the spatial variability in the groundwater concentrations at the orchard scale. Spatial variability in nitrate leaching from the vadose zone was caused by a combination of soil heterogeneity plus variable nitrogen and water application and uptake related to tree age (Chapter 2). Soil heterogeneity in the saturated zone affects the overall shape of the average breakthrough curve.

The actual spatial variability in nitrate concentrations in recharge is probably much larger than what was modeled in this study. This is based on nitrate concentrations measured in porewater collected from below the root zone at this orchard and several other orchard study sites in the Central Valley (Baram et al. 2016, Onsoy et al. 2005). The 1D vadose zone model restricts potential flow pathways and would reduce variability in nitrate leaching compared to a 3D heterogeneous vadose zone model. But, 3D vadose zone models face computational limitations. Unless models are refined to the pore scale, models will always upscale or simplify spatial variability to some extent. This study has also evaluated the effect of upscaling, or homogenizing, spatial variability to the orchard scale. Homogenizing spatial variability in nitrate leaching across the orchard produced similar average nitrate concentrations in the monitoring wells as the fully heterogeneous model when the homogenized nitrate leaching was combined with a homogenized geologic model. When combined with a heterogeneous geologic model, there was earlier

breakthrough and the first temporal moment (i.e., center of the plume with respect to time) is earlier due to the presence of preferential flow pathways. These findings are consistent with a related study considering the impacts of spatial variability on nonpoint nitrate transport at the scale (Henri et al. 2020). Henri et al. (2020) found that at the regional scale, models that upscale geologic and leaching variability are also reasonably representative of average conditions predicted by fully heterogeneous models, especially due to the mixing effects along well screens.

While homogenization of spatial variability may produce adequate results for long-term planning purposes (Henri et al. 2020), this type of model is lacking in that it does not predict 1) the distribution of contaminant concentrations in groundwater, or, 2) early breakthrough or tailing of contaminants in wells, which is known to occur in heterogenous geologic media. Early breakthrough and tailing are characteristics of anomalous transport, which is not suitably modeled using the advection-dispersion equation. If capturing these aspects of anomalous transport are important to the model purpose, it is shown in this study, as well as Henri et al. (2020) and other studies such as Salamon et al. (2007), that including a representation of the heterogenous geology in combination with the advection-dispersion equation can reproduce characteristics of anomalous transport such as early breakthrough.

This study models spatial variability in nitrate leaching at one scale. Nitrate concentrations in recharge in the model inputs varied based on the monitoring well spacing, which on average is 118 m. The scale of the nitrate input variability happened to be close to the average distance of the monitoring wells from their source areas (150-180 m). While there is likely to be more spatial variability in nitrate leaching than what was modeled, modeling nitrate leaching variability at a scale finer than the well source area size is unlikely to change the predicted concentrations in the wells. However, regional-scale models of nitrate transport typically assign an average estimate for leaching to areas with the same land use and neglect spatial variability within the same crop type (as in Bastani and Harter 2019, Bastani and Harter

- 118 -

2020). This approach will model a narrower distribution of concentrations in shallow wells with small source areas than what would be produced using the correct scale of variability. This may be a concern when modeling a distribution of domestic wells with concentrations above the MCL at the regional scale, if the source areas are small.

The source area dimensions for a domestic well in the vicinity of the orchard is approximated using a simple computation described in Horn and Harter (2004). This method was found to be reasonable for wells with low pumping rates that do not strongly influence the local groundwater flow field (i.e., domestic wells), located in highly permeable aquifers (Horn and Harter 2004). In this method, the source area size depends on the pumping and recharge rates. The source areas tend to be several times longer than they are wide, especially when the recharge rate is small compared to the horizontal hydraulic conductivity and the lateral head gradient (as is the case at the orchard study site). Typical domestic source area widths of 1 to 60 m are described by Horn and Harter (2004). Pumping at a rate of 1 ac-ft/year, with a 10 m screen at an average depth of 46 m (Table 3-6), the source area of a domestic well near the orchard is estimated to be about 1 km long and 30 m wide. This source area size suggests that modeling spatial variability in recharge at a scale no larger than 1 km would be suitable for modeling domestic wells in this area. This scale is slightly larger than the orchard study site itself, which means that a simple model like Scenario 4 might be appropriate for predicting nitrate concentrations in a domestic well. The scale of spatial variability in the model is less likely to be an issue for wells with large source areas, like deep public supply wells with high pumping rates. Future research can evaluate the relationship between modeled spatial variability in nitrate leaching from the vadose zone and the distributions of predicted concentrations in pumping wells with different source area sizes.

3.7 Conclusion

Long-term solutions to addressing nitrate pollution of groundwater focus on reducing leaching from farms by improving nitrogen use efficiency in agriculture. This study developed a numerical groundwater model to simulate the response in shallow groundwater quality to a change in nitrogen management practices at an almond orchard that increased the NUE. Different model scenarios were performed to find what causes nitrate concentrations measured in shallow groundwater across the 56-ha study orchard site to vary by an order of magnitude.

Tracking nitrogen impacts on groundwater quality requires consideration of the distribution of nitrate concentrations in wells. Nitrate concentrations in a shallow well network spanning the orchard scale vary just as much as at the regional scale. Spatial variability in nitrate concentrations observed at the sub-orchard scale is found to be primarily caused by nonuniformity in nitrate leaching from the vadose zone. Modeling spatial variability in nitrate leaching from the vadose zone was necessary to reproduce the distribution of nitrate concentrations observed at the orchard monitoring wells. In order to use groundwater models to predict the probability distribution for nitrate concentrations in wells within a region to be below a certain threshold, it will be important to model leaching variability at a scale appropriate to the well source area sizes of concern. If spatial variability in nitrate leaching is not fully modeled, then the predicted nitrate distributions will be narrower, centered around the average. However, it was also found that simple models which upscale spatial variability are easy to develop and predict the average response well.

In this study, the dry climate in California's Central Valley, combined with high efficiency irrigation at the orchard, results in low recharge rates and therefore slow vertical groundwater flow to shallow wells. This means that in semiarid areas, even if nitrate leaching at the surface is reduced, it will take 40-50 years to start seeing improvements in shallow groundwater quality. It was noted earlier in

Hansen et al. (2017) that in Denmark, groundwater quality improvements were most likely possible within 30 years. This was possible under a wetter climate, because Denmark annually receives on average three times the precipitation of California's Central Valley. Artificially increasing recharge rates on farms through Managed Aquifer Recharge (MAR) has the capacity to cut the delay in groundwater quality improvements by decades. The results of this study encourage future research to investigate the use of MAR in improving groundwater quality. Additionally, these results highlight how in dry climates, relying on nitrogen efficiency goals alone may, in some regions, not improve shallow groundwater quality within our lifetimes.

3.8 References

Allen, Richard G., Albert J. Clemmens, Charles M. Burt, Ken Solomon, and Tim O'Halloran. 2005. "Prediction Accuracy for Projectwide Evapotranspiration Using Crop Coefficients and Reference Evapotranspiration." *Journal of Irrigation and Drainage Engineering* 131 (1): 24. https://doi.org/10.1061/(ASCE)0733-9437(2005)131:1(24).

Allen, Richard G., Luis S. Pereira, Terry A. Howell, and Marvin E. Jensen. 2011. "Evapotranspiration Information Reporting: I. Factors Governing Measurement Accuracy." *Agricultural Water Management* 98 (6): 899–920. https://doi.org/10.1016/j.agwat.2010.12.015.

Badr, M. A., A. S. Taalab, and W. A. El-Tohamy. 2011. "Nitrogen Application Rate and Fertigation Frequency for Drip-Irrigated Potato." *Australian Journal of Basic and Applied Sciences* 5 (7): 817–25.

Baram, S., V. Couvreur, T. Harter, M. Read, P. H. Brown, J. W. Hopmans, and D. R. Smart. 2016. "Assessment of Orchard N Losses to Groundwater with a Vadose Zone Monitoring Network." *Agricultural Water Management* 172 (July): 83–95. https://doi.org/10.1016/j.agwat.2016.04.012.

Baram, S., V. Couvreur, T. Harter, M. Read, P.H. Brown, M. Kandelous, D.R. Smart, and J.W. Hopmans. 2016. "Estimating Nitrate Leaching to Groundwater from Orchards: Comparing Crop Nitrogen Excess, Deep Vadose Zone Data-Driven Estimates, and HYDRUS Modeling." *Vadose Zone Journal* 15 (11): 1–13. https://doi.org/10.2136/vzj2016.07.0061.

Bastani, Mehrdad, and Thomas Harter. 2019. "Source Area Management Practices as Remediation Tool to Address Groundwater Nitrate Pollution in Drinking Supply Wells." *Journal of Contaminant Hydrology* 226 (October): 103521. https://doi.org/10.1016/j.jconhyd.2019.103521.

———. 2020. "Effects of Upscaling Temporal Resolution of Groundwater Flow and Transport Boundary Conditions on the Performance of Nitrate-Transport Models at the Regional Management Scale." *Hydrogeology Journal* 28 (4): 1299–1322. https://doi.org/10.1007/s10040-020-02133-x.

Bellvert, Joaquim, Karine Adeline, Shahar Baram, Lars Pierce, Blake L. Sanden, and David R. Smart. 2018. "Monitoring Crop Evapotranspiration and Crop Coefficients over an Almond and Pistachio Orchard Throughout Remote Sensing." *Remote Sensing* 10 (12): 2001. https://doi.org/10.3390/rs10122001.

Botros, Farag E., Yuksel S. Onsoy, Timothy R. Ginn, and Thomas Harter. 2012. "Richards Equation–Based Modeling to Estimate Flow and Nitrate Transport in a Deep Alluvial Vadose Zone." *Vadose Zone Journal* 11 (4): vzj2011.0145. https://doi.org/10.2136/vzj2011.0145.

Brown, Patrick. 2010. "Development of a Nutrient Budget Approach to Fertilizer Management in Almond." Final Report 2008-13 10-0039SA. CDFA Fertilizer Research and Education Program. https://www.cdfa.ca.gov/is/ffldrs/frep/pdfs/completedprojects/10-0039-SA_Brown.pdf.

Brown, Patrick, Sebastian Saa, Saiful Muhammad, and Sat Darshan Khalsa. 2020. "Nitrogen Best Management Practices." Almond Board of California. https://www.almonds.com/sites/default/files/2020-12/ABC_Nitrogen_8.5x11_vmags.pdf.

California Water Boards. 2022. "Groundwater Issue: Groundwater Quality." April 11, 2022. https://www.waterboards.ca.gov/water_issues/programs/groundwater/issue_gq.html.

Carle, Steven. 1999. "T-PROGS: Transition Probability Geostatistical Software." https://www.researchgate.net/profile/Steven-Carle/publication/284548821_T-PROGS_Transition_Probability_Geostatistical_Software_Version_21/links/604127ef4585154e8c77e100/T-PROGS-Transition-Probability-Geostatistical-Software-Version-21.pdf.

Doll, David, and Kenneth Shackel. 2016. "Drought Management for California Almonds." *Crops & Soils* 49 (2): 28–35. https://doi.org/10.2134/cs2016-49-2-9.

Domenico, P. A., and M. D. Mifflin. 1965. "Water from Low-Permeability Sediments and Land Subsidence." *Water Resources Research* 1 (4): 563–76.

Drechsler, Kelley, Allan Fulton, and Isaya Kisekka. 2022. "Crop Coefficients and Water Use of Young Almond Orchards." *Irrigation Science* 40 (3): 379–95. https://doi.org/10.1007/s00271-022-00786-y.

Dubrovsky, N. M., K. R. Burow, G. M. Clark, J. A. M. Gronberg, P. A. Hamilton, K. J. Hitt, D. K. Mueller, M. D. Munn, L. J. Puckett, and B. T. Nolan. 2010. "Nutrients in the Nation's Streams and Groundwater, 1992–2004, Circular 1350." *US Geological Survey, Reston, VA, USA*. https://pubs.usgs.gov/circ/1350/.

EU Nitrogen Expert Panel. 2015. "Nitrogen Use Efficiency (NUE) an Indicator for the Utilization of Nitrogen in Food Systems." Wageningen University, Alterra, Wageningen, Netherlands.

Farneselli, Michela, Paolo Benincasa, Giacomo Tosti, Eric Simonne, Marcello Guiducci, and Francesco Tei. 2015. "High Fertigation Frequency Improves Nitrogen Uptake and Crop Performance in Processing Tomato Grown with High Nitrogen and Water Supply." *Agricultural Water Management* 154 (May): 52–58. https://doi.org/10.1016/j.agwat.2015.03.002.

Faunt, Claudia. 2009. "Groundwater Availability of the Central Valley Aquifer, California." U.S. Geological Survey Professional Paper 1766. https://pubs.usgs.gov/pp/1766/PP_1766.pdf.

———. 2012. "Contours of Corcoran Clay Depth in Feet from Page (1986) for the Central Valley Hydrologic Model (CVHM)." USGS Science Data Catalog. 2012. https://data.usgs.gov/datacatalog/data/USGS:2eedd7e1-0522-465f-9478-c47e5263a46e.

Feddes, R. A., P. J. Kowalik, and H. Zaradny. 1978. *Simulation of Field Water Use and Crop Yield*. Simulation Monographs. Wageningen: Center for agricultural publishing and documentation.

Fetter, C. W. 2001. *Applied Hydrogeology*. 4th ed. Upper Saddle River, N.J: Prentice Hall.

Fetter, Charles Willard, Thomas Boving, and David Kreamer. 2017. *Contaminant Hydrogeology*. Waveland Press.

Fitts, Charles R. 2002. *Groundwater Science*. Amsterdam ; Boston: Academic Press.

Fleckenstein, Jan H., and Graham E. Fogg. 2008. "Efficient Upscaling of Hydraulic Conductivity in Heterogeneous Alluvial Aquifers." *Hydrogeology Journal* 16 (7): 1239–50. https://doi.org/10.1007/s10040-008-0312-3.

Fogg, Graham E. 1986. "Groundwater Flow and Sand Body Interconnectedness in a Thick, Multiple-Aquifer System." *Water Resources Research* 22 (5): 679–94. https://doi.org/10.1029/WR022i005p00679.

Gurevich, Hanna, Shahar Baram, and Thomas Harter. 2021. "Measuring Nitrate Leaching across the Critical Zone at the Field to Farm Scale." *Vadose Zone Journal* 20 (2): e20094. https://doi.org/10.1002/vzj2.20094.

Gurevich, Hanna, Iael Raij-Hoffman, Sat Darshan Khalsa, Patrick Brown, and Thomas Harter. n.d. "The Fate of Surplus N in an Almond Orchard: Mass Balance vs. Model."

Hansen, Birgitte, Lærke Thorling, Jörg Schullehner, Mette Termansen, and Tommy Dalgaard. 2017. "Groundwater Nitrate Response to Sustainable Nitrogen Management." *Scientific Reports* 7 (1): 8566. https://doi.org/10.1038/s41598-017-07147-2.

Harbaugh, Arlen W., Christian D. Langevin, Joseph D. Hughes, Richard G. Niswonger, and Leonard F Konikow. 2017. "MODFLOW-2005: USGS Three-Dimensional Finite-Difference Groundwater Model." U.S. Geological Survey. https://doi.org/10.5066/F7RF5S7G.

Harter, T., and J. R. Lund. 2012. "Addressing Nitrate in California's Drinking Water; Report for the State Water Resources Control Board." *Center for Watershed Sciences, University of California: Davis, CA, USA*. https://groundwaternitrate.ucdavis.edu/files/139110.pdf.

Harter, Thomas, Yuksel S Onsoy, Katrin Heeren, Michelle Denton, Gary Weissmann, Jan W Hopmans, and William R Horwath. 2005. "Deep Vadose Zone Hydrology Demonstrates Fate of Nitrate in Eastern San Joaquin Valley." *California Agriculture* 59 (2): 124–32. https://doi.org/10.3733/ca.v059n02p124.

Healy, Richard W. 2010. *Estimating Groundwater Recharge*. Cambridge university press.

Heath, Ralph C. 1998. *Basic Ground-Water Hydrology*. Vol. 2220. US Department of the Interior, US Geological Survey.

Henri, Christopher Vincent, Thomas Harter, and Efstathios Diamantopoulos. 2020. "On the Conceptual Complexity of Non-Point Source Management: Impact of Spatial Variability." *Hydrology and Earth System Sciences* 24 (3): 1189–1209. https://doi.org/10.5194/hess-24-1189-2020.

Herman, Jon, and Will Usher. 2017. "SALib: An Open-Source Python Library for Sensitivity Analysis." *The Journal of Open Source Software* 2 (9): 97. https://doi.org/10.21105/joss.00097.

Khalsa, Sat Darshan S., David R. Smart, Saiful Muhammad, Christine M. Armstrong, Blake L. Sanden, Benjamin Z. Houlton, and Patrick H. Brown. 2020. "Intensive Fertilizer Use Increases Orchard N Cycling and Lowers Net Global Warming Potential." *Science of The Total Environment* 722 (June): 137889. https://doi.org/10.1016/j.scitotenv.2020.137889.

Kourakos, George, Frank Klein, Andrea Cortis, and Thomas Harter. 2012. "A Groundwater Nonpoint Source Pollution Modeling Framework to Evaluate Long-Term Dynamics of Pollutant Exceedance Probabilities in Wells and Other Discharge Locations." *Water Resources Research* 48 (6). https://doi.org/10.1029/2011WR010813.

Lockhart, K. M., A. M. King, and T. Harter. 2013. "Identifying Sources of Groundwater Nitrate Contamination in a Large Alluvial Groundwater Basin with Highly Diversified Intensive Agricultural Production." *Journal of Contaminant Hydrology* 151 (August): 140–54. https://doi.org/10.1016/j.jconhyd.2013.05.008.

Mann, Michael E., and Peter H. Gleick. 2015. "Climate Change and California Drought in the 21st Century." *Proceedings of the National Academy of Sciences* 112 (13): 3858–59. https://doi.org/10.1073/pnas.1503667112.

Maples, Stephen R., Graham E. Fogg, and Reed M. Maxwell. 2019. "Modeling Managed Aquifer Recharge Processes in a Highly Heterogeneous, Semi-Confined Aquifer System." *Hydrogeology Journal* 27 (8): 2869–88. https://doi.org/10.1007/s10040-019-02033-9.

Marr, Jenny, Devinder Dhillon, David Arrate, Shem Stygar, and Romain Maendly. 2018. "FLOOD-MAR: Using FLood Water For Managed Aquifer Recharge to Support Sustainable Water Resources." White Paper. CA Department of Water Resources. https://cawaterlibrary.net/document/flood-mar-using-flood-water-for-managed-aquifer-recharge-to-support-sustainable-water-resources/.

Meisinger, J. J., and G. W. Randall. 1991. "Estimating Nitrogen Budgets for Soil-Crop Systems." In *Managing Nitrogen for Groundwater Quality and Farm Profitability*, 85–124. John Wiley & Sons, Ltd. https://doi.org/10.2136/1991.managingnitrogen.c5.

Onsoy, Y. S., T. Harter, T. R. Ginn, and W. R. Horwath. 2005. "Spatial Variability and Transport of Nitrate in a Deep Alluvial Vadose Zone." *Vadose Zone Journal* 4 (1): 41–54. https://doi.org/10.2113/4.1.41.

Phillips, Steven, Karen Burow, D.L. Rewis, Jennifer Shelton, and Bryant Jurgens. 2007. "Hydrogeologic Setting and Ground-Water Flow Simulations of the San Joaquin Valley Regional Study Area, California," January, 4–31.

Phillips, Steven P., Diane L. Rewis, and Jonathan A. Traum. 2015. "Hydrologic Model of the Modesto Region, California, 1960-2004." Scientific Investigations 2015–5045. US Department of the Interior, US Geological Survey.

Pollock, D. W. 2016. "User Guide for MODPATH Verison 7–a Particle Tracking Model for MODFLOW. Open-File Report 2016–1086." US Geological Survey, Washington, DC.

Rajput, T. B. S., and Neelam Patel. 2006. "Water and Nitrate Movement in Drip-Irrigated Onion under Fertigation and Irrigation Treatments." *Agricultural Water Management* 79 (3): 293–311. https://doi.org/10.1016/j.agwat.2005.03.009.

Salamon, P., D. Fernàndez-Garcia, and J. J. Gómez-Hernández. 2007. "Modeling Tracer Transport at the MADE Site: The Importance of Heterogeneity." *Water Resources Research* 43 (8). https://doi.org/10.1029/2006WR005522.

Schulze-Makuch, Dirk. 2005. "Longitudinal Dispersivity Data and Implications for Scaling Behavior." *Groundwater* 43 (3): 443–56. https://doi.org/10.1111/j.1745-6584.2005.0051.x.

Selker, John S., James T. McCord, and C. Kent Keller. 1999. *Vadose Zone Processes*. CRC Press.

Silva, Sebastian Saa, Saiful Muhammad, Blake Sanden, Emilio Laca, and Patrick Brown. 2013. "Almond Early-Season Sampling and In-Season Nitrogen Application Maximizes Productivity, Minimizes Loss." *Almond Board of California*, 9.

Simunek, Jirka, Jan Hopmans, and Naftali Lazarovitch. 2010. "A New Compensated Root Water and Nutrient Uptake Model Implemented in HYDRUS Programs," May.

Simunek, Jirka, M. Th Van Genuchten, and M. Sejna. 2013. "The HYDRUS-1D Software Package for Simulating the One-Dimensional Movement of Water, Heat, and Multiple Solutes in Variably-Saturated Media, Version 4.17." *HYDRUS Software Series 3*, 342.

Spalding, R. F., and M. E. Exner. 1993. "Occurrence of Nitrate in Groundwater—A Review." *Journal of Environmental Quality* 22 (3): 392–402. https://doi.org/10.2134/jeq1993.00472425002200030002x.

State Water Resources Control Board. 2017. "GROUNDWATER INFORMATION SHEET: Nitrate." GAMA Program. https://www.waterboards.ca.gov/gama/docs/coc_nitrate.pdf.

Stewart, W. M., D. W. Dibb, A. E. Johnston, and T. J. Smyth. 2005. "The Contribution of Commercial Fertilizer Nutrients to Food Production." *Agronomy Journal* 97 (1): 1–6. https://doi.org/10.2134/agronj2005.0001.

Storlie, Craig A., Philip E. Neary, and James W. Paterson. 1995. "Fertilizing Drip-Irrigated Bell Peppers Grown on Loamy Sand Soil." *HortTechnology* 5 (4): 291–94. https://doi.org/10.21273/HORTTECH.5.4.291.

Syvertsen, J. P., and J. L. Jifon. 2001. "Frequent Fertigation Does Not Affect Citrus Tree Growth, Fruit Yield, Nitrogen Uptake, and Leaching Losses." In *Proc. Fla. State Hort. Soc*, 114:88–93.

Syvertsen, J. P., and S. M. Sax. 1999. "Fertigation Frequency, Wetting Patterns and Nitrate Leaching from Lysimeter-Grown Citrus Trees." In *Proceedings of the Florida State Horticultural Society*, 112:9–14.

Tanachaichoksirikun, Pinit, Uma Seeboonruang, and Graham E. Fogg. 2020. "Improving Groundwater Model in Regional Sedimentary Basin Using Hydraulic Gradients." *KSCE Journal of Civil Engineering* 24 (5): 1655–69. https://doi.org/10.1007/s12205-020-1781-8.

Thompson, Thomas L., Scott A. White, and Michael A. Maurer. 2000. "Development of Best Management Practices for Fertigation of Young Citrus Trees," October. https://repository.arizona.edu/handle/10150/223854.

Thompson, Thomas L., Scott A. White, James Walworth, and Greg J. Sower. 2003. "Fertigation Frequency for Subsurface Drip-Irrigated Broccoli." *Soil Science Society of America Journal* 67 (3): 910–18. https://doi.org/10.2136/sssaj2003.9100.

UNESCO. 2022. *The United Nations World Water Development Report 2022: Groundwater: Making the Invisible Visible*. Paris. https://unesdoc.unesco.org/ark:/48223/pf0000380721.

U.S. Geological Survey. n.d. "National Water Information System Data Avilable on the World Wide Web (Water Data for the Nation)." Accessed May 16, 2022. http://waterdata.usgs.gov/nwis/.

Van Groenigen, J. W., G. L. Velthof, O. Oenema, K. J. Van Groenigen, and C. Van Kessel. 2010. "Towards an Agronomic Assessment of N2O Emissions: A Case Study for Arable Crops." *European Journal of Soil Science* 61 (6): 903–13. https://doi.org/10.1111/j.1365-2389.2009.01217.x.

Vrugt, J. A., M. T. van Wijk, J. W. Hopmans, and J. Šimunek. 2001. "One-, Two-, and Three-Dimensional Root Water Uptake Functions for Transient Modeling." *Water Resources Research* 37 (10): 2457–70. https://doi.org/10.1029/2000WR000027.

Weissmann, G. S., and G. E. Fogg. 1999. "Multi-Scale Alluvial Fan Heterogeneity Modeled with Transition Probability Geostatistics in a Sequence Stratigraphic Framework." *Journal of Hydrology* 226 (1): 48–65. https://doi.org/10.1016/S0022-1694(99)00160-2.

Weissmann, Gary S., Steven F. Carle, and Graham E. Fogg. 1999. "Three-Dimensional Hydrofacies Modeling Based on Soil Surveys and Transition Probability Geostatistics." *Water Resources Research* 35 (6): 1761–70. https://doi.org/10.1029/1999WR900048.

Zhang, Yonggen, and Marcel G. Schaap. 2017. "Weighted Recalibration of the Rosetta Pedotransfer Model with Improved Estimates of Hydraulic Parameter Distributions and Summary Statistics (Rosetta3)." *Journal of Hydrology* 547 (April): 39–53. https://doi.org/10.1016/j.jhydrol.2017.01.004.

Zheng, Chunmiao, and Gordon D. Bennett. 1995. *Applied Contaminant Transport Modeling: Theory and Practice*. New York Albany Paris [etc.]: Van Nostrand Reinhold ITP.

Zheng, Chunmiao, and P. Patrick Wang. 1999. "MT3DMS: A Modular Three-Dimensional Multispecies Transport Model for Simulation of Advection, Dispersion, and Chemical Reactions of Contaminants in Groundwater Systems; Documentation and User's Guide."

3.9. Appendix

Table 3-A1. Nitrate Concentration Measured in Shallow Groundwater Monitoring Wells

MW	1	2	3	4	5	6	7	8	9	10
Sampling Event					NO3-N (mg/L)					
11/6/2015	9.11	4.31	11.06	14.40	16.94	13.07	16.94	16.64	13.64	10.85
10/29/2017	4.46	5.97	9.69	25.05	16.25	18.33	19.21	22.97	6.77	16.73
5/7/2018	4.65	3.49	10.25	33.05	20.57	23.85	21.29	10.65	5.52	17.13
7/23/2018	13.44	9.49	10.13	37.29	19.21	19.73	19.21	25.49	6.73	17.19
9/11/2018	12.79	11.19	10.15	35.27	17.91	18.47	18.47	25.43	6.48	16.59
11/26/2018	10.93	9.37	10.27	39.20	16.72	17.28	17.92	28.48	6.04	16.21
1/24/2019	9.69	8.61	11.09	34.17	17.37	17.73	18.41	26.61	6.57	16.09
3/11/2019	9.59	6.90	10.82	30.18	16.82	17.22	17.94	26.10	6.25	15.34
4/26/2019	12.21	6.66	10.13	31.81	16.21	16.85	17.73	25.49	6.21	15.17
6/5/2019	13.97	16.18	10.50	38.26	16.74	17.30	18.02	25.86	6.29	15.26
7/19/2019	13.66	18.38	10.54	38.94	16.94	18.86	19.42	36.82	6.02	15.50
9/9/2019	12.53	15.54	11.14	33.62	17.06	18.34	19.86	31.06	6.28	15.38
10/25/2019	10.00	9.67	10.56	30.43	16.00	17.47	20.99	26.75	6.31	15.15
12/5/2019	8.41	8.22	10.62	32.38	17.18	18.94	24.86	30.62	6.01	15.74
1/31/2020	6.63	7.41	10.57	31.69	18.25	18.97	25.21	33.81	6.28	15.61
3/19/2020	9.95	11.84	11.36	45.44	20.32	19.56	27.92	51.68	8.48	18.00
5/5/2020	10.33	10.25	11.29	46.49	19.69	19.37	28.57	52.41	6.72	16.97
6/16/2020	11.23	13.07	12.03	45.23	21.23	19.79	27.95	48.35	6.81	19.11
8/11/2020	11.15	12.19	11.07	43.47	18.43	19.71	27.39	45.31	6.64	18.19
10/15/2020	8.13	7.65	10.96	30.56	16.00	18.64	30.64	38.00	6.29	17.12
11/23/2020	6.91	7.31	11.22	31.86	16.18	19.06	34.02	37.54	6.48	18.18
1/20/2021	6.30	7.26	11.91	31.43	16.47	19.03	36.15	36.63	7.20	18.31
3/11/2021	6.09	7.75	12.63	36.75	17.39	19.39	32.63	35.63	7.19	17.57
4/29/2021	7.03	10.64	12.08	42.48	18.00	19.28	34.56	37.76	7.16	16.56
6/1/2021	7.00	11.13	12.37	46.45	18.37	20.13	38.53	38.69	7.62	17.73
7/29/2021	7.96	12.63	13.03	46.55	17.83	20.15	40.87	39.43	7.99	17.83
9/8/2021	8.36	10.28	13.48	41.80	17.64	19.88	42.52	37.44	8.52	18.36
1/24/2022	6.04	8.37	14.21	28.45	17.41	19.89	42.77	40.37	8.05	18.33
3/15/2022	6.46	9.98	16.46	45.74	21.58	20.30	45.26	39.66	8.38	17.86

Table 3-A2. Nitrate Concentration Measured in Shallow Groundwater Monitoring Wells

MW	11	12	13	14	15	16	17	18	19	20
Sampling Event					*NO3-N (mg/L)*					
11/6/2015	53.33	27.70	61.60	31.95	46.12	55.50	31.09	10.90	23.87	34.39
10/29/2017	23.37	27.05	56.89	31.21	42.57	20.81	33.93	16.01	8.41	27.13
5/7/2018	22.33	24.89	49.37	36.57	55.85	20.25	25.45	18.89	18.97	20.41
7/23/2018	23.09	28.73	56.43	32.25	53.71	26.37	31.93	22.69	18.37	36.12
9/11/2018	21.99	28.07	59.51	30.55	50.47	25.91	31.51	23.67	16.79	33.39
11/26/2018	21.44	27.04	60.00	30.08	50.72	26.24	31.68	24.16	17.12	33.64
1/24/2019	21.81	27.01	59.78	30.37	44.41	24.97	31.69	24.69	18.65	34.03
3/11/2019	21.30	26.50	60.82	29.14	46.42	23.78	30.74	23.98	21.54	35.54
4/26/2019	20.45	24.77	61.97	30.37	51.17	24.77	28.77	23.09	21.65	37.33
6/5/2019	21.62	25.54	64.50	32.74	58.34	26.58	29.78	23.62	22.42	37.82
7/19/2019	21.18	25.26	69.34	35.66	65.78	25.98	32.14	25.22	24.54	41.18
9/9/2019	21.94	25.46	80.82	35.06	56.90	23.86	31.22	25.46	21.30	39.62
10/25/2019	21.79	25.15	93.63	34.11	69.79	20.19	30.75	24.99	20.67	36.94
12/5/2019	23.82	27.18	110.69	38.46	78.06	20.78	33.98	27.82	24.70	41.07
1/31/2020	23.53	26.49	113.29	38.25	78.01	21.69	33.85	27.97	25.13	39.66
3/19/2020	22.32	27.52	107.53	42.96	67.36	22.96	34.64	29.20	27.04	45.36
5/5/2020	22.33	27.05	107.54	43.37	67.45	23.13	34.65	27.93	27.93	44.86
6/16/2020	21.95	27.79	111.90	44.51	69.79	24.03	35.63	28.11	29.87	50.11
8/11/2020	20.99	26.99	106.79	42.03	70.35	22.51	33.87	26.99	29.79	55.07
10/15/2020	21.12	26.88	91.04	40.32	66.96	20.80	33.76	27.52	27.84	55.36
11/23/2020	21.54	28.42	92.69	43.62	69.86	23.14	35.46	29.54	30.70	50.82
1/20/2021	21.99	27.99	91.01	44.95	77.11	23.99	35.91	30.55	31.51	48.28
3/11/2021	20.47	25.55	81.39	44.70	69.82	23.83	32.51	28.87	31.31	47.95
4/29/2021	19.76	26.96	76.14	42.56	70.00	24.40	33.76	30.88	30.28	55.36
6/1/2021	20.85	27.09	80.05	47.17	82.13	29.73	36.13	33.41	33.33	56.81
7/29/2021	20.47	27.75	76.23	46.71	89.11	29.35	35.35	34.31	35.11	56.51
9/8/2021	20.52	27.96	79.80	45.80	78.12	26.84	35.00	34.80	34.92	56.12
1/24/2022	22.13	29.49	44.45	73.41	64.45	20.77	35.33	37.89	37.81	56.97
3/15/2022	21.26	29.18	74.14	47.98	65.98	23.90	34.78	39.50	38.54	60.76

CHAPTER 4. Concluding Remarks

Nitrate is the most common groundwater contaminant in the Central Valley observed exceeding its respective drinking water limits for public health. According to the State Water Resources Control Board, the public drinking water supply for 31 million Californians relies on groundwater, and 2 million Californians rely on private domestic wells. Despite groundwater being a coveted resource, contamination of groundwater with nitrates has been increasing historically and is likely to worsen without intervention. Regional groundwater trends since the 1950s exhibit increasing nitrate concentrations in the shallow and deep aquifers in the eastern fan subregion of the Central Valley (Burow et al. 2013). Numerical groundwater modeling of the Modesto basin forecasts that under current management practices, nitrate concentrations in nearby public supply wells will steadily increase to 20% above the MCL over the next 50 years (Bastani and Harter 2019). The regulatory strategy selected to address deteriorating groundwater quality due to nitrate in the Central Valley is to improve nutrient management at farms and reduce leaching from agriculture, which is the greatest contributor of nitrogen loading to groundwater. This study predicts how highly efficient nutrient and water management at an almond orchard would impact nitrogen loading rates and groundwater quality at the field scale over the next 30 years.

Chapter 2 found that nutrient management practices which closely match the crop uptake (HFLC) have the potential to significantly reduce nitrate leaching, even on already well-managed farms following standard management practices. Under the prior standard practice, average NUE was estimated to be around 83%. This NUE is already considered to be excellent, but the average NUE is predicted to increase to 90% under HFLC, which is pushing the upper practical limit for nutrient efficiency. While HFLC management increased crop yields, lowered fertilizer applications, and improved NUE right away, actual nitrogen loading rates demonstrate high spatial and temporal variability. Temporal variability over the scale of 5-10 years is caused by differences in climate (precipitation) and irrigation efficiency with

tree age. Spatial variability in nitrogen loading is found even within the same orchard blocks and is caused by nonuniform water flow through heterogeneous geologic media. Due to high intra-land use variability, modeling at the field scale over a period of several decades was required for the decreasing trend in nitrogen loading to emerge.

Modeling spatial variability in nitrogen loading rates (Chapter 2) was found to be necessary to reproduce the variability of nitrate concentrations measured in groundwater monitoring wells at the orchard (Chapter 3). When using groundwater models to evaluate probabilistic nitrate concentrations in wells, spatial variability in nitrogen loading inputs to the model should match the scale of the well source area size. If the well source area is smaller than the land use category scale, then it may be important to consider intra-land use spatial variability in nitrogen loading. While public supply wells and irrigation wells have source areas that typically span many land uses, domestic wells may have small enough source areas where this should be considered.

However, models which simplify spatial variable nitrogen loading rates as an average were found to represent average field-scale responses. In Chapter 2, the nitrogen mass balance model predicted HFLC would have a similar impact on nitrogen loading as the numerical model. In Chapter 3, a groundwater model without geologic or nitrate source variability predicted average nitrate concentrations in monitoring wells as well as a complex heterogeneous model. Simple models like these can be scaled up to the regional scale, whereas the level of detail used in the models in this study is too computationally intensive at a larger scale.

Lastly, Chapter 2 predicted low recharge rates (on average 7 cm/year) caused by dry climate and efficient irrigation at the orchard. As a result, Chapter 3 predicted long response times (up to 50 years or more) in field-scale improvements in shallow groundwater quality. The outcome of this project was tied to deep percolation/groundwater recharge rates beneath the orchard. Not only does the low recharge rate

translate to slow changes in nitrogen loading rates and groundwater quality, but it also means nitrate leaching from the orchard is concentrated into a smaller volume of water. Despite having some of the highest nutrient efficiencies expected in a commercial orchard, the average concentration of nitrate in groundwater recharge was predicted to remain above 10 mg/L. Under these conditions, long-term average nitrate concentrations in shallow groundwater are also likely to remain above the MCL.

Agriculture in the Central Valley is transitioning to highly efficient irrigation methods to adjust to diminishing surface water and stressed groundwater supplies. Deep percolation from applied water is decreasing, as demonstrated by the low groundwater recharge rates at the orchard in this study. The average recharge rates modeled at the orchard in this study for the period 2013-2021, 7 cm/year, were an order of magnitude less than simulated recharge rates modeled in the Modesto regional groundwater model for the period 1960-2004, 60-90 cm/year (Phillips et al. 2015). Over time, patterns of regional groundwater flow will adapt to the changing landscape; wells will draw from larger and/or more distant source areas. Wells which have the potential to source water from rivers may adapt to lower irrigated land recharge by pulling a greater fraction of relatively clean river recharge. Wells whose source areas include rivers tend to have lower nitrate concentrations (Castaldo et al. 2021). Future work should consider the impact reduced recharge from irrigation will have on well source areas and, in turn, regional groundwater nitrate concentrations in wells.

4.1 References

Bastani, Mehrdad, and Thomas Harter. 2019. "Source Area Management Practices as Remediation Tool to Address Groundwater Nitrate Pollution in Drinking Supply Wells." *Journal of Contaminant Hydrology* 226 (October): 103521. https://doi.org/10.1016/j.jconhyd.2019.103521.

Burow, Karen R., Bryant C. Jurgens, Kenneth Belitz, and Neil M. Dubrovsky. 2013. "Assessment of Regional Change in Nitrate Concentrations in Groundwater in the Central Valley, California, USA, 1950s–2000s." *Environmental Earth Sciences* 69 (8): 2609–21. https://doi.org/10.1007/s12665-012-2082-4.

Castaldo, Giovanni, Ate Visser, Graham E. Fogg, and Thomas Harter. 2021. "Effect of Groundwater Age and Recharge Source on Nitrate Concentrations in Domestic Wells in the San Joaquin Valley." *Environmental Science & Technology* 55 (4): 2265–75. https://doi.org/10.1021/acs.est.0c03071.

Phillips, Steven P., Diane L. Rewis, and Jonathan A. Traum. 2015. "Hydrologic Model of the Modesto Region, California, 1960-2004." Scientific Investigations 2015–5045. US Department of the Interior, US Geological Survey.